Spatiotemporal variability of hydrology in Moanatuatua drained peatland and its influence on CO_2 emissions and surface oscillations

A thesis

submitted in partial fulfilment

of the requirements for the degree

of

Master of Science (Research) in Earth Sciences

at

The University of Waikato

by

Georgia Louise Glover-Clark

THE UNIVERSITY OF
WAIKATO
Te Whare Wānanga o Waikato

The University of Waikato

2020

Abstract

Drained agricultural peatlands can be highly productive but problematic ecosystems, including releasing substantial carbon dioxide (CO_2) emissions to the atmosphere as peat decomposes. The ongoing and permanent loss of soil carbon from drained peatlands worldwide represents approximately 5% of global anthropogenic CO_2 emissions, which are accompanied by long-term irreversible subsidence of the peatland surface, affecting land management. Hydrology, particularly with respect to water table depth and soil moisture content, is seen as an important control on soil physical and hydraulic properties, reversible and irreversible subsidence, and biogeochemical processes including the emission of CO_2. The globally unique peatlands of Aotearoa New Zealand, including in their drained state, have a relatively limited research history when compared to those in the Northern Hemisphere. As such, we lack a comprehensive understanding of hydrological regimes and how they act to influence environmental effects.

To improve our understanding, I have conducted a spatially and temporally detailed hydrological investigation over a one-year period within Moanatuatua drained peatland in the Waikato region of Aotearoa New Zealand. My primary objective was to determine the controls on spatiotemporal variation in hydrology and its influence on CO_2 emissions and oscillations in peat surface elevation, by comparing and contrasting two dairy farms with similar management practices but different drainage designs and drainage histories. Using a combination of manual and automatic measurement techniques, water table depth (relative water level, RWL) and soil moisture (volumetric moisture content, VMC) were measured, as well as peat physical properties, water vapour and CO_2 fluxes, and peatland surface oscillations (PSO).

Both RWL and VMC were spatially and temporally variable. Spatial patterns of RWL were very similar between sites, indicating limited control of drainage design during a climatically warm and dry year. The deeper drains at Site 2 did, however, appear to increase RWL depth. Temporal patterns of RWL and VMC at both sites responded to water storage changes largely driven by the water balance components of precipitation and evaporation. Evident hydrological differences between sites appeared to be predominantly influenced by soil physical properties, which led to

more variable VMC at Site 1 and more variable RWL at Site 2. Lower VMC at Site 1 initiated hydrophobicity in surface peat over an extended drought period, while Site 2 was little affected. Deep capillary zones at both sites indicated subsurface moisture redistribution, the depths of which far exceeded those in published literature. A dependent relationship between RWL and VMC was only apparent when peat was near saturation, otherwise displaying considerable long and short-term hysteresis caused by different and delayed responses of RWL and VMC to rainfall.

CO_2 emissions at both sites were primarily influenced by VMC and were not at all correlated with RWL, raising questions for the continued use of RWL as a proxy to estimate near-surface moisture conditions in carbon studies. Soil temperatures also influenced emissions, and appeared to be the dominant control only when VMC was high. The ability of soil at Site 2 to retain more moisture during an extended summer drought meant that ecosystem respiration (ER) was not constrained by water limitations to the extent it was at Site 1. As gross primary production was very similar at the two sites, the ongoing differences in ER initiated in late January led to accumulated emissions over the full year of 5.6 t C ha^{-1} greater than at Site 2.

Over a 10 month period, PSO at both sites were in the upper range of values published in international literature, and were between 2.5 – 3.5 times greater than the annual average irreversible subsidence rate for the Waikato region. PSO was correlated with rainfall, RWL and VMC, each of which had varying influence during the measurement period. Considerable hysteresis was measured in the relationship between surface elevation and RWL, distinctly separating drying and wetting cycles. Short term hysteresis was likely induced by a delay between equilibration of effective stresses within the peat matrix before a change in surface elevation incurred. Higher bulk density at Site 2 acted to reduce the magnitude of PSO, a phenomenon that was also noted at both sites adjacent to drainage channels.

Overall, this research has revealed the importance of hydrology, drainage history, and their effects on peat physical properties, each of which strongly influenced CO_2 emissions and PSO, raising questions about their continued use for agriculture.

Acknowledgements

My Masters research project would not have been possible without the unwavering support and guidance from those around me, so I would like to take this opportunity to give thanks to the following:

First and foremost, my supervisor, Associate Professor David Campbell. Thank you for introducing me to the fascinating world of peatlands, first pristine and then drained. Your passion for peat is infectious, and you have undoubtedly passed the bug on to me! Thank you for the wonderful opportunity to undertake a research project in such a remarkable yet incredibly complex ecosystem. It has been an absolute honour to work with you over the past year as part of the PEATWISE team. You have taught me more than I ever thought possible, and I am forever grateful for the countless hours of guidance, help and support which you have given to me. I really appreciate the kindness that you and Annie have shown me.

Thank you to Chris Morcom for your constant willingness to help with fieldwork, data processing, and whatever else needed doing. It was well beyond the call of duty. Dean Sandwell, for your crucial help with laser surveying, the establishment of my benchmarks, and always emphasising the importance of control points! Joss Ratcliffe for assistance and guidance with my deep soil cores and lab work. Thank you to Emily Fensham and Alice Wheatley-Wilson for your valuable work on developing site-specific calibrations of the soil moisture probes and soil heat flux plates. Thank you to Louis Schipper, for generously organizing funding, giving insightful advice and suggestions regarding my project, and for all our interesting and thought-provoking conversations. Noel Bates for assistance in the soils lab. Aaron Wall for all your helpful suggestions, sorting out my Matlab issues and showing me new shortcuts and tricks. Thank you to Jack Pronger and Justin Wyatt for all your assistance with the PSO side of my project, and valuable suggestions. Jacob Hamill for help with fieldwork.

Thank you to J.D. and R.D. Wallace Ltd. for permitting the establishment of our research sites on their farms, to farm managers Shaun Olsen and Christian Hohepa for access, and Harry Snell for all your assistance.

This project was supported by the PEATWISE consortium, of which the Aotearoa New Zealand component was funded through the Ministry for Primary Industries. I would also like to acknowledge generous funding through scholarships from the University of Waikato, the Waikato Regional Council, DairyNZ, and the Waikato Graduate Women Educational Trust. Thank you.

To the rest of the WaiBER group, it has been a privilege working alongside you all, and I can't wait to see the great things each of you will achieve. An extra special thanks to Seb Hoepker, Dori Torres-Rojas and Thomas Corbett, for always lifting my spirits and being keen for a chat. Kris Numa, you are an absolute star and it has been a real pleasure to study alongside you over the past two years. Thank you for always being there for me, whether it was thesis related or not. To Jacko White and the rest of the MSc cohort, Kate Rogers, Celeste Davies-Calway, Charlotte Robertson, Matt House and Maddie Hansen, it has been a great few years getting to know each of you.

Sara, Ella and Courtney, you three have been my shining lights that have kept me going throughout all of this. Thank you for the constant support, interest in the foreign language of peat, and for the many great trips away. I don't know what I would have done without you. Lindsay, Lucy, Tyla, and the rest of my friends near and far, thank you for always being in my corner and distracting me from study whenever I needed a break. Especially all of you Project Blue legends!

My incredible Mum and Dad, I love you to the moon and back. I can't thank you enough for being such amazing role models, giving endless encouragement and support, as well as allowing me to drive you mad with all the talk about peat. Granny, you are incredible, and none of this would have been possible without your support, so I thank you from the bottom of my heart. This thesis is for you and Grandpa. To Hollie, Felix, Uncle Stevie, Uncle Ian, Sophie, Daisy, and the rest of my family, thank you for your unwavering support and for always taking such an interest in whatever I do. You're all amazing! And last, but most definitely not least, my Aunty Jill. One of the strongest, happiest and most inspirational people I know. Your attitude towards life and its hurdles makes absolutely all of this worth it. I love you.

Table of Contents

Chapter 1

Introduction

1.1 Background

Terrestrial ecosystems are crucial elements in the carbon (C) exchange system between soil and the atmosphere (Davidson & Janssens, 2006). Peatlands are of global importance within this exchange, containing 30% of the global soil C stock (Blodau, 2002), despite covering a disproportionately low 2.8% of Earth's land surface area (Xu et al., 2018). In recent centuries, increasing demand for land has resulted in widespread drainage of peatlands for agricultural and urban expansion (Holden et al., 2006). An estimated 65 million hectares (Mha) of peatlands have been drained worldwide (Kaat & Joosten, 2009), representing a substantial loss of high-value ecosystem services (Clarkson et al., 2013) and leading to significant environmental impacts (Schwärzel et al., 2006).

Over coming years, the stability of food supply is projected to decrease; while simultaneously there will be increased food demand (International Panel for Climate Change, IPCC, 2019). Ongoing C losses from drained peatlands adds to the atmospheric CO_2 burden, the magnitude of which has been estimated to represent approximately 5% of anthropogenic carbon dioxide (CO_2) emissions (Joosten et al., 2016). If drained peatlands continue to be used for agricultural production, implementation of mitigation measures which reduce their environmental impact are essential. To achieve this, a deeper understanding of drained peatlands, and the underlying processes affecting their productivity and greenhouse gas emissions, is required.

1.2 Effects of peatland drainage

When peatlands are drained, C dynamics are significantly altered. Hydrological conditions largely control the C balance of a peatland (Holden et al., 2004), because the position of the water table (WT) and associated capillary fringe determine the thickness of the oxic layer within the peat profile (Waddington & Price, 2000). Lowered WTs facilitate increased oxygen diffusion into the soil; increasing decomposition rates and leading to the permanent loss of soil organic matter

through oxidation (Heathwaite et al., 1993). CO_2 emissions are released through this process (Armentano & Menges, 1986), and peatlands shift from being C sinks in their natural state to substantial C sources once drained (Tubiello et al., 2016).

Peatland drainage not only impacts carbon gas dynamics but also has fundamental implications for peat processes and characteristics (Holden et al., 2004). Peatland surface subsidence is a well-documented issue, caused by a combination of peat shrinkage, oxidation and consolidation (Pronger et al., 2014). It is mostly dependent on the intensity of drainage and the degree of decomposition (Schwärzel et al., 2002). Subsidence processes are initiated immediately following drainage (Petersen & Madsen, 1978), and continue to occur until management practices that stop this process are adopted, or the organic deposits completely disappear (Deverel et al., 2016).

In addition to the ongoing and irreversible subsidence, the peatland surface will oscillate due to changing water contents that impose different effective stresses on the highly porous, and easily deformable, peat matrix (Ingram, 1983). These oscillations have been referred to as 'bog breathing' (Morton & Heinemeyer, 2019) or peatland surface oscillation (PSO; Fritz et al., 2008), amongst others. PSO in drained peat occurs to a lesser degree than in pristine peat but remains an essential process with regards to water storage changes (Price & Schlotzhauer, 1999), and seasonal variability of peat physical and hydraulic properties (Price, 1997).

Following drainage, soil physical characteristics are substantially altered, further constraining effective land management (Berglund & Berglund, 2011). Initial pore dewatering and the ensuing consolidation of peat acts to rearrange soil particles (Hobbs, 1986). As a result, macroporosity and total porosity are decreased, and bulk density is increased (Schwärzel et al., 2002; Dettmann et al., 2014). Soil properties vary through time; seasonally due to PSO processes, as well as ongoing variation from decomposition (Boelter, 1965). Changes to porosity and bulk density considerably reduce hydraulic conductivity, affecting water movement within drained peatlands (Ingram, 1983; McLay et al., 1992).

Effective control of water table depth (WTD) and soil moisture content (SMC), through the construction of drainage channels, is essential for agricultural

productivity and minimising adverse environmental effects (Norberg et al., 2018). However, low hydraulic conductivity in drained peat soils may frequently render drainage operations unsuccessful or uneconomic, as close drain spacings have been required at numerous study sites to lower the WT to a depth adequate for productive agriculture (Hudson & Roberts, 1982; Holden et al., 2004). Complicating this further is that a strong relationship between WTD and SMC holds for some peat soils (Schlotzhauer & Price, 1999), but not others (Parmentier et al., 2009). Consequently, there is no universal best management practice for all drained peatlands, and they must be evaluated on a case-by-case basis.

1.3 Drained peatlands in Aotearoa New Zealand

In Aotearoa New Zealand (NZ), peatlands once covered an estimated 166,000 ha of land (Holden et al., 2004), around 100,000 ha of which were located in the Waikato Region of Te Ika-a-Māui (North Island). Over the past 150 years, more than 90% have been drained and developed for agriculture (Clarkson et al., 2004), representing substantial peat losses that, relative to original peatland extent, exceed most other countries in the developed world (Mitsch & Gosselink, 2000). The Waikato Region now contains over 75,000 ha of drained peat soils (Pronger et al., 2014), the majority of which are under year-round, rotational dairy grazing (Campbell et al., 2015). In a region that comprises approximately one-fifth of NZ's dairy production (DairyNZ, 2019), dairy grazing on drained peat contributes significantly to the economy. Based on an estimate of the 2018-2019 dairy season (DairyNZ, 2019) and the 60% of drained peat under dairy grazing in the Waikato Region, the value of dairy production on peat was estimated at $462M (NZD; J. Wyatt, personal communication, September 27, 2019).

1.4 Aims and objectives

To improve management practices on Waikato drained peat soils under dairy farm grazing, an improved understanding of their hydrology and its influence on environmental impacts is required. The overarching aim of this thesis was to determine the controls on spatiotemporal variation in hydrology and its influence on PSO and CO_2 emissions; on two dairy farms with similar management practices but different drainage designs and drainage histories.

Four objectives were developed to achieve this:

i. Establish the spatiotemporal variability of water table depth and soil moisture content over a one-year period;
ii. Identify the relationships between water table depth and soil moisture content;
iii. Investigate the roles of the surface water balance, peat physical properties, and drainage design as potential controls on hydrological variability;
iv. Determine the hydrological influences on CO_2 emissions;
v. Quantify the spatiotemporal variability of changes in peat surface elevation and identify the influences of hydrology and soil physical properties.

1.5 Thesis outline

Chapter 2 reviews the relevant literature concerned with drained peatland physical processes, hydrology, irreversible and reversible surface subsidence, the production and emission of CO_2, and measurement techniques; and further identifies the knowledge gaps this thesis will aim to fill.

Chapter 3 presents a description of the Moanatuatua peatland and its drainage history, as well as detailing the two research sites established on adjacent working dairy farms. Methodology relevant to both Chapters 4 and 5 is described.

Results chapters 4 and 5 are structured similar to journal articles, each with a brief introduction, methods, results and discussion sections. Chapter 4 describes the spatiotemporal behaviour of hydrology, controls acting upon this, and how hydrology influenced CO_2 emissions over a year-long study period. Chapter 5 describes the spatiotemporal variability of peat surface elevation at the two sites over ten months.

Chapter 6 integrates the findings of Chapters 5 and 6. Conclusions and recommendations are given, on how the findings of this research can serve to inform best management practices on peat soils under dairy grazing to mitigate negative environmental consequences. Knowledge gaps that require further investigation are also outlined.

Chapter 2

Literature review

2.1 Introduction

On a global scale, drained peatlands currently cover approximately 50.9 Mha of land (Leifeld & Menichetti, 2018). The disturbance of hydrological conditions causes these ecosystems to react sensitively, having multiple implications for local hydrology, peat physical properties, and biogeochemical processes such as CO_2 emissions (Dettmann et al., 2014). With current pressure on greenhouse gas (GHG) inventories and national emission reduction commitments, carbon dynamics of drained peatlands are receiving significant interest and extensive research, particularly in Europe where they are widely distributed and have been drained for many decades (e.g. Norberg et al., 2018; Säurich et al., 2019b; Tiemeyer et al., 2020).

Leifeld and Menichetti (2018) estimated that annual global CO_2 emissions from drained peatlands are ~1.91 Gt CO_2-equivalent, which amounts to approximately 5% of all anthropogenic GHG emissions on less than 1% of global land surface area (Joosten et al., 2016). The substantial and permanent loss of soil carbon to the atmosphere as CO_2 and associated loss of peat deposits, not only has an impact on the global climate, but it also acts to challenge the productive agricultural use of peat soils (Verhoeven & Setter, 2010).

It is becoming increasingly apparent that the continuation of current management practices on drained peat soils will have persistent drawbacks (Brouns et al., 2015), to both land management and the environment. With this in mind, CO_2 losses from drained peatlands have a high mitigation potential (Ferré et al., 2019), a potential which has been estimated as greater than the capacity to sequester carbon in mineral soils on all agricultural land (Leifeld & Menichetti, 2018). It has been widely accepted that a decrease in the thickness of the peat unsaturated zone will largely reduce the impacts of drainage, and mitigation measures have therefore focused on controlling the hydrology. Raising water tables to an optimum depth (Renger et al., 2002; Regina et al., 2014) and submerged drains (Van den Akker & Hendriks, 2017)

have been suggested to reduce CO_2 emissions and subsidence, but in practice, it is difficult to maintain the water table at a specific level (Ferré et al., 2019). Furthermore, high water tables conflict with intensive agricultural use (Ferré et al., 2019). Improved knowledge of drained peatlands and their hydrological processes is required to remediate negative environmental effects and maintain agricultural productivity to meet food demands for an increasing global population.

2.2 Defining peat

Peat soils and organic soils are, by definition, different. Organic soils are defined in the 2006 IPCC Guidelines (Annex 3A.5, Chapter 3 in Volume 4) on the basis of criteria 1 and 2, or 1 and 3 (IPCC, 2006):

1. Thickness of organic horizon greater than or equal to 10 cm. A horizon of less than 20 cm must have 12% or more organic carbon when mixed to a depth of 20 cm.
2. Soils that are never saturated with water for more than a few days must contain more than 20% organic carbon by weight (i.e., about 35% organic matter).
3. Soils are subject to water saturation episodes and has either:
    a. At least 12% organic carbon by weight (i.e., about 20% organic matter) if the soil has no clay; or
    b. At least 18% organic carbon by weight (i.e., about 30% organic matter) if the soil has 60% or more clay; or
    c. An intermediate proportional amount of organic carbon for intermediate amounts of clay.

Peat soils are organic soils which are derived only from peatlands, and are composed of partially decomposed plant remains with over 65% organic matter by dry weight (Charman, 2002).

2.3 Peat physical processes

In pristine peatlands, a network of different physical and hydrological properties exist; their formation which has been contingent on local hydrology, vegetation, sediment inputs, and underlying surface characteristics (Erkens et al., 2016). Superimposing the already complex structure and characteristics of pristine

peatlands, are the changes in physical structure that occur upon drainage, due to the initiation of secondary pedogenic processes such as aggregate formation and earthification (Schwärzel et al., 2002; Säurich et al., 2019a), as well as the influence of time since drainage (Laiho, 2006). Consequently, soil physical characteristics of drained peatlands contrast greatly with their pristine counterparts (Säurich et al., 2019a), and are spatially heterogeneous even over short distances (Norberg et al., 2018).

Soil structure is the three-dimensional arrangement of solid soil particles, and the pore spaces located between them (Egglesmann, 1984). Soil pores may either be micropores, with a diameter less than 0.3 mm, or macropores, with a diameter greater than 0.3 mm (Jarvis, 2007). In the process of lowering the water table through artificial drainage of peatlands, a reduction in pore water pressure leads to the collapse of many macropores (Howie & Hebda, 2018), and subsequent rearrangement of soil particles (Hobbs, 1986). Consequently, total porosity is decreased, and the proportion of micropores is increased (Schwärzel et al., 2002; Dettmann et al., 2014). Such changes are ongoing through time, as they are directly related to the degree of decomposition[1] (Boelter, 1965).

Bulk density, the dry mass of soil particles per unit volume (Sinclair et al., 2020), is another fundamental soil characteristic altered by drainage. The decreased proportion of macropores and total porosity directly increases bulk density (Waddington & Price, 2000), which in turn is related to the degree of decomposition (Clymo, 1963). An initially rapid increase in bulk density is typical when a peatland is drained, after which there is a gradual increase over time (Liu & Lennartz, 2019). In addition to long-term increases in bulk density, peat soils exhibit seasonal changes in response to changing soil moisture content (Faul et al., 2016). Price (1997) found peaks in bulk density to correspond with drier periods. Short-term changes in bulk density have been seen to express a large degree of hysteresis with respect to soil moisture (Price & Schlotzhauer, 1999), indicating further variability.

Total porosity, alongside the distribution of pore sizes within peat and degree of decomposition, is an important control on the movement of water through the soil,

[1] Decomposition of peat will reduce total porosity through the breakdown of plant debris into smaller fragments, thus reducing the volume of interparticle pore spaces (Moore et al., 2005).

as well as the availability of water for plants (Egglesmann et al., 1993). The increased proportion of micropores within the unsaturated zone will increase the vertical capillary flows of water compared to pristine peat, due to increased matric forces (Price et al., 2003). Additionally, greatly reduced vertical and horizontal hydraulic conductivity is seen when peatlands are drained because micropores transmit water less rapidly than macropores (Price, 2003; Whittington et al., 2007). The peat is thus less easily drained (Waddington & Price, 2000), which may render some drainage networks uneconomic (Holden et al., 2004). Further complicating the efficacy of drainage networks is the variability of hydraulic conductivity, between peat types and within drained peatlands (Boelter, 1965).

Natural peat has a high water holding capacity, from the abundance of coarse organic particles that can hold a substantial amount of water (Huat et al., 2011). This capacity is enhanced upon drainage, because water is withdrawn into the smallest pores and correspondingly retained at a lower pore water pressure (Price et al., 2003). Alongside this, McLay et al. (1992) found that water can be strongly sorbed to organic matter, further increasing water retention in drained peat soils. Although drained peat has a higher capacity to retain water than pristine peat, a large amount of this soil water is held at suctions above the permanent wilting point of most plants, therefore being unavailable and hydrophilically sorbed (McLay et al., 1992), which has implications for plant growth during periods of limited precipitation. Boelter (1969) demonstrated that peat with a higher bulk density is characterised by a much greater water holding capacity, and is dependent on the degree of decomposition (Kuntze, 1965). Furthermore, Rothwell et al. (1996) found that water holding capacity of drained peat closest to drainage ditches was higher relative to the rest of the paddock, following the spatial pattern of bulk density.

Despite the high water retention ability of peat soils, they have a tendency to become hydrophobic (Holden et al., 2006). Hydrophobicity is a phenomenon where the soil becomes repellent to water and is typically associated with organic compounds derived from living or decomposing vegetation or microorganisms (Szajdak & Szatylowicz, 2010). It has also been attributed to excessive drying of the soil during prolonged drought periods (Egglesmann et al., 1993). Schwärzel et al. (2002) demonstrated the effect of hydrophobicity at the end of a summer drought, which caused inhibition of soil water uptake by plants and preferential flow of water

to the water table after a rainfall event, rather than replenishing near-surface soil moisture. Often, once a peat soil has become hydrophobic it cannot regain the initial moisture content (Egglesmann et al., 1993), having implications for hydrological processes and plant growth.

The organic matter content of peat soils is often high, but spatially and temporally variable (Ingram, 1983; Norberg et al., 2018). For example, within a single drained peatland, Rowson et al. (2010) found total organic content from several soil samples to range between 64 and 94%. As time since drainage increases, and so too does degree of decomposition, mineralisation processes decrease the size of organic particles (Huat et al., 2011), and consequently, highly decomposed peat contains a lower ratio of organic matter to mineral matter (Petersen & Madsen, 1978).

The great variation in peat soil properties between peatlands, within peatlands, and through time, portrays the importance of treating peat soils as being as different from each other as they are from mineral soils (Dettmann et al., 2019). More importantly, it highlights the need to obtain site-specific data for studies of processes that are associated with or intrinsically linked to physical soil properties.

2.4 Hydrology

The hydrology of drained peatlands is intricately linked with soil physical properties (Rezanezhad et al., 2016), resulting in distinct hydraulic properties and processes compared to those of pristine peatlands (Dietrich et al., 2019; Liu & Lennartz, 2019). To effectively manage peat soils, with regards to both agricultural use and mitigation of environmental effects, it is essential to have a thorough understanding of hydrological processes, as well as their associated controls (Schwärzel et al., 2006; Mustamo et al., 2016).

It has long been established that CO_2 fluxes, and other processes associated with peatland drainage such as subsidence, are sensitive to changes in hydrology (Holden et al., 2004). The environmental implications of these drainage effects have meant that the majority of research on the hydrology of drained peatlands has been centred around the role and influence of hydrology to carbon fluxes and subsidence processes (e.g. Renger et al., 2002; Camporese et al., 2008). Correspondingly, there

is a paucity of published research that has focused solely on the controls of hydrology and its spatiotemporal variability (Regan et al., 2019).

2.4.1 Water balance

To begin to understand the hydrology of a drained peatland, all inputs and outputs of water must be considered; which as described by Campbell and Jackson (2004) can be summarised by a simple water balance equation applicable to all wetlands (Equation (2-1)).

$$\Delta S = (P + Q_{in} + G_{in}) - (E + Q_{out} + G_{out}) \quad (2\text{-}1)$$

Inputs of water include precipitation (P), surface inflows (Q_{in}) and groundwater inflows (G_{in}). Outputs include evaporation (E), surface outflows (Q_{out}) and groundwater outflows (G_{out}). In drained peatlands, not all of these water balance components are relevant. Due to the typically low horizontal and vertical hydraulic conductivity (e.g. Mustamo et al., 2016), lateral flows in and out of the drained subsurface (G_{in} and G_{out}) are often negligible (e.g. Lloyd, 2006). Furthermore, there are commonly no surface inflows (Q_{in}) as the primary role of peatland drainage is to remove water from the system. The water balance of drained peatlands can, therefore, be simplified to Equation (2-1),

$$\Delta S = P - (E + Q_{out}) \quad (2\text{-}2)$$

where each of the components has varying importance throughout the year. In periods of dry weather, E may be the largest component (Ingram, 1983), so when drainage ditches are not actively transporting water the water balance equation can be simplified to $\Delta S = P - E$. In wet periods when the drains are once again transporting water, Q_{out} becomes relevant. Furthermore, while meteorological conditions drive the water balance of a drained peatland, components of the water balance are in turn controlled by drainage design and depth, vegetation, and soil properties (Stenberg et al., 2018).

Storage changes (ΔS) driven by the water balance, manifest as changes in the amount of water stored in the unsaturated zone over time, where a negative value represents a loss of water from the drained peatland and a positive represents a gain, both of which drive changes in soil moisture content (SMC) and water table depth (WTD). Specific yield is a parameter that describes the relationship between changes in WTD with changes in storage (Price & Schlotzhauer, 1999). By definition, it is the change in WTD associated with the amount of stored water lost or gained, and allows estimation of the available pore space within the unsaturated zone (Logsdon et al., 2010). In a soil which has a low specific yield, a small volume of water infiltrating to the saturated zone will cause a large rise in WTD (Price et al., 2003).

2.4.2 Soil moisture

SMC describes the amount of water stored within the unsaturated zone, and in peat soils is typically expressed volumetrically (volumetric moisture content, VMC); water volume per unit volume of soil (Ingram, 1983). Alternatively, the water-filled pore space (WFPS) is the proportion of total pore space filled by water (Balaine et al., 2013). In peat soils, SMC or WFPS act as controls on the exposure of soil organic matter to oxygen, having a direct influence on processes such as CO_2 emissions and subsidence (Carlson et al., 2015; Marwanto et al., 2019).

When the water table (WT) is close to the peat surface, a connection between SMC and WTD exists due to the capillary zone, which acts to replenish surface moisture lost through evaporation and vegetation demands, from the WT (Wessolek et al., 2002). There have been studies which have disputed this relationship, finding a weak link between WTD and SMC (e.g. Parmentier et al., 2009), studies that find this relationship to be true only for certain periods (e.g. Price, 1997), and in some drained peatlands, research has shown this relationship may hold almost year-round (e.g. Wessolek et al., 2002).

The hydrological variable of key focus for the majority of studies on peat soils has been the water table depth (WTD), likely due to ease of measurement when compared to soil moisture content (SMC). As such, WTD is often used as a proxy to estimate near-surface moisture conditions (Tiemeyer et al., 2016). This practice

is problematic, however, because SMC is not a direct function of WTD (Kellner & Halldin, 2002), and there is evidence which suggests that when the WT gets below a certain depth, SMC and WTD are no longer connected by the capillary zone (Price, 1997). Among others, Parmentier et al. (2009) concluded that SMC has a low dependency on WTD, and the relationship between them is peatland specific as a result of contrasting soil physical properties. Furthermore, direct measurements of SMC, rather than the use of WTD as a proxy, better represent the influence of drought and wetness on processes such as CO_2 emission, subsidence, and plant well-being (Ritchie, 1998; Tiemeyer et al., 2016), highlighting the need for measurements of SMC in addition to WTD within drained agricultural peatlands.

2.4.3 Water table

The position of the water table (WT) lies where the hydrostatic pressure of water held within soil pores is equal to atmospheric pressure (Ingram, 1983). The depth of the WT can be expressed in one of two ways (Figure **2.1**): the WTD relative to the ground surface (relative water level, RWL); and the position of the WT above an absolute elevation datum (absolute water level, AWL), such as mean sea level (Fritz et al., 2008). It is important to define whether WTD has been measured as RWL or AWL; the difference between them is not negligible due to the influence of shrinkage processes affecting peatland surface elevation (described in Section 2.5).

The WT does not always define the upper boundary of the saturated zone, which instead is determined by the position of the capillary fringe (Ingram, 1983), only if there is one present. The capillary fringe is a volume immediately above, and connected to, the WT, where soil pores are saturated due to matric suction forces, despite having negative hydrostatic pressure (Ingram, 1983). The relative position of the WT and capillary zone can often have a degree of influence on near-surface moisture conditions, especially in peat soils, acting to redistribute moisture up the peat profile (Schwärzel et al., 2006). This is a process known as capillary rise.

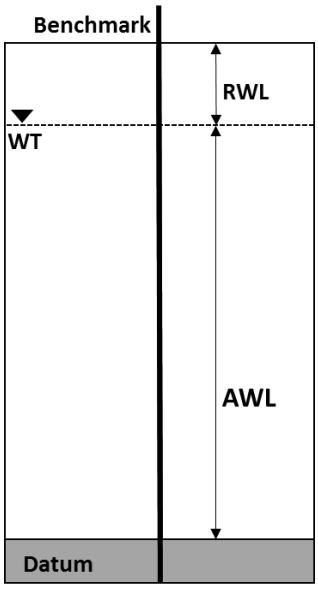

Figure 2.1 Diagram showing the two ways of expressing the position of the water table (WT); relative water level (RWL) and absolute water level (AWL). A benchmark, such as a steel rod anchored into the substratum, provides a stable datum for measurement of AWL. Adapted from Fritz et al. (2008).

Artificial drainage channels increase the temporal variation of WTD, as well as influencing the spatial pattern (Holden et al., 2006; Luscombe et al., 2016). As a result, WT dynamics in drained peatlands are characterised by significant spatial and temporal variation (Silins & Rothwell, 1999; Holden, 2005), making effective hydrological control for agricultural use or mitigation measures complicated (Lloyd, 2006).

2.4.4 Spatial variation

Considerable heterogeneity in soil properties over short distances, particularly hydraulic conductivity, strongly affects water movement within peat soils (Baden & Egglesmann, 1963), and consequently on the spatial pattern of WTD and SMC. Furthermore, the depth and spacing of drainage ditches will also influence spatial variation (Holden et al., 2006).

Considering a large spatial scale, mean WTD varies significantly between drained peatlands, likely driven by differences in climate and management, and confounded by site-specific properties. In an Indonesian drained peatland, Evans et al. (2019) measured mean WTD of 60 cm, which they found to be highly spatially variable. In the Netherlands, Schothorst (1977) found the mean WTD for one drained

peatland to be 64 cm, while another peatland that had been drained for a longer period was 15 cm. Tiemeyer et al. (2020) found the average WTD in drained peatlands across Germany to be between 43 cm and 60 cm, while various studies have found mean WTD to exceed 1 m (e.g. Leifeld et al., 2011).

On a smaller spatial scale, WTD and SMC will vary across a drained peatland. While Camporese et al. (2008) demonstrated that narrow drain spacings can result in a spatially uniform WT, this is not a common finding. More typically, the WT will be drawn down near drains (Sinclair et al., 2020) and closer to the surface over the paddock, with deeper drains resulting in greater WT drawdown and lower SMC. Spatially, WT drawdown has traditionally been assumed to be equal on either side of a drain, as a simple function of hydraulic conductivity and depth of the drain (e.g. Boelter, 1972). Due to the variability in soil properties, this assumption does not hold in reality for many peatlands (e.g. Rothwell et al., 1996; Silins & Rothwell, 1999). Such variation is evident when considering the optimum drain spacing for agricultural use, between peatlands. Burke (1967) demonstrated that the WT was only affected within 2 m of a drain, recommending a drain spacing of 4 m; Stewart and Lance (1983) concluded that effective drain spacing was 1 m; while McLay et al. (1992) found the WT to be affected within 50 m of drainage channels.

A lack of monitoring programmes to observe spatial variability of WTD and SMC has been noted by a number of authors (e.g. Holden et al., 2004; Luscombe et al., 2016), yet, other than attributing variability to soil physical or hydraulic characteristics, drainage design and describing greater WT drawdown near drains, the spatial controls remain largely unstudied.

2.4.5 Temporal variation

WTD and SMC regimes vary over time with respect to depth and proximity to drains (Petersen & Madsen, 1978). Fluctuations are greatest in areas close to drainage channels (Holden et al., 2011), and deeper drains (Luscombe et al., 2016). For example, Holden et al. (2011) observed a relatively uniform seasonal hydrological pattern across a drained peatland, but the degree of fluctuation varied between measurement points, depending on the location with respect to drains.

The degree of decomposition, along with seasonal changes associated with shrinkage will influence hydraulic properties and. correspondingly, hydrological dynamics over time. However, whilst variations in soil hydraulic properties appear to be the major influence on the spatial heterogeneity of WTD, both within and between drained peatlands, they do not vary over time to the same extent. Temporally, the water balance, $P - E$ has been suggested as the dominant control on fluctuations in WTD (e.g. Ingram, 1983; Parmentier et al., 2009). When $P - E$ is negative, precipitation inputs are exceeded by evaporative losses, a loss of stored water within the peat profile will occur; often manifesting as a drop in the WT. Summer periods frequently have a negative water balance, when there are warmer temperatures and higher solar irradiance driving evaporation, and less precipitation to recharge moisture. Correspondingly, dry conditions that cause maximum WTD and minimum SMC are observed, while in the winter the opposite is true (Holden et al., 2011).

At the beginning of summer when peat soils have high water content, the WT will drop in response to evaporation and plant water demands, however, there is a depth where the WT and capillary fringe become disconnected from the surface-atmosphere exchange (Price et al., 2003). Any further water demands will cause a change in SMC, rather than WTD (Price, 1997). The WTD at which this occurs depends on site-specific hydraulic properties and has been suggested to be 0.6 m, 0.7 m, or as deep as 1 m (Price, 1997; Wessolek et al., 2002; Price et al., 2003). At the end of a drought period, the relationship between SMC and WTD may be altered through soil cracking promoting preferential flow pathways and the effects of hydrophobicity. In this situation, infiltrated water will recharge the WT, rather than SMC (Schwärzel et al., 2002), causing hysteresis in the SMC/WTD relationship. Further hysteresis in this relationship can occur due to the seasonally variable pore size distribution as a result of peat shrinkage (Schlotzhauer & Price, 1999), causing emptying and filling of soil pores to occur at different potentials.

The effect of vegetation has also been suggested as a control on WTD and SMC (e.g. Stenberg et al., 2018), compounding the influence of the water balance. Different types of vegetation have varying water demands and rooting depth[2], so

[2] Peat is acidic in nature (Anshari et al., 2010), and so plant rooting depth and development can be inhibited.

the control of vegetation will vary between land uses (e.g. pastoral and arable agriculture). Furthermore, the influence of vegetation introduces diurnal variation in WTD, where a decrease in WTD occurs during the day and evening, but not during the night when plants are not photosynthesising (Holden et al., 2011).

2.5 Surface subsidence

Significant land surface elevation changes occur in drained peatlands. The gradual and non-reversible lowering of the peat surface over time, subsidence, is a major issue that begins immediately following drainage (Petersen & Madsen, 1978). Subsidence will continue through time until complete disappearance of the organic deposits or management practices are adopted that stop this process (Deverel et al., 2016). In addition to long-term subsidence, the surface elevation is variable over short time periods, due to shrinking and swelling processes resulting from changes in water content (Camporese et al., 2006). There are a number of undesirable environmental and economic consequences associated with subsidence, including increased infrastructure and management costs and an ongoing need to deepen drains (Pronger et al., 2014).

2.5.1 Processes contributing to subsidence

The processes that contribute to subsidence in drained peatlands are well known, and consist of three main volume change mechanisms, owing to the highly deformable nature of peat (Hobbs, 1986). These mechanisms are consolidation, oxidation and shrinkage (Zanello et al., 2011), each of which operates on different time scales.

Dewatering of surface peat due to peatland drainage causes an immediate loss of buoyancy, as the peat matrix is no longer supported by water held within pore spaces (Hooijer et al., 2012). Also, strain on the peat within the saturated zone is increased, and rapid consolidation through compaction ensues (Hooijer et al., 2012). Of the three subsidence processes, consolidation is the first to occur. It is an irreversible process that leads to an increase in peat bulk density (Motorin et al., 2018).

Biological oxidation of organic matter within peat is the dominant cause of long-term subsidence (e.g. Schothorst, 1977; Deverel & Leighton, 2010), where it has been suggested that between 35 to 100% of subsidence results from oxidation (e.g. Armentano & Menges, 1986; Couwenberg et al., 2010). The exposure of previously anoxic peat to oxygen initiates the rapid decomposition of organic matter, and carbon is irreversibly lost through the efflux of CO_2 to the atmosphere (Hooijer et al., 2012). Oxidation does not directly lead to an increase in bulk density (Hooijer et al., 2012), but it does cause a progressive increase in the mineral fraction of upper peat layers, which can be used to indicate the degree of decomposition (Drzymulska, 2016).

Shrinkage, often coupled with compaction, is a volume reduction process within the unsaturated zone, leading to increased bulk density (Hooijer et al., 2012). Shrinkage is the drying and contraction of organic fibres, while compaction is a result of surface loading such as heavy farm machinery or livestock (Hooijer et al., 2012). Separation of these two processes is difficult (Hooijer et al., 2012), and so for the purpose of this thesis, they will be hereafter referred to as shrinkage.

While consolidation and oxidation are irreversible mechanisms, the high porosity of the peat matrix has the capacity to shrink and swell in response to changing water contents (Ingram, 1983), causing oscillations in surface elevation (Strack et al., 2005) that may often be hysteretic in nature (Egglesmann, 1984). Oscillations have been measured in drained peatlands over time periods that range from hourly to seasonally (Egglesmann, 1984; Camporese et al., 2006; Hooijer et al., 2012), and with magnitudes of several centimetres (Morton & Heinemeyer, 2019). Surface elevation will typically be greatest in winter, but the largest changes in peat volume will occur early in summer when the peat is near saturation (Price & Schlotzhauer, 1999). Shrinking and swelling behaviour will bring about seasonal changes to hydraulic and physical properties, such as bulk density, hydraulic conductivity, and water retention (Price, 2003). Furthermore, as a consequence of variable surface elevation, the WT may reside closer to the peat surface in summer than it otherwise would (Price & Schlotzhauer, 1999).

2.5.2 Spatiotemporal variability of subsidence

The rate at which a peatland surface subsides and its spatiotemporal variability is dependent on a number of factors, such as thickness of the peat layer, peat type, peat decomposition rate, peat density, intensity of drainage, and climatic conditions (Egglesmann, 1976). As a result, subsidence rates vary significantly between drained peatlands on a global scale, ranging from a few millimetres to more than 10 cm yr^{-1} (e.g. Armentano, 1980; Armentano & Menges, 1986; Deverel et al., 2016; Berglund et al., 2019).

Following drainage, subsidence rates are initially rapid (Figure **2.2**), after which they stabilise and continue to decrease over time, but at a diminished rate (e.g. Armentano, 1980; Hooijer et al., 2012; Pronger et al., 2014). There is good agreement in the literature that peat consolidation is responsible for the initial rapid subsidence rates, and the succeeding long-term decline represents a shift to dominance of oxidation processes (e.g. Pronger et al., 2014).

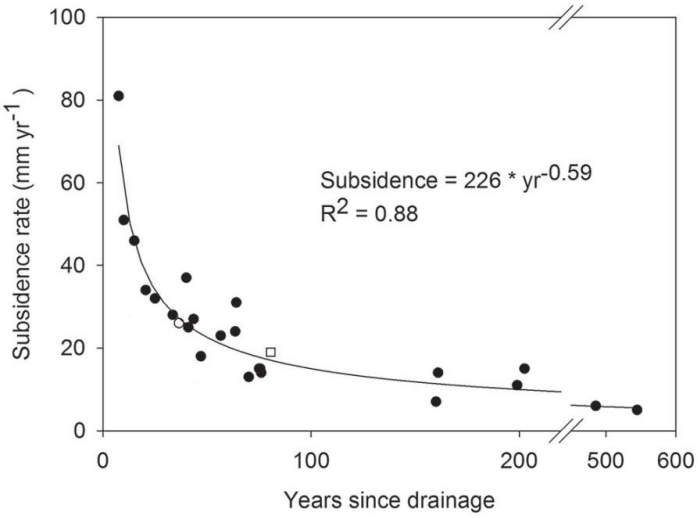

Figure 2.2 Relationship between subsidence rate and time since drainage with a line of best fit fitted to international data (closed circles). Average subsidence rates in the Waikato region as calculated in 2002 (open circle; 26 mm yr^{-1}) and 2012 (open square; 19 mm yr^{-1}) were overlaid onto the relationship. Adapted from Pronger et al. (2014).

Alongside temporal variation, subsidence is highly spatially heterogeneous (Leifeld et al., 2011; Ferré et al., 2019). In part, this is caused by drainage design (Wosten et al., 1997; van der Schaaf, 2012; Haapalehto et al., 2014). Subsidence will follow the shape of the WT between drains, leading to a parabolic soil surface with highest elevation halfway between drains, and lowest near the drains (Wosten et al., 1997).

Water table depth, directly influenced by the drainage depth, will further influence subsidence, where deeper drains will result in increased subsidence (Shih et al., 1998). The variability of peat physical properties will cause spatial differences in subsidence rates (Strack et al., 2005), and Dawson et al. (2010) suggested that subsidence may also be influenced by the geographical distribution of peat types and their underlying mineral deposits.

2.5.3 Management implications and mitigation

Subsidence complicates land management. Firstly, there is an ongoing need to deepen drains. If drain depths are kept constant while the surface is subsiding, the thickness of the unsaturated zone will reduce; leading to increasing soil moisture, which might constrain pasture or crop production, and limit stocking density of the land (Wosten et al., 1997). Therefore, drains must be periodically cleared and deepened, to ensure sufficiently low WTs for effective land use. This practice causes further subsidence, which requires even deeper drains and constitutes a drainage-subsidence cycle (Pronger et al., 2014).

In part due to ongoing drain maintenance, increased costs are a consequence of subsidence. In areas of low lying drained peatlands, such as in the Netherlands, pumped removal of excess water is essential (Holden et al., 2004). As the surface elevation approaches sea level, more and more water must be removed to maintain agricultural productivity, affecting the economic sustainability of farm enterprises. Subsidence impacts infrastructure, such as damage to building foundations and farm races, issues which have affected stakeholders for decades (Brouns et al., 2015).

Mitigation of subsidence and the associated implications can, according to the current state of knowledge, be achieved by maintaining higher WT depths (Ferré et al., 2019) which can be done by blocking drains, or implementing subsurface drains that irrigate in the summer and drain in the winter (Querner et al., 2012). Furthermore, changing land-use practices such as cultivation intensity (Kasimir-Klemedtsson et al., 1997) or limiting nutrient amendments (Hooijer et al., 2012) have also been shown to reduce subsidence rates. However, in doing so, massive challenges to intensive land use are introduced, and agriculture becomes much less

profitable on peat soils (Ferré et al., 2019); a major barrier towards improved environmental sustainability.

2.5.4 Measurement techniques

A range of techniques have been used to measure subsidence in drained peatlands, the nature of which has strongly depended on the scale of research. A large proportion of published subsidence work has focused on quantifying seasonal or annual scale subsidence rates (e.g. Pronger et al., 2014), usually on a regional basis. Other studies have concentrated on fine-scale short-term oscillations in surface elevation (e.g. Zanello et al., 2011), which are typically focused on shrinking/swelling phenomena rather than oxidation processes. Subsidence data have also been used to calibrate and validate subsidence models (e.g. Camporese et al., 2006), which can range between peatland specific and national scales.

Schipper and McLeod (2002) sampled a number of cores from a pristine peatland and adjacent drained land in Waikato region, Aotearoa New Zealand, to calculate total subsidence since drainage, average annual subsidence rates and carbon loss. They did this by comparing the distance and peat carbon content between the surface and a reference tephra layer (Taupo Tephra) between the pristine and drained peatlands, obtaining estimates of average annual subsidence and total subsidence over 40 years (Schipper & McLeod, 2002). The average subsidence rate of 3.4 cm yr^{-1} was generally higher than rates elsewhere in the world, which they attributed to the short time since drainage. A different method was used in the same region by Pronger et al. (2014), where they quantified historic (1920 – 2000) and contemporary (2000 – 2012) subsidence rates by comparing peat depth surveys taken in 1920, 2000, and 2012. They determined historic and contemporary subsidence to be 2.6 cm yr^{-1} and 1.9 cm yr^{-1}, respectively; two different rates which are indicative of the temporal relationship shown in Figure **2.2**.

In the Netherlands, Brouns et al. (2015) generated soil subsidence maps by modelling spatially-explicit soil, land use, ditch water level and ground level information; with a model based on measured long-term subsidence data. A number of factors were used to determine annual subsidence rates, such as peat thickness and relative height of ditches. They estimated annual subsidence rates to be 3 cm

yr^{-1}, aligning well with values from the international literature. Furthermore, a shift from intensive to extensive agriculture and higher ditch water levels acted to reduce subsidence rates whilst maintaining the economic feasibility of land use.

Camporese et al. (2006) continuously measured ground surface displacement with an extensometer in the Zennare Basin, Italy. The experimental set up included three displacement transducers connected to an aluminium plate resting on the soil surface at one end, and to a steel tripod at the other, which had piles anchored to the underlying substrate (Camporese et al., 2006). Considerable oscillations upwards of around 10 mm in peat surface elevation were measured in response to drying and wetting cycles. Swelling of the peat matrix was seen to occur rapidly following a rainfall event, while shrinkage was a slower process, taking place over time scales between hours and weeks.

In a pristine Aotearoa New Zealand peatland, Fritz et al. (2008) measured fine-scale changes in peat surface elevation. Along with monthly manual measurements of two dipwell transects, a paired water-level transducer set up was implemented. One transducer was attached to the peat surface (free to move) and the other was attached to a steel rod anchored into the substratum (fixed), whereby differences between recorded water levels of the two transducers were caused by oscillations in peat surface elevation (Fritz et al., 2008).

2.6 The carbon balance of drained peatlands

2.6.1 Definition of terms

The net ecosystem carbon balance (NECB) describes the overall rate of carbon loss from, or accumulation within, an ecosystem (Chapin et al., 2006). Indicative of whether the ecosystem is functioning as a source or sink of carbon, the NECB considers all carbon removal and addition pathways (Chapin et al., 2006), including supplementary feed or the harvesting of crops in agricultural systems. In drained peatlands, studies of carbon dynamics are generally more concerned with the net ecosystem exchange (NEE), as NEE represents the most variable and largest component of interannual carbon budgets (e.g. Roulet et al., 2007). NEE represents

the net efflux or sink of CO_2 between an ecosystem and the atmosphere[3] and excludes pathways such as dissolved organic carbon (Baldocchi, 2003). NEE expresses the balance between gross primary production (GPP) and ecosystem respiration (ER), as described by Equation (2-3) (Chapin et al., 2006).

$$-\mathrm{NEE} = \mathrm{GPP} - \mathrm{ER} \tag{2-3}$$

GPP describes the assimilation of CO_2 by autotrophs, while ER is a loss of carbon as CO_2 through the respiratory processes of autotrophs (above and below ground) and heterotrophs; all of which are represented in Figure **2.3**. For drained peat, ER includes respiration from plants, newly formed plant-derived organic matter, as well as oxidation of peat (Berglund & Berglund, 2011); the latter being most relevant for CO_2 studies of these ecosystems. Peat oxidation causing rates of ER to surpass that of GPP has meant that on an annual basis drained agricultural peatlands typically have an annual net loss of CO_2 to the atmosphere (Maljanen et al., 2010).

Net primary production (NPP) is the uptake of carbon through photosynthesis, excluding that which has been lost through autotrophic respiration (Chapin et al., 2006). Like NEE, net ecosystem production (NEP) is expressed as the balance between GPP and ER, although with opposite sign convention[4]. NEE and NEP are often used interchangeably, their use depending on the study focus within the carbon cycle.

The production of CO_2 within soils (soil respiration, SR) is predominantly attributed to the microbial decomposition of organic matter (heterotrophic respiration, HR), and root respiration (belowground autotrophic respiration, AR_b). Wessolek et al. (2002) concluded that within peat, HR of organic matter far outweighs the contribution of AR_a and AR_b to ER, and HR is hence the variable of most interest to studies on drained peatlands.

[3] NEE follows the atmospheric sign convention, where a positive value represents a net loss of carbon from an ecosystem to the atmosphere (Chapin et al., 2006).
[4] NEP is defined from an ecosystem perspective, rather than an atmospheric one (Chapin et al., 2006).

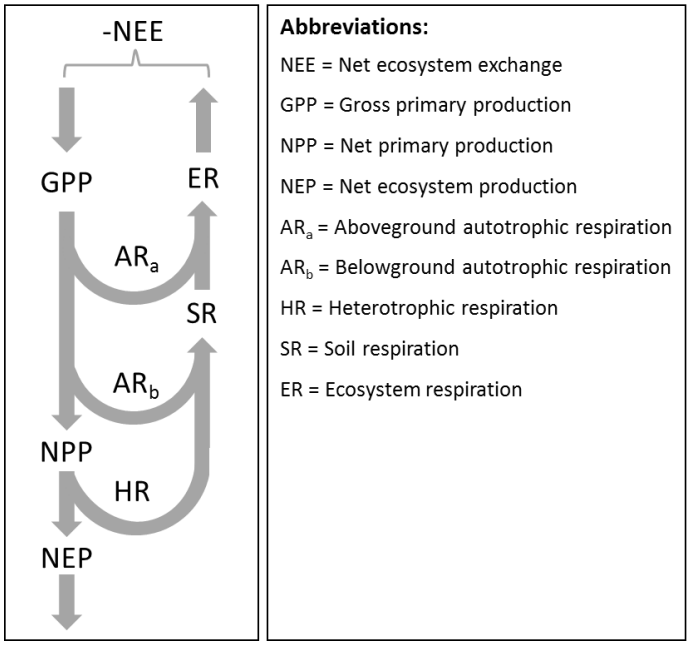

Figure 2.3 Summary of terms used to describe components of the carbon balance related to NEE. Adapted from Luyssaert et al. (2007).

2.6.2 CO_2 production in peat soils

In peat soils, the production of CO_2 is contingent on a number of factors, including: the depth of the water table or near-surface moisture conditions (Mäkiranta et al., 2009; Carlson et al., 2015); soil properties (Minkkinen et al., 2007); management practices (Maljanen et al., 2003); and, like all chemical and biochemical reactions, temperature (Davidson & Janssens, 2006). The controls do not affect ER in isolation, and there are instead multiple complex interactions between them (Laiho, 2006; Tiemeyer et al., 2016), which makes it difficult to disentangle the individual effects of each control (Säurich et al., 2019a). As a result, considerable spatial and temporal variation exists in the efflux of CO_2 between and within drained peatlands (Camporese et al., 2008).

2.6.2.1 Soil water

Soil heterotrophic respiration is subject to water limitations (Davidson & Janssens, 2006), and at low soil moisture contents, plant growth and microbial activity are constrained (Gaumont-Guay et al., 2006). Conversely, when a soil is too wet, gas diffusion is restricted, limiting oxygen availability for respiration (Gaumont-Guay et al., 2006), and so an optimal range of moisture conditions exists.

In drained peatlands, the depth of the water table is considered the dominant factor controlling the production and efflux of CO_2 (e.g. Berglund & Berglund, 2011; Carlson et al., 2015). Many field and laboratory studies have shown that as depth to the water table increases, so too will CO_2 emission (Couwenberg, 2011), as a greater volume of peat is exposed to oxygen, allowing increased oxidation. Furthermore, dry conditions limit plant growth, decreasing GPP relative to ER. For example, Renger et al. (2002) measured a decrease in crop production, while CO_2 emissions doubled when the WT was adjusted from 30 cm to 80 cm. In contrast, Berglund and Berglund (2011) measured a decrease in CO_2 emissions by changing the WTD from 40 cm to 80 cm, and without reference to a depth, concluded that an intermediate WTD was required for optimum plant growth. Mäkiranta et al. (2009) found the relationship between WTD and CO_2 efflux to follow a bell-shaped curve, with maximum emissions occurring at a WTD of 60 cm. Similarly, Säurich et al. (2019a) found a bell-shaped curve, instead measuring WFPS, where maximum CO_2 efflux rate was observed between 0.77 and 0.88 (Figure **2.4**). There are also some studies which have demonstrated a poor correlation between WTD and CO_2 (e.g. Maljanen et al., 2001).

In addition to the large variation in peat soil properties, a lack of response of CO_2 production to changes in WTD can be caused by a disconnection of surface peat and the water table (Marwanto et al., 2019), meaning that SMC or WFPS is a more representative measurement. Norberg et al. (2018) found that the SMC in surface peat is often less than what is indicated by the WTD, and Candra et al. (2016) demonstrated that the relationship between SMC and SR had a stronger correlation than the relationship between WTD and SR.

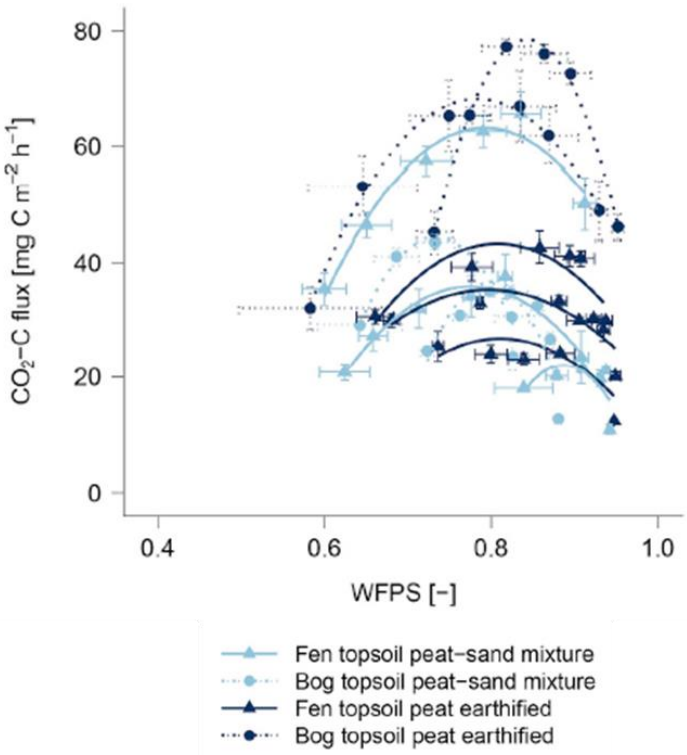

Figure 2.4 Carbon dioxide (CO2) fluxes and water-filled pore space (WFPS) in various peat topsoil samples. Curves represent fitted quadratic polynomial functions. Adapted from Säurich et al. (2019a).

2.6.2.2 Temperature

A positive correlation between SR and temperature exists, and a relatively small rise in soil temperature can considerably increase respiration rates (Lloyd & Taylor, 1994; Fang & Moncrieff, 2001). In a drained peatland, Berglund and Berglund (2011) emphasised the importance of temperature after measuring CO_2 efflux rates in the growing season that were up to eight times greater than in the winter. Minkkinen et al. (2007) found that 53 – 74% of temporal variation in CO_2 emissions could be explained by soil temperature at a 5 cm depth.

Temperature and soil water status are linked, where a higher moisture content can dampen the effects of temperature on CO_2 production (Oechel et al., 1998), and when temperatures are higher, CO_2 production is influenced more by soil moisture (Wessolek et al., 2002). Soil water, or as a proxy, WTD, is predominantly considered the main driving variable of CO_2 production in peat soils, however, most studies accept that increased peat temperatures lead to higher CO_2 emissions (e.g. Waddington et al., 1998). Despite this, some research has shown that soil temperature is the main driving variable of CO_2 emissions from peat soils

(Mäkiranta et al., 2009). Discrepancies between studies are likely due to the high variability of peat properties.

2.6.2.3 Soil properties and farm management

While WTD or SMC and temperature are considered the dominant controls on NEE, there are other factors which control CO_2 emissions to some degree. Soil chemical properties, such as nutrient status, is one example (Berglund & Berglund, 2011). Soil organic compounds are the energy substrate for microorganisms involved in peat decomposition (Waddington & Price, 2000) and, accordingly, the availability and quality of carbon in soil drives microbial activity. Peatlands with a higher degree of decomposition are characterised by a lower organic fraction (Drzymulska, 2016), and so nutrient status can be influenced by drainage history. Furthermore, substrate quality will vary with depth, and it has been argued that the upper part of the peat profile produces the most CO_2 (Waddington et al., 2001; Berglund & Berglund, 2011). Berglund and Berglund (2011) measured more CO_2 from a topsoil than a subsoil with a lower carbon availability; suggesting soil with more decomposed organic matter may emit greater CO_2, which Regina et al. (2004) and Säurich et al. (2019b) also found. Along with SR, nutrient status affects GPP, whereby greater plant production will occur when essential nutrients are not a limiting factor.

In soil, the availability of inorganic nutrients, such as nitrogen and phosphorus, will affect carbon assimilation and mineralisation (Swift et al., 1979). Farm management practices, such as fertilisation, can alter the availability of nutrients in the topsoil, and therefore the production of CO_2 (Säurich et al., 2019a). Multiple studies have shown an increase in SR following nutrient amendments of potassium, nitrogen and phosphorus (e.g. Larmola et al., 2013; Pinsonneault et al., 2016), while others have found fertilisation has a weak effect on CO_2 (e.g. Tiemeyer et al., 2016). Peat soils are acidic in nature, and the addition of lime to amend soil pH will generate more favourable conditions for plant growth and microbial decomposition, increasing CO_2 production (Fuentes et al., 2006). Soil disturbance, through ploughing or compaction from livestock, alters the diffusion and transport of oxygen within the soil, subsequently influencing SR (Maljanen et al., 2010). Furthermore, grazing cycles for pastoral peatlands can affect NEE, whereby

Campbell et al. (2015) measured greater CO_2 emissions directly following grazing events, which they attributed to reduced GPP rather than increased ER.

2.6.3 CO_2 studies on drained peatlands

The measurement of CO_2 fluxes between drained peatlands and the atmosphere can be challenging (Couwenberg, 2011). Methodologies used to measure these fluxes has included direct and indirect techniques, as well as estimating their response to driving variables through modelling. The majority of direct CO_2 measurements have been sampled using the chamber technique (Rowson et al., 2010; Berglund & Berglund, 2011; Karki et al., 2016; Tiemeyer et al., 2016). For example, Tiemeyer et al. (2016) synthesised a large dataset from 48 sites on 12 drained peatlands under pasture across Germany, where CO_2 fluxes were measured using identical methodology at each site. A combination of opaque and dark chambers were used to measure ER and NEE, respectively, over a series of biweekly or monthly field campaigns; from which they derived GPP (Tiemeyer et al., 2016). They found CO_2 emissions to increase with deeper mean WTD until a depth of approximately 40 cm, but large variation between sites resulted in considerable scatter in the data, illustrated in Figure **2.5**.

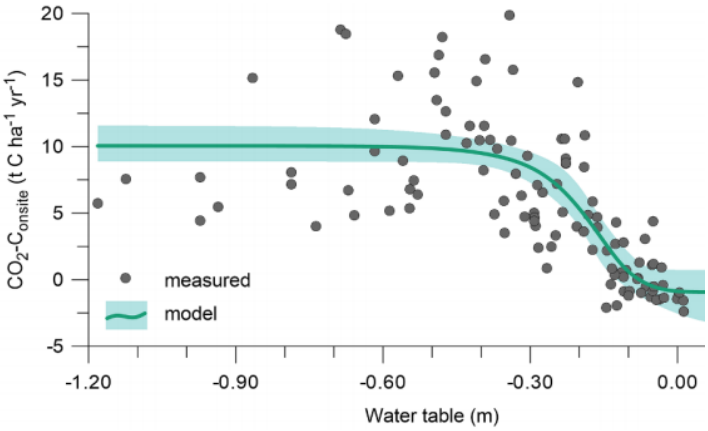

Figure 2.5 Response of CO_2 emissions from peat and organic soils in Germany to mean annual water table depth. Adapted from Tiemeyer et al. (2020).

The eddy covariance (EC) technique[5] has been utilised to a much lesser degree for measuring CO_2 emissions in drained peatlands, despite its ability to spatially

[5] The EC technique is reviewed in Section 2.7.

integrate fluxes over large areas (e.g. Baldocchi & Meyers, 1988), and subsequent capacity to account for the high degree of spatial variability. A review published by Maljanen et al. (2010) found that only two studies out of over 50 reviewed used the EC technique, which by 2015 had increased to 6 (Campbell et al., 2015). In Aotearoa New Zealand, Campbell et al. (2015) measured CO_2 fluxes from two sites on a drained agricultural peatland, using two EC towers (one permanent, one mobile) to evaluate the spatial variation of NEE. EC data were processed, quality checked and subsequently gap filled (see Section 2.6.2), to ensure representative flux measurements; and when compared to five EC CO_2 flux studies published in international literature, net CO_2 losses were consistent (Campbell et al., 2015). They found that when WTDs were lower, CO_2 emissions were increased due to a decrease in GPP rather than increasing ER. Furthermore, CO_2 emissions were strongly affected by grazing cycles.

Indirect quantification of CO_2 emissions relies on subsidence rates, and more specifically the relative contribution of oxidation processes to ongoing subsidence (Kasimir-Klemedtsson et al., 1997). This technique is not as accurate as direct measurements, because the oxidative component of subsidence can vary between a few percent and 100% (Armentano & Menges, 1986), and care must be taken to ensure that primary consolidation is not included in CO_2 efflux estimates (Kasimir-Klemedtsson et al., 1997). Furthermore, spatial and temporal variation cannot be quantified. Using this methodology, drained peatlands in the Netherlands were studied by Erkens et al. (2016), to estimate total CO_2 emitted between 1000 and 2005 AD. Figure **2.6** illustrates a simplified version of their methodology. The key component of this technique is the separation of subsidence into oxidation, which produces CO_2, and consolidation, which does not produce CO_2. In this study, they compared the bulk density between pristine and drained peat samples, to determine the average contribution of consolidation to subsidence; estimated to be 28% (Erkens et al., 2016). From the 72% volume change caused by oxidation, organic matter density was calculated, and peat carbon losses were converted to CO_2 emissions.

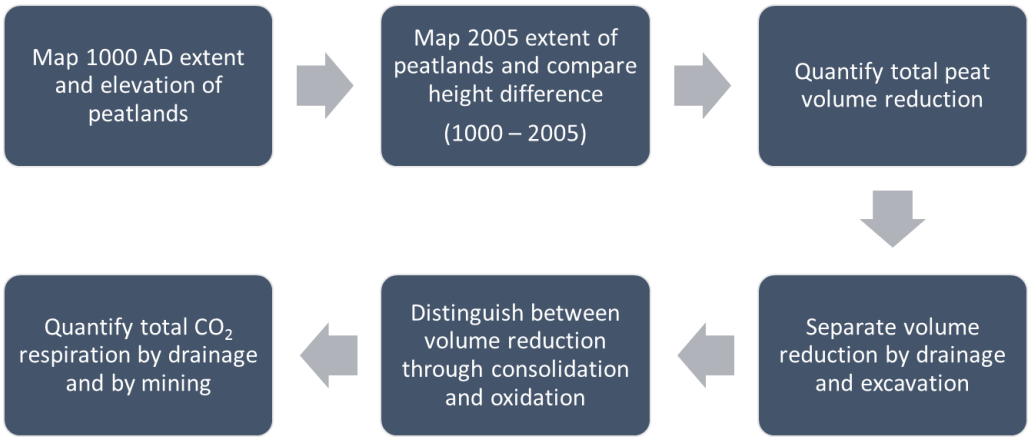

Figure 2.6 Flow chart depicting the process of quantifying CO_2 respiration through subsidence. Adapted from Erkens et al. (2016).

Modelling CO_2 efflux in response to environmental driver variables, such as WTD, is another technique used in GHG emission accounting (e.g. Warner, 1999; Wessolek et al., 2002), which must be calibrated with measured data. Wessolek et al. (2002) developed a simple model to predict CO_2 release from drained peatlands, as a function of climate and WTD. The model was calibrated using data derived from lab experiments of soil cores prepared with varying water contents, as well as long-term field data of chamber measured CO_2 release and associated soil hydrology (Wessolek et al., 2002). To obtain a function of CO_2 release, multiple non-linear regression analyses were carried out; to which Wessolek et al. (2002) concluded the simulation model accurately predicted CO_2 emissions for various soils, moisture conditions, and climates. In contrast, Tiemeyer et al. (2016) found it impossible to model CO_2 exclusively as a function of WTD across 12 drained peatlands, highlighting the heterogeneous nature of peat soils and their properties.

2.6.4 IPCC emissions inventory

Countries that have ratified the United Nations Framework Convention on Climate Change (UNFCCC) are committed to reporting national anthropogenic GHG emissions (Intergovernmental Panel on Climate Change, IPCC, 2014). The 2006 IPCC Guidelines detail methodologies for estimation of national GHG inventories, based on three tiers. Tier 1 outlines default emission factors (EF) to be used with the IPCC equation, Equation (2-4); where A is the activity data, representing the area of drained peat under a given land use.

$$\mathrm{CO_2\ emission} = A \times EF \quad (2\text{-}4)$$

Tier 2 incorporates country-specific data and can include subcategories such as time since drainage and classification of the management system. Tier 3 allows emission estimates to be further refined, where modelling may be used for developing relationships with variables that drive emissions, or the simulation of temporal variation in water table depths (IPCC, 2014).

Since 2006, considerable scientific advances have been made with regards to organic soils; leading to the publication of the 2013 Wetlands Supplement (IPCC, 2014). The Wetlands Supplement provides an improvement on the estimation of GHG emissions for several managed[6] wetland categories, such as drained inland organic soils, within which various land-uses were defined. In addition to land-use, Tier 1 EFs (Table **2.1**) are specific to climate and vegetation zones, nutrient status, and drainage depth, indicating a significantly updated framework (IPCC, 2014).

Table 2.1 Summary of Tier 1 CO_2 emission factors (EF) and 95% confidence intervals for grasslands within the 2013 Wetlands Supplement for drained inland organic soils. Adapted from IPCC (2014).

Land-Use	**Climate/ Vegetation zone**	**EF (tonnes CO_2-C ha^{-1} yr^{-1})**	**95% Confidence interval**	
Grassland, drained	Boreal	5.7	2.9	8.6
Grassland, drained	Tropical	9.6	4.5	17.0
Grassland, drained, nutrient-poor	Temperate	5.3	3.7	6.9
Grassland, shallow-drained, nutrient-rich	Temperate	3.6	1.8	5.4
Grassland, deep-drained, nutrient-rich	Temperate	6.1	5.0	7.3

Although Tier 1 IPCC EFs for CO_2 have been derived from internationally published subsidence and flux data, there is considerable uncertainty surrounding

[6] Subject to human activities (IPCC, 2014).

accuracy (e.g. Couwenberg, 2011; Tiemeyer et al., 2016), highlighted by the 95% confidence intervals. For accurate emission accounting, there is a need to develop country-specific EFs following IPCC Tier 2 and 3 methodologies. This has been done in Germany by Tiemeyer et al. (2020).

2.7 Eddy covariance measurements of water and carbon fluxes

Fluxes of water vapour and carbon (CO_2, CH_4) between terrestrial ecosystems and the atmosphere can be directly quantified using the eddy covariance (EC) approach. The EC technique works by applying micrometeorological theory to the covariance between vertical wind velocity, measured with a sonic anemometer, and fluctuations in scalar concentrations, measured with infrared gas analysers (Baldocchi, 2003). These data are typically measured at a high sampling frequency (10-20 Hz), and calculated for half-hourly periods using Reynolds decomposition (Burba, 2013), resulting in flux data that can range from hours to years (Baldocchi, 2008). The area sampled, known as the flux footprint, has a spatial coverage of paddock to ecosystem scales, which is dependent on the height of the EC sensors (Baldocchi, 2008). These features allow measurements to take into account the high spatial and temporal variability of drained peatlands.

2.7.1 Uncertainties associated with flux measurements

Owing to the complexity of the EC technique, flux measurement, data processing and gap-filling practices can produce errors, constraining accuracy (Baldocchi, 2008).

A number of EC site requirements must be satisfied to ensure accurate flux measurement. These include; sensors that are able to capture the smallest and fastest eddies, flat and uniform terrain, extended and homogenous vegetation upwind of the EC tower, and steady atmospheric conditions (Baldocchi, 2008; Burba, 2013). In the absence of ideal conditions, such as when the sensors are wet or the wind is coming from an undesirable direction, measurements are removed through a quality control process (Baldocchi, 2003). The rejection of data introduces gaps to the dataset, giving an annual flux coverage that typically ranges between 65-75% (Falge et al., 2001).

Repeatable annual flux sums can be produced with data gaps surpassing 40% (Falge et al., 2001), but there is a need to fill these gaps when considering shorter timescales. Gap filling approaches vary in complexity, from interpolating between missing data points, appropriate for short gaps, to the use of artificial neural networks (Baldocchi, 2008). Statistical analyses are used to ensure the overall accuracy of gap filling, such as comparing multiple gap-filling runs (e.g. Campbell et al., 2015).

The friction velocity (u^*) correction is the most controversial gap-filling correction made to EC data (Baldocchi, 2008). When turbulence is low, such as when thermal stratification becomes stable at night, CO_2 may drain out of the measured air volume without being recorded by the EC sensors (Baldocchi, 2008). To prevent the underestimation of fluxes, particularly ecosystem respiration (ER), data are rejected during these periods when the u^*, or standard deviation of vertical wind speed, is below a site-specific threshold (Baldocchi, 2003). Determining the critical threshold value is controversial, and is more straightforward at some sites than others (Loescher et al., 2006). To limit uncertainty in the choice of threshold, sensitivity evaluation to various u^* thresholds can be carried out (Loescher et al., 2006).

The EC approach produces a direct measure of net CO_2 exchange between an ecosystem and the atmosphere (NEE), but is unable to distinguish between its subcomponents of carbon gain through GPP, and carbon loss through ER (Baldocchi, 2003). Methods exist to partition NEE into GPP and ER, although results are subject to potential bias due to assumptions made within these procedures (Oikawa et al., 2017). Most partitioning approaches make use of the hypothesis that daytime ER mirrors the same temperature response that night-time ER does (Wehr et al., 2016). Photosynthesis cannot occur without light, and so measurements of night-time NEE are assumed to be equal to night-time ER, allowing daytime ER and therefore GPP to be estimated. Partitioning techniques that make these assumptions have been found to overestimate GPP and ER, by up to 10% in some cases, as they ignore the presence of the Kok effect, which is the inhibition of leaf respiration by light (Oikawa et al., 2017). More recently developed methodologies, such as isotopic partitioning, have been shown to be more accurate

(e.g. Wehr et al., 2016; Oikawa et al., 2017), however, wide adoption has not yet occurred due to limitations with measurement cost and ease of use.

A long-standing issue and source of uncertainty in micrometeorology is the lack of energy balance closure, caused by a tendency to underestimate latent and sensible heat fluxes (Kutikoff et al., 2019). The approach is a formulation of the first law of thermodynamics; where the sum of measured latent and sensible heat fluxes must be equal to all other energy sinks and sources (Wilson et al., 2002). The magnitude of the lack of closure is frequently used as an indicator for the accuracy and reliability of EC flux data, based on the assumption that other fluxes may have been inaccurately measured if there is an inability to close the energy balance (Leuning et al., 2012). A few studies have been able to close the energy balance within reasonable limits (e.g. Lamaud et al., 2001; Jacobs et al., 2008). However, these successes are rare, with typical underestimation of surface energy fluxes being between 10-30% (e.g. Wilson et al., 2002; Grachev et al., 2020).

Reasons suggested for the lack of closure includes, but is not limited to; instrument measurement uncertainty; low-frequency mesoscale transport; spatial sampling scale differences (e.g. between EC fluxes and soil heat flux plates); and data processing inaccuracies (Leuning et al., 2012). Closure can be substantially improved if careful attention is paid to all sources of measurement and data processing errors, as well as an accurate determination of all components of available energy (Leuning et al., 2012). Furthermore, Grachev et al. (2020) recommended that by increasing the averaging time to longer intervals such as daily, monthly or sub annually, surface energy imbalance can be substantially reduced; giving more confidence to flux measurements.

2.8 Peatlands in Aotearoa New Zealand

Peatlands in Aotearoa New Zealand are compositionally different from those in the Northern Hemisphere, being characterised by primary peat formers from the Restionaceae family, which are endemic to NZ (Clarkson et al., 1999). Making NZ peatlands as equally unique, especially in the Waikato Region, is the ability to sustain peat accumulation despite the warm, dry summers and negative annual

water balances, whereas typically peatland formation requires considerable rainfall, and moist, cool summer conditions (McGlone, 2009).

Despite the factors that separate NZ peat from elsewhere in the world, drained peatlands have not received the same degree of interest in NZ as in tropical and high latitude areas. In part, this can be attributed to a comparatively small distribution of peatlands, containing only 0.05% of the world's peat deposits, and a short drainage history compared to European countries (Davoren, 1978).

Previous research on drained peat in Aotearoa New Zealand has aimed to quantify; the effect of drainage of physical soil properties (McLay et al., 1992); annual irreversible subsidence rates and associated carbon loss (Schipper & McLeod, 2002; Pronger et al., 2014); nitrous oxide emissions (Kelliher et al., 2016); and the annual CO_2 exchange (Nieveen et al., 2005; Campbell et al., 2015). To date, there has been no published work on spatiotemporal variability of hydrology, its controls, nor has there been any on the short-term reversible surface oscillations in Aotearoa New Zealand drained peatlands. A hydrological understanding is particularly crucial for drained peatlands in NZ, because, as established in this literature review, a myriad of processes and properties are affected and controlled by hydrology.

Chapter 3

Site description and general methods

Moanatuatua (37°55.50′S, 175°22.20′E) is an ombrotrophic peat bog, located approximately halfway between Cambridge and Te Awamutu in the Waikato region of Te Ika-a-Māui (North Island) of Aotearoa New Zealand (Figure **3.1**). Once extending over an estimated 75,000 ha of land (Clarkson et al., 2004), Moanatuatua has been subject to extensive drainage and development that began in the 1930s (Cranwell, 1939). Since then, Moanatuatua wetland has been reduced in size by more than 98%, most of which was done before 1974 (Ratcliffe et al., 2019). The drained land, termed Moanatuatua drained peatland, is predominantly under pasture for dairy grazing (Campbell et al., 2015), with some blueberry orchards. This area experiences annual mean temperatures of 13.8ºC and rainfall of 1167 mm (NIWA, 2017).

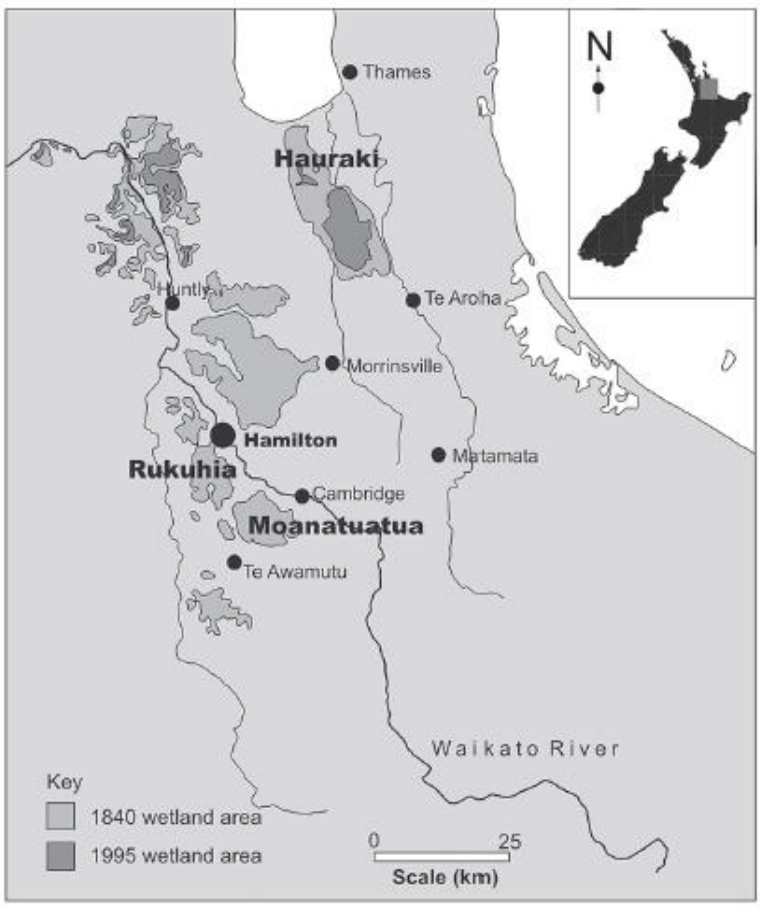

Figure 3.1 Peatland distribution in the Waikato Region, Aotearoa New Zealand, showing historic (1840) and recent (1995) wetland extent. Adapted from Pronger et al. (2014).

For this study, two research sites were established on adjacent farms on Moanatuatua drained peatland, with peat depths that ranged between 5 m and 7 m (Table **3.1**). The sites, comprising two experimental paddocks within each farm, were selected based on having similar grazing management practices but different drainage designs (Figure **3.2**). Gamma Farm, Site 1, had 'hump and hollow' drainage, with shallow drains (0.3 m width, 0.3 m height) spaced approximately every 30 m within each paddock and a deep drain (0.7 m width, 0.6 m height) either end of the transect. Moanaleas Farm, Site 2, had border ditch style drainage, with deep drains (0.8 m width, 1 m height) surrounding each paddock. Site 2 previously had hump and hollow drainage but was recontoured in October 2016 to its current design. The drainage history between sites differs. Site 1 was drained approximately between 1974 and 1979, while Site 2 was between 1974 and 1979 (Table 3.1). Approximate drainage dates were derived by stitching together photographs from the Crown Aerial Film Negative Collection and visually tracking through time when segments of Moanatuatua peatland were drained (H. Óskarsson, personal communication, January 21, 2020).

Table 3.1 Geographic coordinates and approximate peat depths and drainage date of the two sites within Moanatuatua drained peatland.

	Latitude	**Longitude**	**Peat depth**	**Approximate drainage date**
Site 1	37°57.267′S	175°23.123′E	7 m	1975
Site 2	37°58.454′S	175°24.204′E	5 m	1960

At each site, a single transect line extending across two adjacent paddocks centred on eddy covariance (EC) instruments was established in early 2019, to measure the hydrological regime (Figure **3.2**). Transects, composed of several dipwells, lay perpendicular to the drainage channels, to allow for measurement of the spatial variation in water table depth (WTD). The transect at Site 1 was 240 m in length and contained 20 dipwells, while Site 2 had a 190 m long transect with 10 dipwells.

The dipwells each consisted of a 2 m length of slotted closed-bottom polyvinyl-chloride (PVC) tubes, encased in a geotextile filter to prevent peat from entering the tube. Dipwells were inserted vertically into the peat, and their tops were recessed 10 cm below the peat surface. A small volume of peat was removed around the top of each dipwell to facilitate measurement. A removable wooden board at

peat surface level covered each dipwell to prevent livestock or machinery from affecting dipwell position. At monthly intervals, depth to the water table was measured manually along each transect. Initially, this was done with a well depth indicator probe (KLL Electric Contact Meter, SEBA Hydrometrie, Kaufbeuren, Germany), and then a home-made 'bubbler' (plastic tube with a depth scale). In four dipwells across each transect, WTD was additionally measured at 30-minute intervals with pressure transducers (INW LevelSCOUT, Seametrics, Kent, WA, USA).

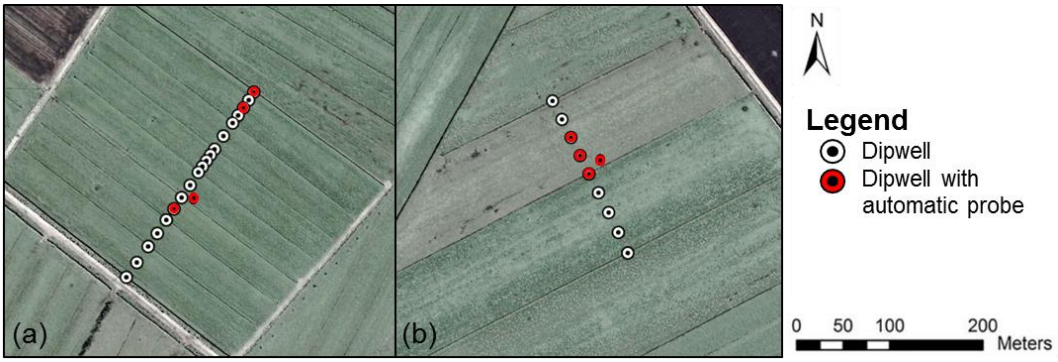

Figure 3.2 Overview of (a) Site 1 and (b) Site 2, illustrating dipwell locations along each transect, as well as the four dipwells with automatic water level probes. Aerial images sourced from Google Earth (2019).

Soil cores with diameter 65 mm and length 50 mm were sampled monthly at various locations along the transects, using a modified cylindrical stainless steel corer. For each sampling event, four cores were collected, at depths between 25 mm and 75 mm. Soil volumetric moisture content (VMC) and bulk density were determined by oven-drying at 105ºC for 72 hours.

EC systems and ancillary instrumentation were established on 28 May 2018 at Site 1 and 14 September 2018 at Site 2. Water vapour and CO_2 flux data collection and processing are described in Chapter 4. Datasets common to Chapters 4 and 5 are as follows. Automatic measurements of VMC were taken from four three-wire time domain reflectometry (TDR) probes (ML3 ThetaProbe, Delta-T Devices, Cambridge, UK) at each EC site; three of which were at 100 mm depth and one at 50 mm depth. The TDR probes had site-specific calibrations applied from laboratory measurements following Delta-T Devices Ltd (2017) specific to organic soils. Soil temperatures were measured with averaging thermocouples (TCAV, Campbell Scientific Inc., Logan, UT, USA); two sets of probes across 20 – 60 mm

(40 mm), as well as at 200 mm depth. At each site, a tipping bucket rain gauge (TR-525M, Texas Electronics, Dallas, TX, USA) recorded rainfall in 0.1 mm increments. All instruments were connected to a datalogger (CR1000X, CSI) with a multiplier (AM16/32B, CSI), and sampled at 10-second intervals before being averaged or totalised over 30 minutes.

Chapter 4

Controls on hydrology and CO_2 emissions from a drained agricultural peatland

4.1 Introduction

The hydrological regime of drained peatlands influences and controls a myriad of processes and properties, including soil physical and hydraulic characteristics (McLay et al., 1992; Price, 1997; Holden et al., 2004), subsidence (Egglesmann, 1976; Schwärzel et al., 2006) and biogeochemical processes such as the emission of carbon dioxide (CO_2; Mäkiranta et al., 2009; Dettmann et al., 2014; Carlson et al., 2015). Effective control of water table depth (relative water level, RWL) and soil volumetric moisture content (VMC) have often been suggested as mitigations for adverse environmental effects (Regina et al., 2014) and to ensure productive agricultural use (Norberg et al., 2018). To do so, a sound understanding of the hydrological regime is required, with respect to both spatiotemporal variability and the factors which drive such variation (Schwärzel et al., 2006; Mustamo et al., 2016). Furthermore, because RWL is commonly used as a proxy to estimate near-surface moisture conditions (e.g. Renger et al., 2002; Berglund & Berglund, 2011), yet there remains a lack of clear consensus in published literature regarding the nature of the relationship between these variables (e.g. Price, 1997; Wessolek et al., 2002; Parmentier et al., 2009), it is vital to understand the connection between RWL and VMC.

In a drained peatland in the Waikato Region, the hydrological regime, peat physical properties, along with water vapour (H_2O) and CO_2 fluxes were measured at two sites for a one year period. The objectives were to quantify the nature of, and controls on, the spatiotemporal variability of RWL and VMC, the relationship between RWL and VMC, and establish the influence of these two variables on CO_2 emissions.

4.2 Methods

4.2.1 Eddy covariance

To measure paddock-scale H_2O and CO_2 fluxes, each EC tower (Figure **4.1**) included a 3D sonic anemometer and open path infra-red gas analyser, details are listed in Table **4.1**. Instruments at Site 1 were mounted at 1.77 m height, and 2.04 m at Site 2. Supplementary meteorological and environmental variables were measured, which included rainfall (Chapter 3), air temperature, relative humidity, net radiation, soil temperature (spaced between 2 – 6 cm depth, referred to as 4 cm depth), soil moisture at 5 and 10 cm depth, water level[7] and soil heat flux at 8 cm depth (Table **4.1**). Both EC systems were controlled by a CR1000X datalogger connected to a multiplexer. EC data were collected at 10 Hz, supplementary data were collected at 10-second intervals, and statistics were calculated and stored at half-hourly intervals.

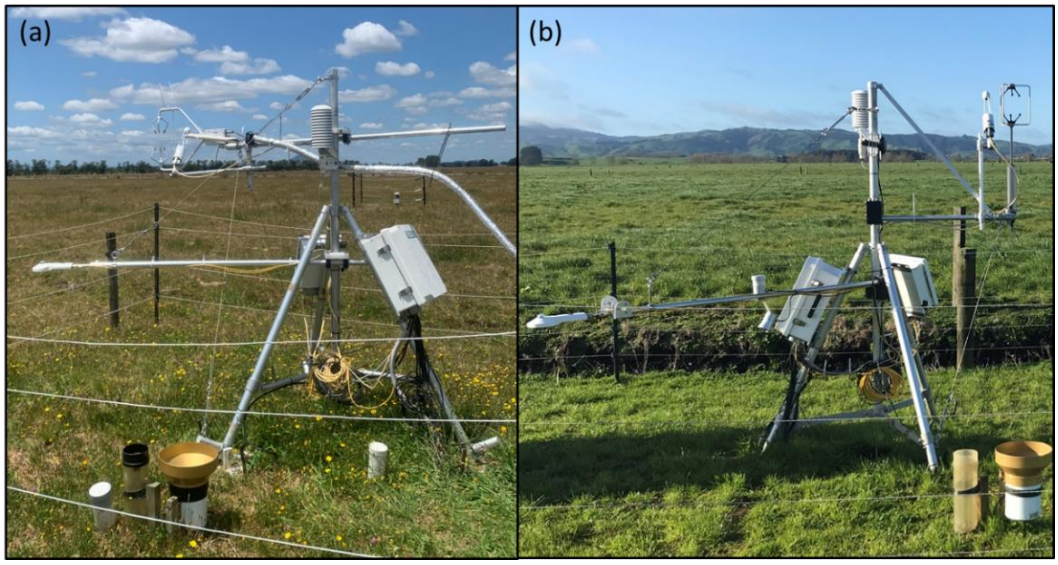

Figure 4.1 Eddy covariance towers at (a) Site 1 and (b) Site 2.

[7] The water level probe located adjacent to the EC tower is detailed in Table **4.1**, while the other three probes are described in Chapter 3.

Table 4.1 Summary of eddy covariance instruments used at each of the sites, including supplementary meteorological and environmental measurements.

Instrument	Site 1	Site 2
Datalogger	CR1000X, Campbell Scientific Inc., Logan, UT, USA	CR1000X, Campbell Scientific Inc., Logan, UT, USA
Multiplexer	AM16/32B, Campbell Scientific Inc., Logan, UT	AM16/32B, Campbell Scientific Inc., Logan, UT
Open path infra-red gas analyser	LI-7500RS, LI-COR Biosciences Inc., Lincoln, NE, USA	LI-7500A, LI-COR Biosciences Inc., Lincoln, NE, USA
Sonic anemometer	CSAT3B, Campbell Scientific Inc., Logan, UT	WindMaster Pro, Gill Instruments Ltd., Lymington, UK
Air temperature and relative humidity	HMP155, Vaisala Inc., Helsinki, Finland	HMP155, Vaisala Inc., Helsinki, Finland
Net radiometer	CNR4, Kipp & Zonen, Delft, Netherlands	CNR4, Kipp & Zonen, Delft, Netherlands
Soil heat flux plates	HFP01SC, Hukseflux Thermal Sensors, Delft, Netherlands	HFP01SC, Hukseflux Thermal Sensors, Delft, Netherlands
VMC	ML3 ThetaProbe, Delta-T Devices, Cambridge, UK	ML3 ThetaProbe, Delta-T Devices, Cambridge, UK
Soil temperature	Four-junction TCAV, Campbell Scientific Inc., Logan, UT	Four-junction TCAV, Campbell Scientific Inc., Logan, UT
Water level	WL1000W, Hydrological Services, NSW, Australia	WL1000W, Hydrological Services, NSW, Australia

Half-hourly fluxes of CO_2 and H_2O were processed from the high-frequency data, using EddyPro software (Version 6.2.2, Li-COR Inc.), with processing options following Wall et al. (2019). Time delays between vertical wind speed and scalar concentrations were accounted for using covariance maximisation, and a two-axis rotation correction was applied for anemometer tilt. High-pass and low-pass

filtering effects were corrected for, and block averaging was used to de-trend scalar concentration time series. High-frequency data spikes were discarded. Fluxes associated with periods of low turbulence (standard deviation of vertical wind speed < 0.13 m s^{-1} following the Reichstein et al. (2005) method for friction velocity), or which originated from an undesirable wind sector (associated with EC tower and site infrastructure) were rejected. With criteria ranging from best (0) to bad (2) based on tests for steady-state and developed turbulent conditions, the EddyPro quality control flagging system was utilised. Only data flagged with values of 0 were accepted.

The quality control measures introduced considerable gaps in the data, which were filled by applying the artificial neural network (ANN) technique (Papale & Valentini, 2003), one model for daytime fluxes and one for night-time. For each flux, a number of input variables were specified ('drivers') to fill gaps (Table **6.1**). Fuzzy variables were generated to describe time (time of day, and season). ANN models were each run a total of 50 times and simulated fluxes were calculated as medians across all 50 runs. For half-hours with missing or flagged poor-quality fluxes, the corresponding ANN simulated values were used.

Fluxes of CO_2 (NEE) were partitioned into ER and GPP. Night-time NEE were assumed to be equal to night-time ER, with no contribution from GPP during this time. Daytime ER were subsequently modelled with the night-time ANN model, to which daytime drivers of ER were applied (Oikawa et al., 2017; Ratcliffe et al., 2019). GPP was then calculated as -NEE + ER.

Random and systematic uncertainties in measured and gap-filled CO_2 fluxes were analysed. Following the method of Dragoni et al. (2007), random uncertainties in measurements and gap-filling were determined. Systematic uncertainty associated with the selection of standard deviation of vertical wind speed was determined, then combined with random uncertainties to calculate annual net ecosystem production (NEP) uncertainty following the procedure used in Wall et al. (2019). Lastly, energy balance closure was assessed, performed on half-hour periods with high-quality flux data. The energy balance closure ratios (Wilson et al., 2002) between 1 January and 31 December 2019 were 89% and 88% at Sites 1 and 2, respectively (Figure **A.1**).

4.2.2 Soil physical properties

To investigate how VMC and bulk density vary with depth, deep soil cores (0 – 1.8 m) were sampled from each site from representative mid-paddock hump positions at two intervals, one to represent dry conditions (20 March 2019) and one for wet conditions (5 August 2019). A Russian D corer was used, consisting of a coring chamber with diameter 50 mm and length 500 mm, to which aluminium rods of varying lengths were attached to reach the desired depths. The chamber had a rotating steel blade, sharp on one side, which cut the peat material and enclosed it within the chamber with a cover flap to obtain cores in undisturbed condition. Four sub cores were sampled, each with a 50 mm overlap at either end to ensure sampling of the whole soil profile. To minimise disturbance, the 'two-borehole technique' was used (De Vleeschouwer et al., 2010), which involved sampling from alternating holes 250 mm apart. In the laboratory, cores were subsampled at 50 mm intervals, for which volumes were determined for saturated peat using volume displacement in a graduated glass beaker. Volumes of unsaturated peat in the 0 – 40 cm depth range were obtained and subsampled with a core of diameter 50 mm and length 50 mm. VMC and bulk density were obtained by oven-drying at 105ºC for 72 hours.

The carbon content of soil from the monthly cores (Chapter 3) and two deep cores were determined by loss on ignition (LOI), whereby 3 g of dried and ground soil samples were placed in a muffle furnace at 550ºC for four hours. The lost mass was attributed entirely to organic matter, from which the carbon content was calculated with the van Bemmelen conversion factor of 0.58 (Minasny et al., 2019).

On October 22, 2019, infiltration rates were measured in the field, and samples were obtained to determine unsaturated hydraulic conductivity (K_{unsat}) at both sites. A ring with diameter 250 mm was pressed approximately 50 mm into the soil surface, within which the infiltration rate was determined by measuring water seepage to soil while maintaining constant water head. For this, the MWLR Infiltrometer was used (Manaaki Whenua Landcare Research, 2019). For K_{unsat}, cores with diameter 100 mm and height 75 mm were sampled at seven depths (0, 10, 20, 30, 45, 65, 95 mm) from each site. Manaaki Whenua Landcare Research conducted K_{unsat} testing in their laboratory, by applying tension (-0.1, -0.4, -0.7 and

-1 kPa) to the upper and lower surfaces of the intact cores, and measuring the flow of water through the water-filled pores (Manaaki Whenua Landcare Research, 2020).

4.3 Results

4.3.1 Climate

Rainfall between 1 January and 31 December 2019 totalled 793 mm for Site 1 and 830 mm for Site 2; 68% and 71% of the long-term average annual ('normal') rainfall of 1167 mm in Cambridge (1981-2010; NIWA, 2017), respectively. In December 2018, before the time period of interest to this study, the sites received 256% of that month's normal rainfall (Figure **4.2**). During the study period, denoted by the grey dashed rectangle, rainfall can be segregated to three distinct periods. Between January and June, rainfall at the sites totalled 66% of normal rainfall. This was followed by a wet period in July, August and September, where rainfall was 120% above average. In the second dry period, October to December, only 38% of normal rainfall fell, which was particularly pronounced in November (14%). During 2019, mean monthly air temperatures (T_{air}) exceeded the long-term averages in all months except April and June. As a result, average T_{air} at Sites 1 and 2 (14.8ºC) exceeded the long-term average by 1ºC (13.8ºC).

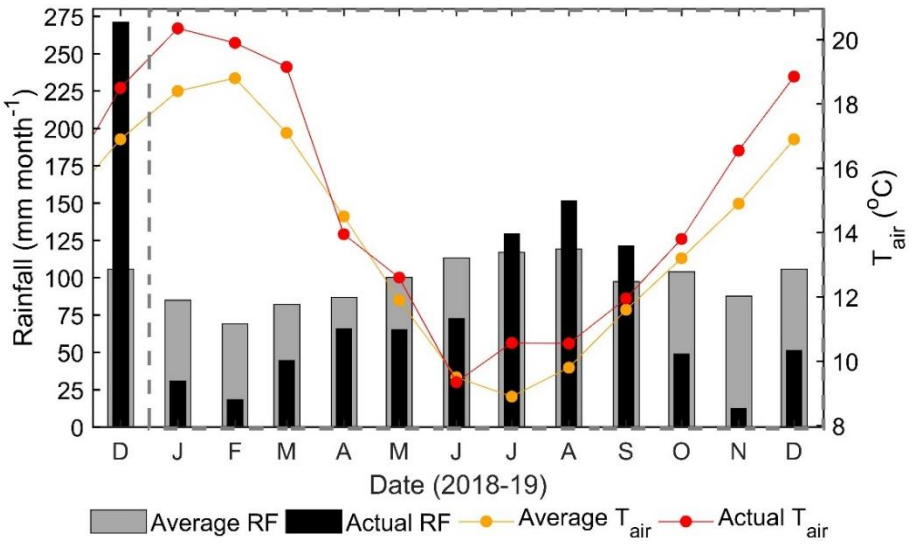

Figure 4.2 Time series of mean monthly rainfall (RF) totals at Sites 1 and 2, long term average (1981-2010); RF (black and grey bars, respectively), monthly average and long-term average air temperature (T_{air}; red and orange dots, respectively). The grey dashed rectangle represents the period of interest (1 January to 31 December 2019). Long-term average rainfall (Cambridge) and air temperature (Hamilton) values from NIWA (2017) and NIWA (2010), respectively.

4.3.2 Spatiotemporal variability of RWL and AWL

RWL at Sites 1 and 2 displayed similar spatial patterns, which did not appear to be influenced by the two different drainage designs (Figure **4.4**). Within the drains, RWL was closer to the peat surface than across the paddocks for both sites, and it appeared there was equal drawdown either side of the drains. For the distribution of manual RWL measurements, the data at Site 2 were spread more evenly either side of the interquartile ranges, although median RWL values were distributed closer to the lower quartile than at Site 1. Over the paddocks, drains, and the whole transect, the total range of RWL was larger at Site 2. At Site 1, the deep drain located 239 m along the transect appeared to draw RWL down further in the adjacent dipwell. Mean RWL values at Site 2 were deeper than at Site 1 across the whole transects and the paddocks, however, both sites were very similar in each of the drains (Table **4.2**).

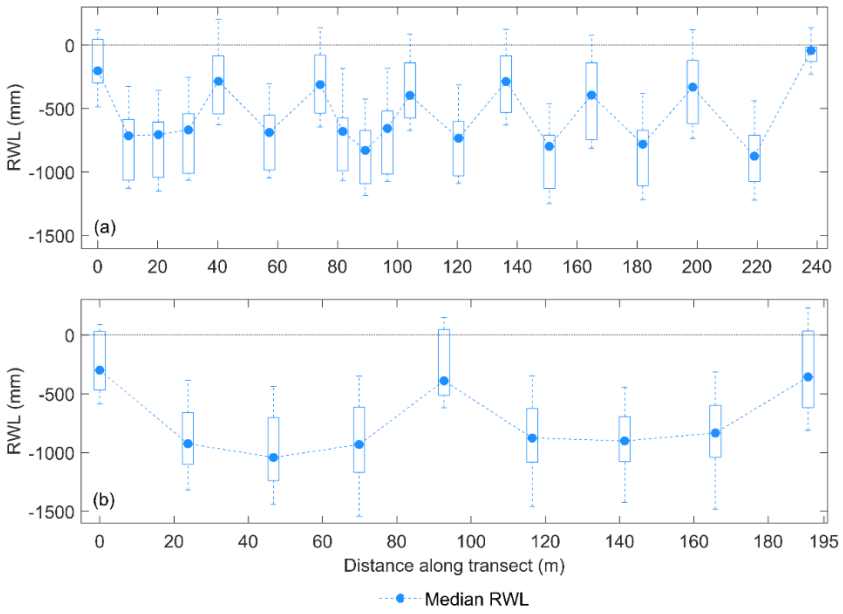

Figure 4.3 Spatial variability of relative water level (RWL) along the transects at (a) Site 1 and (b) Site 2, showing boxplots (upper quartile, median, lower quartile, maximum and minimum) from manual measurements of each dipwell between January 2019 and January 2020. The horizontal black dotted line represents the peat surface. For drain positions refer to Figure **4.4**.

Table 4.2 Summary of spatial relative water levels (RWL) from means of manual measurements across the whole transects and within the drains and paddocks, as well as those derived from the automatic probes (drain, EC, mid-slope, hump) at Sites 1 and 2 between 1 January and 31 December 2019.

	Site 1 (mm)	**Site 2 (mm)**
Manual		
Mean RWL (all)	-568.6	-687.4
Mean RWL (drains)	-269.0	-265.2
Mean RWL (paddocks)	-783.3	-898.5
Automatic probes		
Mean RWL (drain)	-53.8	-35.9
Mean RWL (EC site)	-669.4	-881.5
Mean RWL (mid slope)	-684.3	-772.7
Mean RWL (hump)	-792.9	-843.8

When water tables are plotted as absolute water level (AWL) to account for differences in elevation between landscape features (Figure **4.4**), the shape of the water table is the inverse of Figure **4.3** because the drains are at an elevation much lower than the adjacent paddocks. This formed a parabolic shape in the water table at each of the sites that held year-round at both sites.

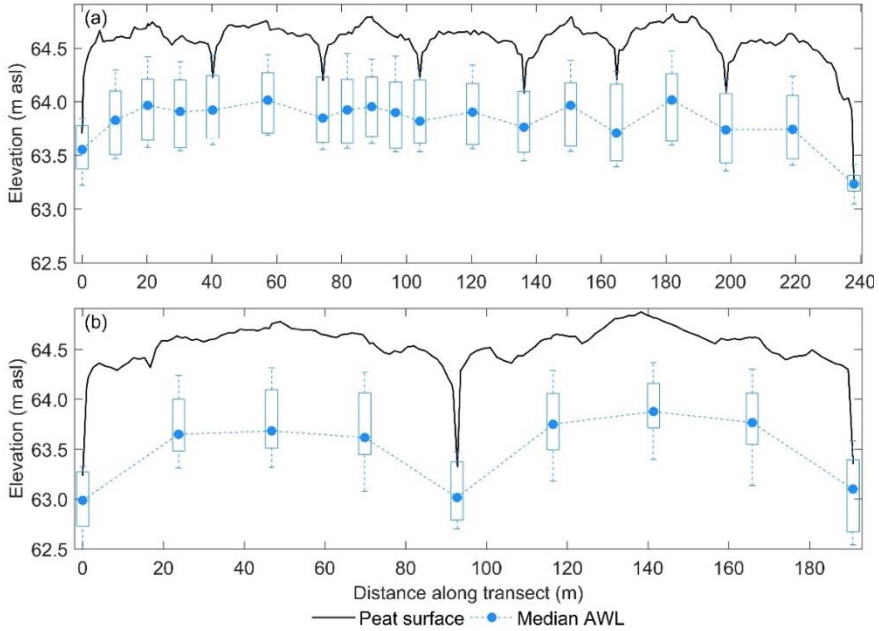

Figure 4.4 Spatial variability of absolute water level (AWL) along the transects at (a) Site 1 and (b) Site 2, showing peat surface elevation and boxplots (upper quartile, median, lower quartile, maximum and minimum) from manual measurements of each dipwell between January and December 2019.

Measurements from the four water level probes at each site, which infer a degree of spatial variability based on their relative positions within the transects, corresponded well with manual measurements made in the same dipwells throughout 2019 (Figure **4.5**; Figure **A.2**). For the whole measurement period, RWL at Site 1 had less spatial variation between each of the dipwells than Site 2, especially over the wet period and second dry period. All measurements indicate that RWL in each of the measured dipwells had a similar seasonal pattern, reaching lowest water levels over the dry periods, and maximum over the wet period; following rainfall patterns. When compared to Site 1, RWL at Site 2 was consistently lower over dry periods and higher over the wet period, resulting in a greater range of RWL (Table **4.2**). Furthermore, it appeared that RWL at Site 2 displayed greater fluctuations after rainfall, which was particularly pronounced in the drain, suggesting the peat at this site had a higher specific yield and was hydrologically more variable.

From the beginning of January 2019, RWL within the EC dipwell at each of the transects drew down rapidly following the extremely wet December 2018. Although the other three automatic probes at each site were not established until 14 February 2019, manual measurements at Site 1 inferred the same trend (Figure **A.2**). RWL across the paddocks at Site 1 appeared to reach maximum depths in April, after which they levelled off. RWL at Site 2, however, continued to draw down until late May. Rainfall events between February and June had little effect on RWL across the paddocks but caused considerable fluctuations in RWL in the drains at both sites, indicating shallow recharge to the water table under the drains, but not to a depth that reached the water table under the paddocks. In June, rainfall after the extended summer drought caused rapid recharge of RWL in all of the automatically measured dipwells. Hump RWL at both sites, as well as the mid-slope RWL at Site 2, were characterised by swift declines in water levels following rainfall at the beginning of June, while RWL in the other dipwells decreased at a slower rate. This pattern was observed again in early June at the hump of Site 2, but not for any of the other dipwells. Consistent rainfall between July and October resulted in oscillating RWLs, which reacted quickly after each rain event in each dipwell. Low and intermittent rainfall between October 2019 and January 2020 caused water table lowering across both transects, with RWL at Site 2 appearing to draw down at a faster rate.

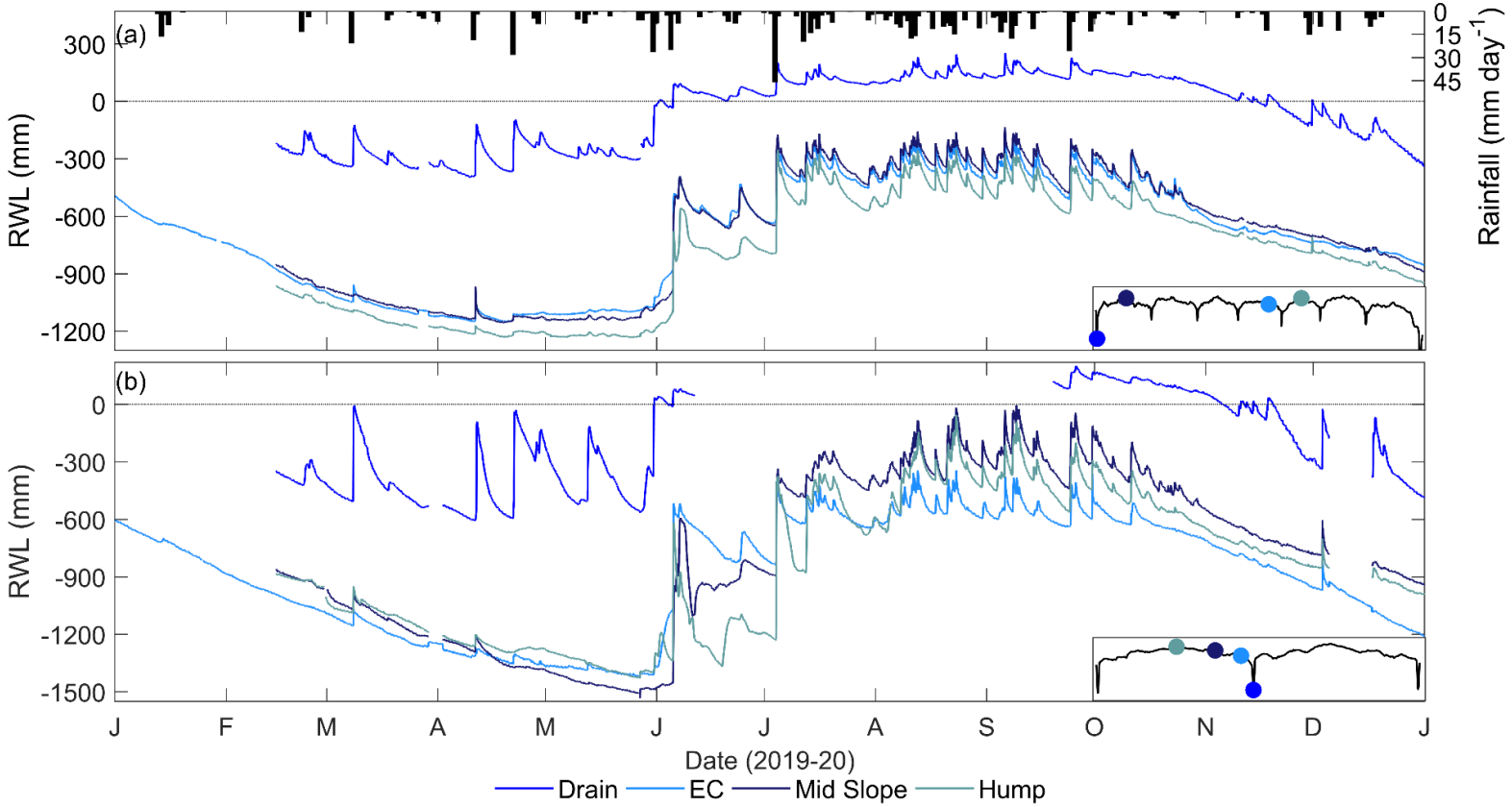

Figure 4.5 Time series of daily rainfall totals and half-hourly mean relative water level (RWL) from automatic probes between 1 January and 31 December 2019 at (a) Site 1 and (b) Site 2, with the inset graphical legend showing relative locations of the automatic probes along each of the transects. The horizontal black dotted line at RWL = 0 represents the peat surface. Note that the values on the Y axes differ between sites, but the ranges are the same, and missing data were caused by instrument failure.

At both sites, RWL was above the surface within the drains for only a short period of the year. At Site 1 this was estimated to be between June and November in the spinner drains, and between July and October in the main drains either side of the transect. RWL was positive at Site 2 for an estimated period between June and November. With regards to the time period when the drains were actively transporting water (active), this was even shorter. Based on an estimation of peak flow events following rainfall, this was approximately 17% of the time that there was water within the drains at both sites.

When plotting water table positions of each of the automatic probes along the transects as AWL at the end of a dry period (April to June 2019, Figure **4.6**), it is apparent there was less spatial variation in AWL at Site 1 than Site 2. For the duration of this period, AWL across the paddocks at Site 1 were consistently higher at the mid-slope position and lowest at the EC. Similarly, AWL at Site 2 was lowest at the EC site, however, highest AWL was measured at the hump which was expected given the spatial pattern of manual measurements in Figure **4.4**. The drains at both sites displayed lowest AWL because of their lower elevation relative to the paddocks.

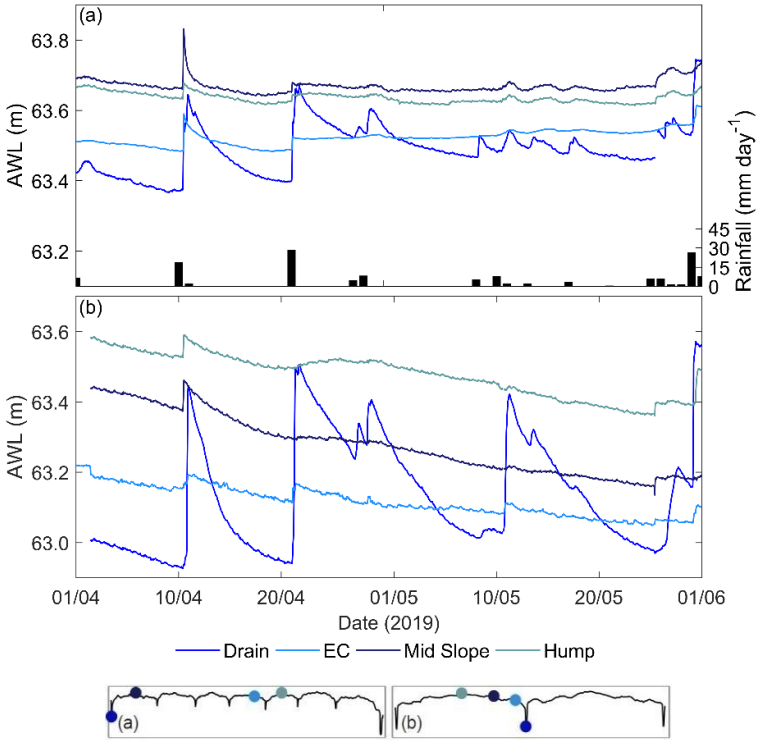

Figure 4.6 Time series plots of daily rainfall totals and half-hourly absolute water levels (AWL) at (a) Site 1 and (b) Site 2 for 61 days starting 1 April 2019, encompassing the end of the first dry period. The graphical legend shows locations of automatic probes along each of the transects. Note that the values on the Y axes differ between sites, but the ranges are the same.

During this time period at both sites, when drainage ditches were not actively transporting water, fluctuations in AWL following rainfall events were greatest in the drains compared to the paddocks. Furthermore, Figure **4.6** encompasses the time period when RWL at Site 1 levelled off while at Site 2 continued to decrease (Figure **4.5**), and the same trend can be seen with AWL.

During the wettest period of 2019, August to October (Figure **4.7**), the same spatial trend was observed across the paddocks, but there was more spatial variation in AWL at both sites when compared to the dry period (Figure **4.6**). Furthermore, with each rainfall event, increased AWL fluctuations were measured across the paddocks than in the drains, because the drains had water levels above the base of the drains. At Site 2, greater change in AWL was observed after each rainfall event, especially at mid-slope and hump positions. Across the paddocks, the same spatial trend was observed as in the dry period.

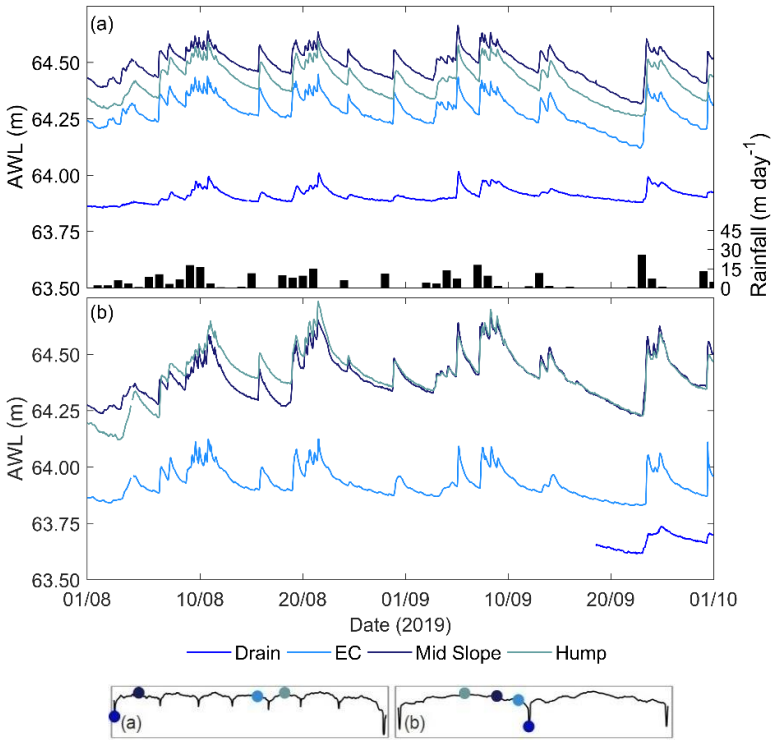

Figure 4.7 Time series plots of daily rainfall totals and half-hourly absolute water levels (AWL) at (a) Site 1 and (b) Site 2 for 61 days starting 1 August 2019, encompassing the wet period. The graphical legend shows locations of automatic probes along each of the transects. Note that missing data for the Site 2 drain were caused by instrument failure.

4.3.3 Spatiotemporal variability of VMC

Spatially, monthly manual soil cores indicated that at both sites VMC was generally lower adjacent to the drainage channels compared to the paddocks, particularly at Site 2 (Table A.2). However, this pattern was not measured on all sampling events, and the sampling design did not allow for a spatial pattern as detailed as RWL.

Based on both temporal automatic probe and manual coring measurements, VMC at Sites 1 and 2 between 1 January and 31 December 2019 decreased over dry periods, and increased during the wet period, exhibiting a strong seasonal pattern (Figure **4.8**). Following high rainfall in December 2018 (Figure **4.2**), VMC was relatively high at the beginning of January 2019 (0.68 cm^3 cm^{-3} and 0.52 cm^3 cm^{-3} for the 10 cm probes at Sites 1 and 2, respectively), after which there was a sharp decline at both sites, at both 5 cm and 10 cm depths. VMC at Site 2 appeared to level off at the beginning of February, whilst VMC at Site 1 continued to decrease, contrasting the RWL pattern within the same period (Figure **4.5**). As a result, VMC of the soil at Site 1 became much lower than at Site 2 (Table **4.3**). Although this trend was measured by both the 5 cm and 10 cm probes, the manual measurements which incorporate a larger spatial area portrayed a lower, but not significantly different VMC at Site 2 during this period.

Between late February and May, intermittent rainfall events wetted the surface peat, causing fluctuations in VMC mostly at 5 cm depth at both sites, but to a much larger magnitude at Site 2. Infiltrated moisture from these rainfall events appeared to be predominantly confined to a very shallow layer of the surface peat, as 10 cm VMC was not affected to the same extent. Despite lower rainfall than the long term average (Figure **4.2**), June 2019 marked the beginning of the wet season, and rainfall events led to increased 5 cm and 10 cm VMC of the peat profile at both sites. VMC at Site 2 was recharged rapidly, and moisture content was similar across both depths. VMC gradually increased over the wet period at Site 1, as the shallow (5 cm) peat appeared to be affected by hydrophobicity from excessive drying over preceding months. Further evidence for this is the VMC at 10 cm depth being higher than VMC at 5 cm depth between June and September 2019. Manual measurements during this time also indicate that Site 1 had lower moisture content than Site 2, however VMC at Site 1 appeared to be slightly higher than what was indicated by the automatic probes.

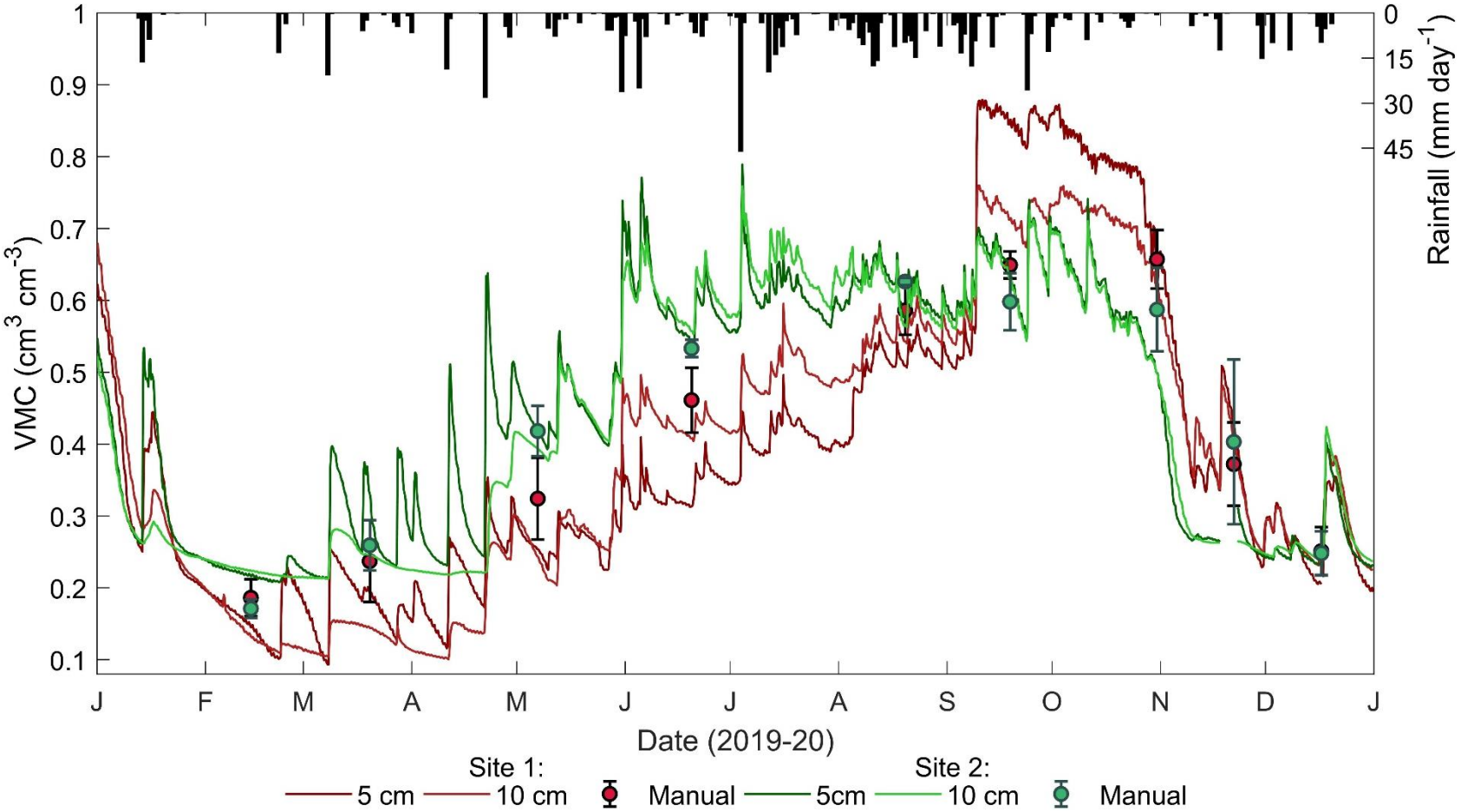

Figure 4.8 Time series of daily rainfall totals, six-hourly mean soil volumetric moisture content (VMC) from the automatic probes at 5 cm and 10 cm depths, and manual measurements (mean ± 1 standard deviation) at 2.5 – 7.5 cm depth along the transects at Sites 1 (red) and 2 (green) between 1 January and 31 December 2019.

On 9 September 2019, 17.9 mm of rain fell at both sites, which triggered a large and sudden increase in VMC at Site 1, particularly evident at 5 cm depth, suggesting hydrophobicity had been overcome. Manual measurements on 19 September also indicate that VMC at Site 1 surpassed that of Site 2, however not to the same magnitude as measured by the automatic probes. Following this event, VMC at Site 1 did not respond in the same way to rainfall as Site 2, and it appeared as if field capacity had been reached at 5 cm depth.

An extremely dry November 2019 initiated rapid drawdown of VMC at both sites, during which VMC at Site 1 remained slightly higher than at Site 2. In late December, VMC at Site 1 became lower than at Site 2 at 5 cm depth only, a trend which continued into January 2020 (Figure **A.3**), mirroring that of late January 2019.

Table 4.3 Summary of minimum and maximum soil volumetric moisture content (VMC) from the automatic probes at 5 cm and 10 cm depths between 1 January and 31 December 2019.

	Site 1 (cm^3 cm^{-3})	**Site 2 (cm^3 cm^{-3})**
$VMC_{5\ cm}$ maximum	0.88	0.79
$VMC_{5\ cm}$ minimum	0.09	0.21
$VMC_{10\ cm}$ maximum	0.76	0.76
$VMC_{10\ cm}$ minimum	0.10	0.21

4.3.4 Relationship between water table and soil moisture

The relationship between RWL and VMC at 5 cm depth displayed substantial hysteretic behaviour at both sites (Figure **4.9**), which can be separated into six segments. In segment A (January 2019), there was a linear relationship between RWL and VMC, when the peat was drying out after a very wet December 2018. At both sites, there was a greater decrease in VMC relative to RWL drawdown, as the surface peat dewatered. VMC at Site 1 declined more than at Site 2, whereas RWL declined more at Site 1 than Site 2 (Table **4.4**). Segment B (February – March 2019) represented a period where the surface peat had already dried out considerably and was characterised by a much larger decrease in RWL relative to VMC. Like Segment A, Site 1 had a greater decrease in VMC (-0.14 cm cm^{-3} and -0.03 cm cm^{-3} at Sites 1 and 2, respectively), while RWL at Site 2 drew down further (-459.40 mm and -499.85 mm). Segment C (April – May 2019) represented the 'green

drought', where rainfall events wetted up the surface peat but were not of sufficient size to substantially affect RWL. During this time, VMC increased at both sites, but more so at Site 2. RWL of Site 1 rose slightly, while at Site 2 it dropped (Figure **4.5**). In this segment, small 'loops' in the data are evident, representing VMC increasing due to rainfall, and then decreasing again as the peat dried.

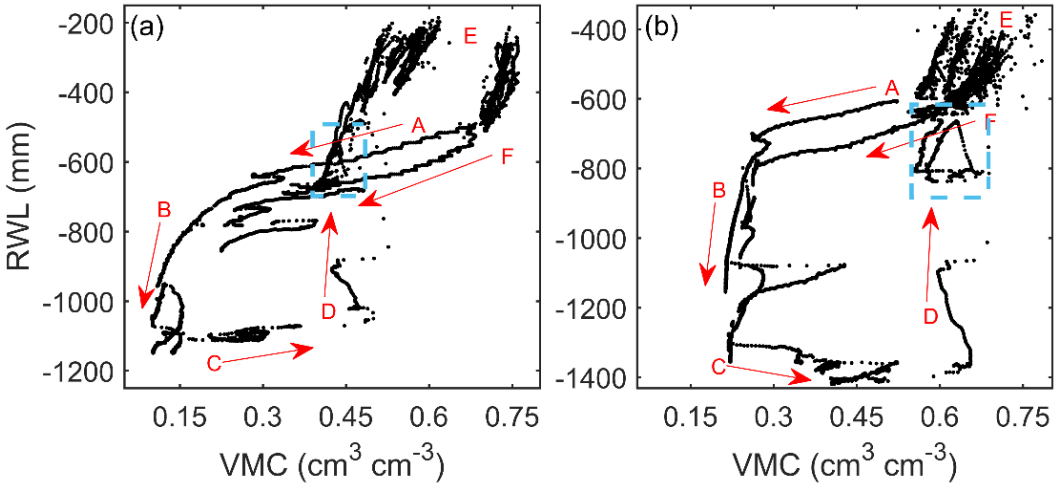

Figure 4.9 Half-hourly values of relative water level (RWL) plotted against 5 cm soil volumetric moisture content (VMC) at (a) Site 1 and (b) Site 2, for the measurement period (January – December 2019). Note that the values on the Y axes differ between sites, but the ranges are the same. Arrows indicate the time sequence, and letters are referred to in the text. The blue dashed rectangles represent short-term hysteresis shown in Figure **4.10**.

In segment D (June – July 2019), the beginning of the wet season, large rainfall events caused VMC to increase only slightly (0.08 cm cm^{-3} and 0.01 cm cm^{-3} at Sites 1 and 2, respectively), but RWL markedly rose at both sites (860.9 mm and 1005.2 mm). Short-term hysteresis was present in this segment, visible as triangular shapes in the data, where there were time lags between increasing VMC and the subsequent increase in RWL (Figure **4.10**). Segment E (August – October 2019) represents when VMC and RWL were at their wettest during the measurement period. Intermittent rainfall events caused fluctuations in RWL and VMC, resulting in considerable scatter of data points within this segment. In September 2019, there was a large jump in VMC at Site 1 (Figure **4.8**), but little to no change in RWL, reflecting the possible change in surface peat from hydrophobic to hydrophilic. Segment F (November – December 2019) was characterised by low rainfall, forming the second drying curve analogous to segment A and the beginning of segment B. Initially, VMC decreased more, relative to RWL increase as the surface peat dewatered, which was followed by a rapid lowering of RWL and little change

in VMC. Different to segments A and B, changes in both VMC and RWL in this segment were greater at Site 2 than at Site 1 (Table **4.4**).

Table 4.4 Summary of relative water level (RWL) and 5 cm soil volumetric moisture content (VMC) changes in each of the five segments (A – F) of the hysteretic relationship.

	Site 1		**Site 2**	
	RWL (mm)	**VMC (cm cm^{-3})**	**RWL (mm)**	**VMC (cm cm^{-3})**
Segment A	-173.4	-0.37	-216.2	-0.27
Segment B	-459.4	-0.14	-499.9	-0.03
Segment C	78.5	0.35	-88.8	0.37
Segment D	860.9	0.08	1005.2	0.01
Segment E	-4.0	0.22	33.4	0.18
Segment F	-461.9	-0.52	-714.0	-0.54

In Figure **4.10**, examination of a ten-day period (20 – 30 June, 2019) within segment D (within the blue dashed rectangle) at each of the sites, short-term hysteretic behaviour in the RWL – VMC relationships were evident. This behaviour, visible as triangular loops, are representative of rainfall events triggering changes in VMC and RWL at different time scales. For ease of comparison, the loops have been separated into three parts. In part A, as shown by the inset plots, VMC at both sites increased on 21 June, which was much more pronounced at Site 2. Shortly after, an increase in RWL was measured at Site 1, which occurred simultaneously with a slight decline in VMC. At Site 2, VMC decreased more than at Site 1, but instead of increasing, RWL decreased slightly. Part B saw RWL, and to a lesser extent VMC, rise concurrently at Site 1. At Site 2, VMC increased just before RWL, causing VMC to already be decreasing before RWL peaked. Part C was characterised by a simultaneous drawdown in RWL and VMC at both sites, however, the relative decrease of RWL to VMC was greater at Site 1, which caused a steeper drying curve.

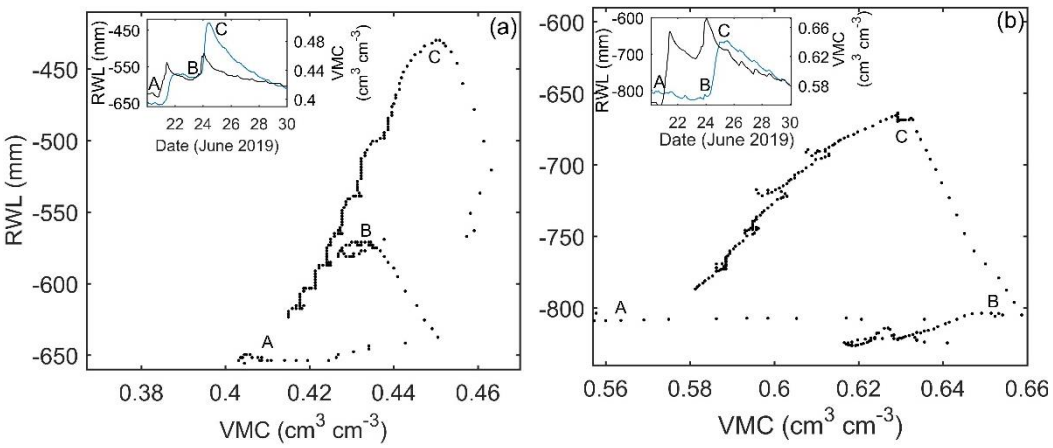

Figure 4.10 Hysteretic relative water level (RWL) – soil volumetric moisture content (VMC) relationship based on half-hourly data over a ten-day period starting 20 June 2019, for (a) Site 1 and (b) Site 2. Insets show time series of RWL (blue line) and VMC (black line) over this period. Note that the X and Y axis values differ between (a) and (b), but the ranges are the same. Labels referred to in text.

From the deep soil cores, further seasonal variation in the relationship between RWL and VMC is evident when comparing RWL and VMC with depth in a dry period (20 March 2019) and a wet period (5 August 2019), as illustrated in Figure **4.11**. For both March and August, the peat appeared to be saturated below a depth of approximately -0.5 m, above which there was an inflection point; marking the upper limit of each of the saturated zones. The inflection point was in relatively the same position for both dates of measurement despite different RWL. For both sites, RWL (dashed lines) was much further down the soil profile than the upper limits of saturation, particularly in March. This area of saturation above the water table indicates a capillary zone with a depth of approximately 0.6 m. In contrast, RWL in August was closer to the peat surface, explaining why VMC was greater in this zone. RWL was higher than the inflection point at Site 1, while at Site 2, RWL was at a similar depth as the inflection, indicating that the capillary zone was not evident in August.

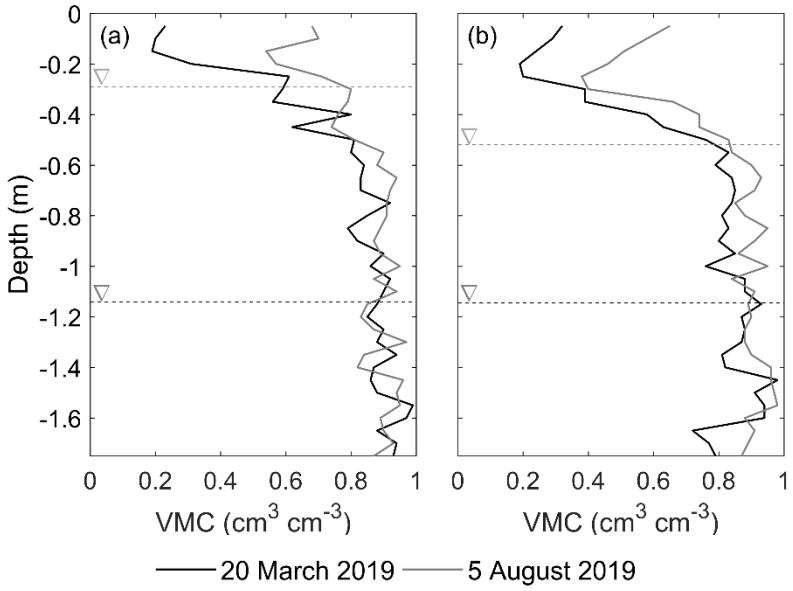

Figure 4.11 Soil volumetric moisture content (VMC) with depth, and its relationship with relative water level (RWL, dashed lines) at (a) Site 1 and (b) Site 2, measured on March 20 and August 5, 2019.

Further evidence for a capillary zone connecting RWL and VMC in dry periods is presented in Figure **4.12**, for the period January to July 2019. The net water flux to and from the peat surface, $P - E$, was negative for the whole period at Sites 1 and 2, reflecting an overall loss of stored water within the soil profiles at both sites. During this period, the cumulative changes in soil water within the top 200 mm of the profiles were initially very similar to $P - E$, until they diverged in late January. This divergence indicates that water removed from the surface peat layer was much less than what was lost as evaporation, suggesting water was being drawn up from deeper in the profile to sustain evaporative losses.

At Site 1, both $P - E$ and soil water change became more negative than at Site 2. Despite this, there was a greater difference between the two variables at Site 2, as indicated by the grey arrows. While this could have been from plant roots abstracting water from deeper in the soil profile, it was most likely due to capillary rise. Capillary rise processes therefore appeared to be more active at Site 2 than Site 1, providing a possible explanation for lower VMC at Site 1 than Site 2 over the first dry period; there was potentially less subsurface moisture redistribution to sustain VMC at Site 1.

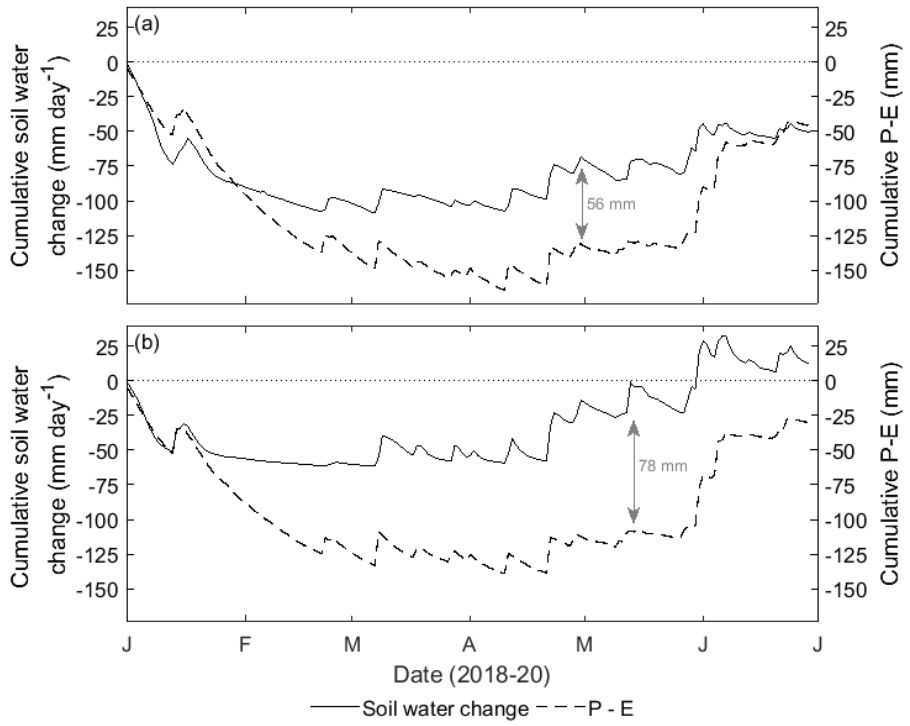

Figure 4.12 Time series of cumulative change in water content in the top 200 mm of the soil profile, and cumulative precipitation minus evaporation ($P - E$) between January and July 2019 at (a) Site 1 and (b) Site 2. Grey arrows and text indicate the date and value of maximum difference between soil water change and $P - E$.

4.3.5 The water balance

Cumulative rainfall and evaporation were relatively similar between Sites 1 and 2 throughout 2019 (Figure 13). From late January onwards, evaporation rates were slightly higher at Site 1, causing cumulative evaporation to diverge between sites. In July, cumulative evaporation at the two sites converged and remained almost identical for the rest of the measurement period. Rainfall was similar at the two sites until October, where greater rainfall at Site 2 caused a slight deviation for the rest of the year. Cumulative evaporation rates exceeded rainfall between January and July 2019, after which cumulative rainfall exceeded evaporation for the remainder of 2019.

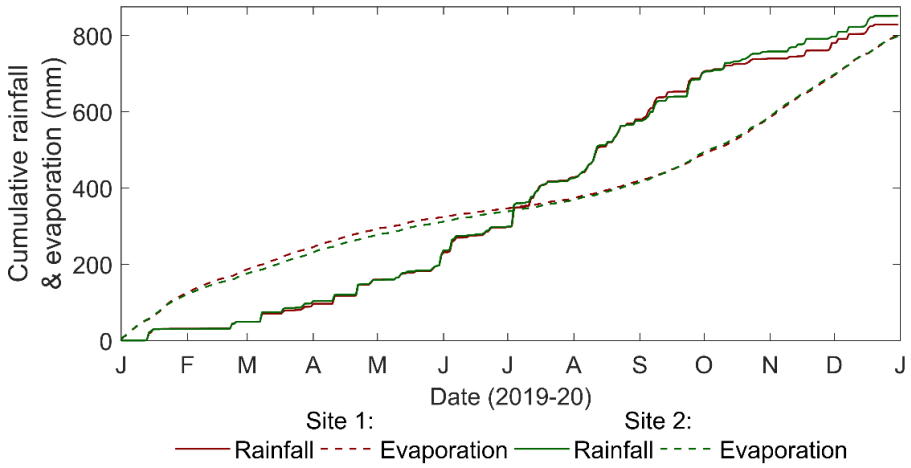

Figure 13 Cumulative rainfall and evaporation based on daily totals at Sites 1 and 2 between 1 January and 31 December 2019.

The surface water balance sum, *P* – *E*, was slightly positive for both sites over the annual period (33.2 mm and 58.5 mm at Sites 1 and 2, respectively), reflecting a net input of water to the systems (Figure **4.14**), far lower than what would be expected in a year with normal rainfall. Evaporation rates exceeded precipitation between January and April 2019, causing cumulative *P* – *E* to become increasingly negative, reflecting a loss of stored water and driving down both RWL and VMC. The control of the water balance was much more apparent on RWL than VMC throughout this period, because once the majority of surface moisture had been depleted in February for Site 2 and March for Site 1 (Figure **4.8**), VMC did not decrease any further. However, RWL depth continued to increase during this time (Figure **4.5**), reflecting the connection between RWL and surface moisture conditions, satisfying evaporative demands by drawing water up the soil profile from the water table. *P* – *E* at Site 1 became more negative than at Site 2, and the date at which the two sites began to differ from one another in late January corresponds with the diversion of VMC at the two sites (Figure **4.8**).

In the month of May, precipitation and evaporation rates were approximately equal, which was reflected by little change in RWL at Site 1 (Figure **4.5**). RWL at Site 2, however, continued to decline during this time, suggesting the influence of another hydrological control; reflecting the capillary rise processes that appeared to be more active at this site (Figure **4.12**). During this time, fluctuations in VMC at both sites were caused by the intermittent rainfall and subsequent evaporation. Between June

and October, considerable precipitation caused $P - E$ to increase, and net water flux to become positive; reflected by the patterns of RWL and VMC at both sites.

Evaporation began to once again exceed precipitation from October 2019, which initially had little effect on RWL and VMC for both sites because the peat was near saturation. Considerable drawdown in RWL and VMC began in mid-October, in response to substantial evaporation during that time, and minimal precipitation.

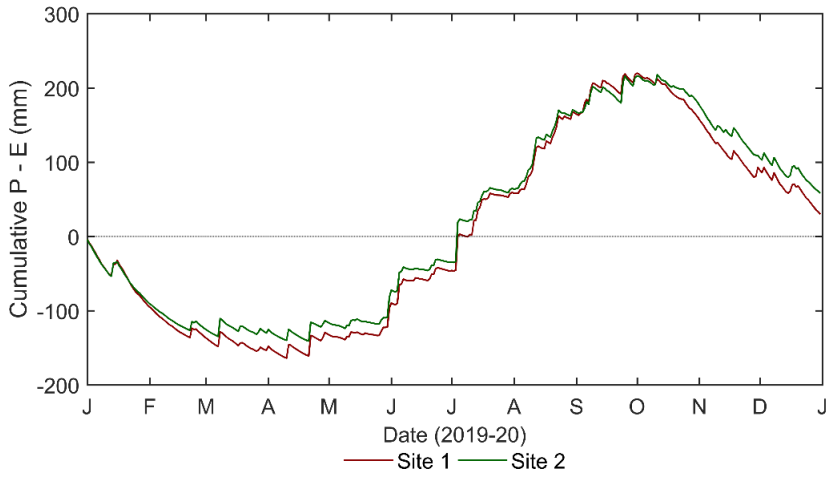

Figure 4.14 Cumulative precipitation minus evaporation (P – E) based on daily totals at Sites 1 and 2 between 1 January and 31 December 2019.

4.3.6 Soil physical and hydraulic properties

Sites 1 and 2 had different soil physical and hydraulic properties (Table **4.5**), for which the differences between bulk density and infiltration rates determined through paired T-tests were statistically significant ($p > 0.05$), and organic carbon contents were not. Site 1 was characterised by lower bulk density, which corresponded well with the higher unsaturated hydraulic conductivity at -0.4 kPa and -1 kPa suctions, when compared to Site 2. Hydraulic conductivities were lower for both sites at higher suctions. The infiltration rate was much higher at Site 2, and the soils at both sites had very similar organic carbon contents.

Table 4.5 Summary of soil physical properties (mean ± 1 standard deviation) measured at Sites 1 and 2. Letters indicate whether the difference between sites was statistically significant ([a]) or not statistically significant ([b]), $p < 0.05$, derived from paired T-tests.

	Site 1	**Site 2**
Bulk density (g cm^{-3})	0.31 ± 0.04[a]	0.37 ± 0.03[a]
$K_{unsat\ -0.4\ kPa}$ (m s^{-1} × 10^{-5})	1.44	0.29
$K_{unsat\ -1\ kPa}$ (m s^{-1} × 10^{-5})	0.29	0.10
Infiltration rate (mm hr^{-1})	24.7 ± 4.8[a]	37.9 ± 13.4[a]
Organic Carbon (%)	49.6 ± 1.8[b]	49.9 ± 2.0[b]

The pattern of soil bulk density with depth (0 – 1.8 m) at Sites 1 and 2 was relatively similar (Figure **4.15**), where bulk density was low (approximately 0.1 g cm^{-3}) between -0.5 m and -1.8 m depth. There was a clear change in physical properties at around -0.4 m at both sites, and above this depth, a sharp increase in bulk density was measured, in both March and August 2019. The surface peat at Site 1 was less dense than at Site 2 (approximately 0.34 and 0.4 g cm^{-3}, respectively), aligning with the monthly surface soil cores, and bulk density was slightly higher in August than March for both the sites.

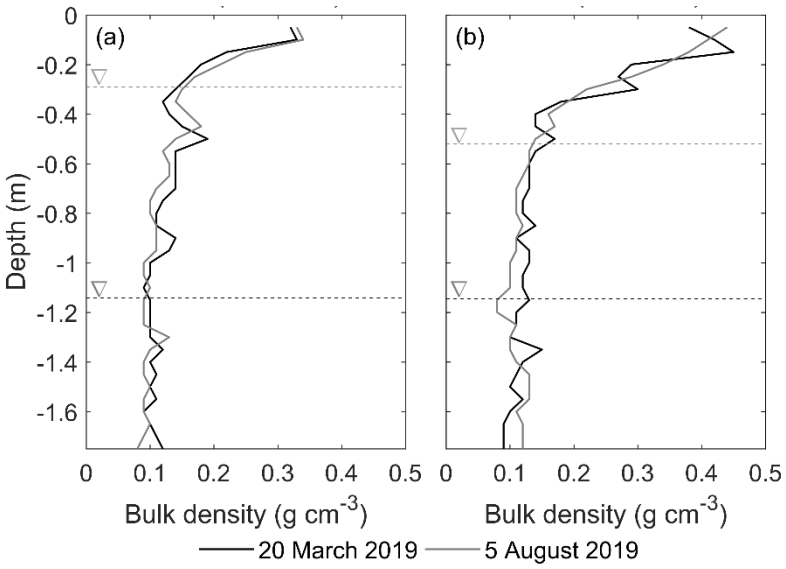

Figure 4.15 Soil bulk density with depth, and its relationship with relative water level (RWL, dashed lines), measured on March 20 and August 5, 2019, at (a) Site 1 and (b) Site 2.

4.3.7 Carbon dioxide fluxes

In 2019, the net ecosystem exchange of CO_2, NEE, was positive for Sites 1 and 2, reflecting a net loss of carbon to the atmosphere (Figure **4.16**). Despite the close geographic proximity of the sites, NEE was substantially greater at Site 2 (6.66 ± 0.63 t C ha^{-1} yr^{-1}), compared to Site 1 (1.05 ± 0.66 t C ha^{-1} yr^{-1}), which can be attributed to differences in ER rather than GPP (Table **4.6**). This difference appears to be mainly a result of ER diverging between sites in late January, with the respiration rate at Site 1 appearing to drop slightly relative to that of Site 2. ER continued to diverge between sites until July, reaching a maximum difference of 4.8 t C ha^{-1} between Sites 1 and 2. In the subsequent months, ER rates remained similar between the two sites. GPP was similar at Sites 1 and 2, with slightly higher rates at Site 1, which caused an annual difference of 1.6 t C ha^{-1} yr^{-1}

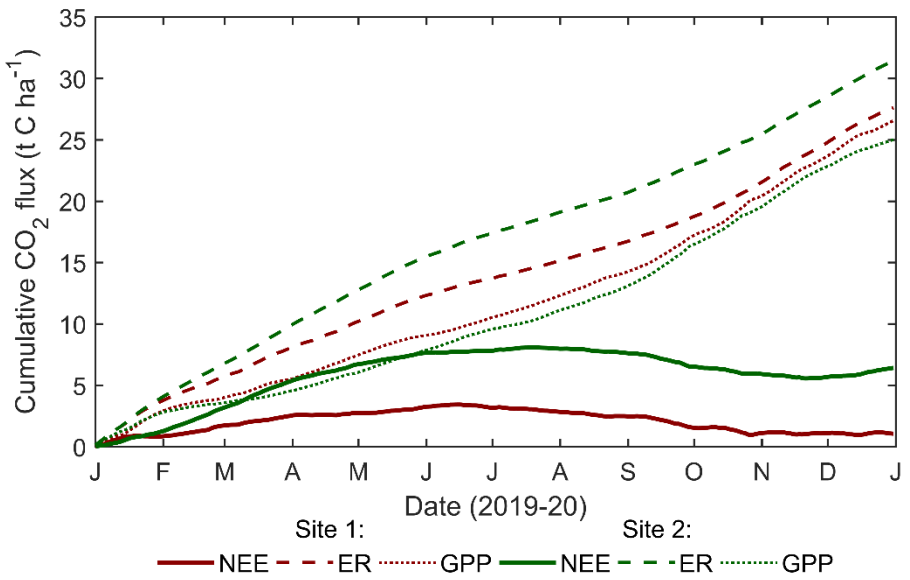

Figure 4.16 Time series plot of cumulative net ecosystem exchange (NEE), ecosystem respiration (ER) and gross primary production (GPP) between 1 January and 31 December 2019 for Sites 1 and 2.

Table 4.6 Summary of annual ecosystem respiration (ER), gross primary production (GPP) and net ecosystem exchange (NEE ± 95% confidence interval) totals for Sites 1 and 2 between 1 January and 31 December 2019.

	Site 1 (t C ha^{-1} yr^{-1})	**Site 2 (t C ha^{-1} yr^{-1})**
ER	27.6	32.4
GPP	26.6	25.0
NEE	1.05 ± 0.66	6.66 ± 0.63

The variation in ER that lead to the contrasting carbon balances between sites appeared to be best explained by VMC and soil temperature, rather than RWL (Figure **4.17**). Furthermore, the differences between sites cannot be explained by different substrate availabilities, as the peat carbon contents were very similar (Table **4.5**).

The divergence of VMC between sites in late January corresponded well with ER, and so it appeared that water limitations were constraining respiration rates at Site 1 (Figure **4.18**). ER at Site 2 was constrained to a much lesser extent, as the soil was able to retain more moisture during this time. Further support for water restricting ER at Site 1 was displayed during the rainfall event that occurred in February. Over a period of three days, 17.7 mm of rain fell at both sites, which led to a sudden increase in ER at Site 1 but had very little effect at Site 2 (Figure **4.18**).

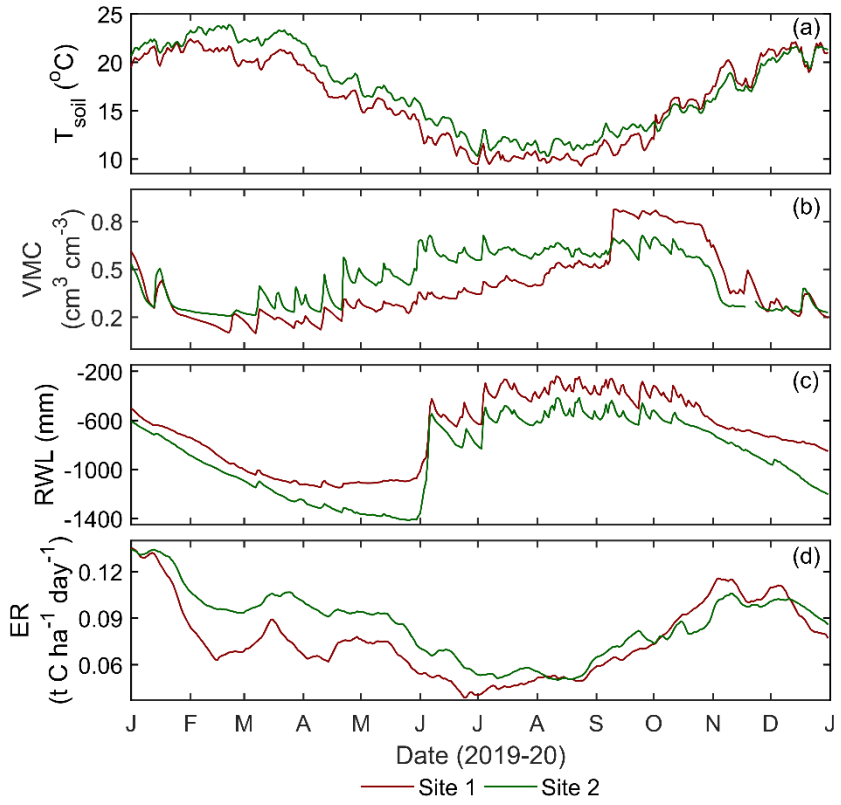

Figure 4.17 Time series plots of (a) soil temperature (T_{soil}), (b) soil volumetric moisture content (VMC) and (c) relative water level (RWL) based on daily means, and (d) 15-day moving means of ecosystem respiration (ER) at Sites 1 and 2 between 1 January and 31 December 2019.

ER rates at both sites appeared to gradually decrease throughout the 'green drought' in the first dry period (March to June; Figure **4.17**), suggesting that higher VMC was able to sustain ER, but the rates were constrained by decreasing soil temperatures and lower plant productivity (GPP; Figure **A.4**). In June and July, ER was lowest across both sites, a period when VMC was higher and soil temperatures were lowest. Soil temperatures remained relatively unchanged between late June and late August, while VMC gradually increased. The increase in ER is most likely a result of GPP increasing during this time, reflecting a higher contribution of recently fixed carbon to ER.

During September, a decrease in rainfall caused RWL and VMC to begin to draw down, and soil temperatures also increased during this time. As a result, both GPP and ER rates substantially increased (Figure **A.4**; Figure **A.5**), which was much more pronounced at Site 1. Low VMC in December appeared to once again limit ER at both sites, particularly at Site 1.

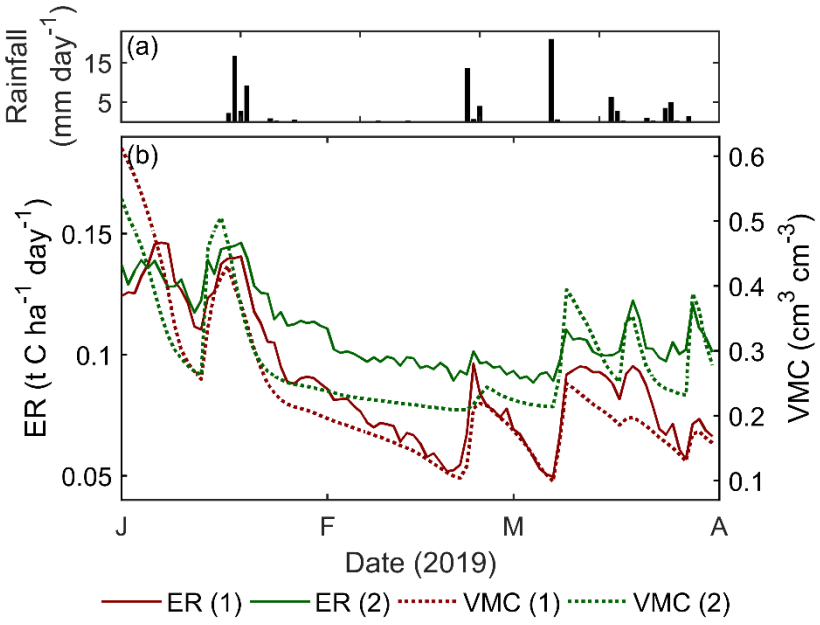

Figure 4.18 Daily totals of (a) rainfall and (b) ecosystem respiration (ER) and daily mean 5 cm soil volumetric moisture content (VMC) between 1 January and 1 April 2019 at Sites 1 and 2.

4.4 Discussion

4.4.1 Spatiotemporal variability of hydrology and its controls

Drained peatlands are characterised by significant spatiotemporal variability in hydrology (Silins & Rothwell, 1999; Holden et al., 2006), which despite the different drainage designs, was evident at both sites in this study. With regards to the spatial patterns, equal RWL drawdown was measured on either side of the drainage ditches at both sites (Figure **4.3**), a pattern also described by Boelter (1972) and Dunn and Mackay (1996). This is likely a result of the relatively flat topography at Sites 1 and 2 when compared to similar studies on upland peatlands that have not found the same effect (e.g. Holden et al., 2006). At Site 2 apparent equal drawdown either side of the drains could be argued to be from a lack of monitoring dipwells in close proximity to the drains, however, the same pattern was measured at Site 1 across the two intensively measured humps (Figure **4.4**), where dipwells were no more than 10 m apart. Because both sites had the same spatial pattern despite the different drainage designs, it appeared that drainage design was not a control on the spatial variability of RWL.

The control on hydrology by the different drainage designs was apparent when comparing depths of RWL between sites. At Site 2, the deeper drains caused greater drawdown in RWL either side of the drainage ditch, which led to increased spatial variability between each of the automatically measured dipwells, when compared to Site 1. Furthermore, the large drains at either end of the transect at Site 1 also resulted in deeper RWL in the adjacent dipwells. This effect is typical of drained peatlands (e.g. Petersen & Madsen, 1978; Luscombe et al., 2016). Ahti (1987) concluded that with increased spacing between drainage channels, deeper RWL would be seen, which also appeared to be true for the differences between Sites 1 and 2. However, Ahti (1987) also found that the distance between drains was not important during dry periods, but the methodology of this study did not allow for investigation into this effect.

In the drainage channels during dry periods, RWL was closer to the peat surface when compared to the rest of the paddocks, which is a pattern that has been noted in other hydrological studies (e.g. Sinclair et al., 2020). When RWL was plotted as AWL to account for differences in elevation between landscape features, a

parabolic shape in the water table across the paddocks was evident. AWL was higher in the middle of the hump when compared to the mid slopes, which could be seen by both manual measurements at Sites 1 and 2 (Figure **4.4**), and automatic measurements at Site 2 (Figure **4.5**). From the automatic measurements, AWL at both sites were lowest in the drains and above which were the EC AWLs. However, instead of AWL being highest at the hump, like it was at Site 2, AWL was greatest at the mid-slope position. Whilst this result was unexpected due to the close proximity of the mid-slope dipwell to the drain, a possible explanation could be the substantial spatial variation in soil physical and hydraulic properties over short distances (Norberg et al., 2018), affecting the movement of water within the peat (Baden & Egglesmann, 1963). Fluctuations in the water table have been found to differ depending on their location with respect to drainage channels, where Petersen and Madsen (1978), and Holden et al. (2011) found that RWL fluctuations were highest adjacent to drainage ditches. This was not a finding at either of the sites in this study and instead, the opposite was found. The different fluctuations may be due to site-specific hydraulic properties, however, it is also likely a result of 2019 being uncharacteristically dry (Figure **4.2**), as reflected by a near-zero water balance which indicated very little net runoff. Consequently, drainage channels were not actively transporting water for most of the year, and may have acted to dampen RWL fluctuations rather than increase them.

VMC has previously been seen to follow a similar spatial pattern to RWL, with lower VMC adjacent to drainage channels (Sinclair et al., 2020), which too was observed in this study. It emerged that the sampling design, with four monthly soil cores from various locations along the transect, was not spatially detailed enough to provide evidence for a distinct spatial pattern compared to that of RWL previously discussed.

Temporally, the hydrology of both sites was highly variable and followed the same pattern, where RWL and VMC reached lowest values over the first dry period, and highest values over the wet period, expected of drained peatlands (Holden et al., 2011). The water balance is often considered to be the driver of hydrological changes (e.g. Ingram, 1983; Parmentier et al., 2009), which was apparent at both sites in this study. $P - E$ controlled whether the systems were losing water, causing RWL and VMC to decline, or gaining water, where RWL and VMC were rising.

However, $P - E$ was not the only hydrological control, and other contributing factors were seen to influence temporal hydrological patterns, such as soil physical properties, which led to intra-site hydrological differences.

Differences also existed when comparing the ranges of RWL and VMC change, where VMC was more variable at Site 1 and RWL was more variable at Site 2. Previous research has suggested that deeper drains increase the range of RWL fluctuation (Petersen & Madsen, 1978; Luscombe et al., 2016), however, because 2019 was such a dry year, this was likely not the case. The differences in the ranges of RWL and its temporal variability between sites can be attributed to different peat specific yields. The change in RWL following a rainfall event has been said to be an estimation of available pore spaces within the unsaturated zone, whereby lower porosity indicates a lower specific yield (Logsdon et al., 2010). Increased RWL fluctuation at Site 2 after rainfall, when compared to Site 1, indicated a lower specific yield, which was an effect also measured by Price (1997).

In late January, $P - E$ at the two sites began to diverge, where evaporation rates became slightly higher at Site 1. During this time, VMC at Site 2 appeared to level off, while at Site 1 it continued to decrease. There are two explanations as to why this may have occurred. Firstly, soil bulk density was significantly higher at Site 2, indicating that, due to the inverse relationship between bulk density and pore size distribution (Waddington & Price, 2000), Site 2 may have been able to retain more moisture at higher suction potentials from greater micropore abundance (Price et al., 2003). Furthermore, increased microporosity will lead to reduced hydraulic conductivity, also measured at Site 2, as micropores transmit water less readily than macropores (Price, 2003; Whittington et al., 2007). Secondly, capillary rise processes appeared to be more active at Site 2 (Figure **4.12**), potentially acting to redistribute more moisture up the soil profile from the water table to sustain a higher surface peat VMC (Schwärzel et al., 2006). In soils with increased microporosity, stronger capillary rise processes have been measured (Price et al., 2003), further explaining intra-site differences.

Greater subsurface moisture redistribution at Site 2 also may explain why, between April and June, RWL levelled off at Site 1 but continued to get deeper at Site 2. It appeared that during this time the capillary zone at Site 1 had disconnected from

surface peat, also seen by Price et al. (2003), and remained more connected at Site 2. The threshold RWL at which the capillary zone is disconnected from surface moisture conditions has previously been estimated at -0.6 m, -0.7 m or -1 m (Price, 1997; Wessolek et al., 2002; Price et al., 2003), yet at Site 2, RWL got as low as -1.5 m, far exceeding these published values.

It is highly plausible that the low VMC at Site 1 over the first dry period initiated hydrophobic behaviour of the surface peat. Hydrophobicity, which causes resistance to rewetting of the peat (Schwärzel et al., 2002) preventing soil from regaining its original moisture content, has been reported to affect peat soils which dry out below a VMC of 0.3 cm^3 cm^{-3} (Berglund & Persson, 1996). Both sites in this study reached a VMC lower than 0.3 cm^3 cm^{-3} (Table **4.3**), however, it appeared that only Site 1 was significantly affected based on rewetting behaviour over the wet period and the sudden VMC increase that occurred in September (Figure **4.8**).

After the first major rainfall event following the extended summer drought (early June), RWL in three of the automatically measured dipwells rose and declined rapidly, not following the typical hydrograph-like curve that was expected, and measured in the other dipwells. While this may be real, it is most likely due to an overreaction of the water table (Ahti, 1987), where infiltrated rainfall preferentially flows into the hollow dipwell, before being redistributed within the peat profile as effective stresses equilibrate. Furthermore, preferential flow pathways could have been created when augering holes for dipwell insertion, as in some instances the auger struck subsurface woody material, and another hole was made adjacent to the original location.

Over the wet period, capillary rise processes were no longer apparent (Figure **4.11**), and fluctuations in both VMC and RWL appeared to only be controlled by the water balance. After each rainfall event, both variables reacted rapidly, and as water was evaporated or redistributed within the soil profile between rainfall events, RWL was drawn down.

4.4.2 Relationship between RWL and VMC

There are contrasting views on the relationship between RWL and VMC in drained peatlands, with evidence to suggest a relationship year-round (Wessolek et al.,

2002), only for certain periods of the year (Price, 1997), or complete lack of relationship (Parmentier et al., 2009). For both sites in this study, a direct relationship between RWL and VMC was only apparent for certain periods of the year and displayed considerable hysteresis. RWL and VMC were highly correlated for both sites at the beginning of dry periods and in the middle of the wet period, both of which occurred when the peat was near saturation. Similarly, Price (1997) found the relationship between RWL and VMC no longer existed once peat had dried out.

Hysteretic behaviour was most apparent following the extended summer drought (Segment D, Figure **4.9**). High-rainfall events led to rapid RWL increase with little VMC change, which can be attributed to preferential flow pathways to the water table caused by surface cracking and, at Site 1, possible hydrophobic behaviour. Both of these are effects that Schwärzel et al. (2006) and Kellner and Halldin (2002) have also commented on in drained peatlands. The initial repellency of surface peat to rewetting was most apparent at Site 1, which was to be expected given the hydrophobic behaviour seen. The small hysteretic loops present later in segment D (Figure **4.10**) were a result of different time lags between cause (rainfall) and effect (RWL or VMC change), where VMC reacted faster than RWL to rainfall given its direct interaction with the atmosphere. This phenomenon was more pronounced at Site 2, likely because the surface peat was less affected by hydrophobicity than at Site 1.

4.4.3 Hydrological influences on CO_2 emissions

Water table depth has frequently been considered to be the dominant factor controlling CO_2 emissions in drained peatlands (e.g. Renger et al., 2002; Berglund & Berglund, 2011; Couwenberg, 2011). At the two sites in this study, CO_2 emissions appeared to have a very low dependency on RWL, and the dominant control was instead VMC, which Candra et al. (2016) and Säurich et al. (2019a) likewise found. Soil temperatures were also seen to influence CO_2 emissions seasonally, but to a lesser extent than VMC. The influence of soil temperature appeared to be most pronounced when VMC was higher at both sites (e.g. January and September 2019), aligning with the findings of Wessolek et al. (2002).

Rates of ER and GPP can be constrained by water limitations in soil (Davidson & Janssens, 2006; Gaumont-Guay et al., 2006), especially in drained peat soils, where research has shown a large proportion of soil moisture may be hydrophilically sorbed to organic matter (McLay et al., 1992). The striking differences in NEE between the two sites do not appear to be from differences in GPP, but instead because of a direct result of water limitations to ER in the first dry period. The ability of the soil at Site 2 to maintain a higher VMC from February, meant that ER was not limited to the same extent as at Site 1 (Figure **4.17**). Further evidence for this was the rainfall event in late February that caused an increase in ER at Site 1, while Site 2 remained relatively unaffected. Known as the Birch effect, this is when pulses of rainfall, within or following a drought period, cause an increase in CO_2 emissions in response to sudden water availability (Unger et al., 2010). These results indicate that, like Säurich et al. (2019a) concluded, soils need to be very dry to limit CO_2 emissions.

Over the wet winter period, particularly between June and August, it appeared that CO_2 emissions were controlled by low soil temperatures and higher VMC, which acted to decrease both ER and GPP at both sites. GPP was also further constrained by decreased light. As temperature could not be controlled in field conditions, it was difficult to disentangle the individual effects of each control, which is what other field studies have found (Säurich et al., 2019a). While it could be argued that gas diffusion through the soil was limited by high moisture content like the bell-shaped curves described by Mäkiranta et al. (2009) and Säurich et al. (2019a), ER at both sites was higher in September despite VMC also being higher. This indicates that soil temperature was the dominant control over the wet period. Similarly, Berglund and Berglund (2011) found CO_2 emissions to be much lower over a winter period and they emphasised the importance of soil temperature. In the spring period, September to October, higher soil temperatures and increased light intensity substantially increased GPP relative to ER, which led to negative NEE at both sites. ER also increased during this period, likely due to the correlation between increased plant productivity and autotrophic respiration.

Soil properties at both sites were not significantly different with regards to the amount of organic carbon by mass within the topsoil, suggesting that substrate availability was not a limiting factor or control on CO_2 emissions. Significantly

higher bulk density at Site 2 indicates there would be more organic matter within the same volume of soil, however, Tiemeyer et al. (2020) found soils with substantially different organic carbon contents did not have significantly different CO_2 emissions. Similarly, Säurich et al. (2019a) found no correlation between CO_2 fluxes and organic carbon content. Decreased porosity has previously been shown to be an indicator of increased decomposition (Moore et al., 2005), and Berglund and Berglund (2011) measured higher CO_2 emissions from a soil that was more decomposed, which may have been a minor factor in the differences between sites.

There have been numerous studies which have concluded that CO_2 emissions will increase as the thickness of the unsaturated zone increases (e.g. Couwenberg et al., 2010; Carlson et al., 2015), implying that CO_2 is emitted from the whole unsaturated soil profile, which the results of this study contradict. At both sites, CO_2 was primarily produced in the shallow surface peat. Firstly, the profile of VMC with depth illustrates that moisture was not limiting below 50 cm depth in March (Figure **4.11**). Secondly, the rainfall event in late February that increased VMC at 5 cm depth and initiated a rapid increase in ER (the Birch effect) at Site 1, indicated that CO_2 emissions largely originated from the surface peat. These findings emphasise the importance of measuring VMC rather than RWL in CO_2 emission studies, and provide potential reasoning behind why there have been so many contradicting results with respect to the influence of RWL on CO_2 emissions from drained peatlands (e.g. Renger et al., 2002; Berglund & Berglund, 2011).

4.5 Conclusions

Spatially, RWL and VMC varied at both sites, where RWL was lower, and soils generally drier, in close proximity to the drains. The drainage design appeared to have no control on the spatial pattern of RWL, and at both sites, drawdown was equal either side of the drainage channels. This pattern was apparent with both drainage styles year-round. VMC appeared to follow a similar trend to RWL, but the sampling design was not spatially detailed enough to provide conclusive evidence. Deeper drains did appear to have some influence on the depth of the water table, where RWL was generally lower at Site 2, as well as RWL in dipwells adjacent to the deep drains either side of the transect at Site 1. The climatically warm and dry year in 2019, which meant that the drains were active only for a very

short period of the year, appeared to dampen RWL fluctuations in close proximity to the drains.

Temporally, the water balance appeared to be the dominant hydrological control, where changes in storage driven by precipitation and evaporation resulted in a strong seasonal variation of RWL and VMC at both sites. Soil physical properties and to a much lesser extent, drainage design, were minor hydrological controls, the effects of which caused differences between sites. At Site 1, VMC was more variable, while at Site 2, RWL was more variable. Soil physical properties at Site 2, with respect to higher soil bulk density and reduced hydraulic conductivity, appeared to prevent VMC from becoming as low as at Site 1 during the first dry period. This was attributed to the inverse relationship that exists between bulk density and pore size distribution, likely increasing water holding capacity at Site 2 during times of high suction potential, such as that of the first dry period. The reduced ability of Site 1 to retain soil moisture at high suctions initiated hydrophobic behaviour in the surface peat, which Site 2 did not appear to be influenced by. Deep capillary zones were measured at both sites, both of which well exceeded depths in published literature. It appeared capillary rise processes were stronger at Site 2, which caused the continued lowering of RWL between April and June that was not measured at Site 1. Rainfall events following the extended summer drought caused rapid RWL fluctuations at both sites, and were attributed to preferential flow pathways (deep soil cracks) at both sites as well as hydrophobic surface peat at Site 1. Hydrophobicity of Site 1 caused VMC to increase at a slower rate than at Site 2 over the wet period, which was particularly pronounced at 5 cm depth. Greater fluctuations in RWL at Site 2 over the wet period were likely due to a lower specific yield, potentially a result of higher bulk density.

At both sites, the relationship between RWL and VMC was hysteretic, and a strong relationship was only evident when surface peat was near saturation; at the beginning of the two dry periods, and the middle of the wet period. RWL and VMC decreased linearly with respect to one another at the beginning of the dry periods, until VMC was depleted and a strong relationship between them was no longer apparent at either site. In the middle of the wet period, as intermittent rainfall events caused fluctuations in RWL and VMC, the two variables were correlated. Hysteretic behaviour was most prevalent following the extended summer drought,

where VMC and RWL displayed different, and delayed, responses to rainfall; likely a result of preferential flow pathways and hydrophobic surface peat. Short-term hysteretic loops were more apparent at Site 2, as the soil was less affected by hydrophobicity.

CO_2 emissions from both sites had a very low dependency on RWL, and instead appeared to be dominantly driven by changes in VMC, and to a lesser extent, soil temperature. The effect of soil temperature was only apparent when VMC was higher, especially over the wet winter period. During the extended dry period, the increased water holding capacity at Site 2 caused ER to continue at a higher rate than at Site 1, where ER appeared to be constrained by water limitations. The Birch effect provided further evidence towards this. Rates of GPP were very similar between sites, leading to the conclusion that the striking difference in NEE, of 5.6 t C ha^{-1} greater at Site 2, was caused by the large deviation in ER between sites initiated in late January and continued throughout the extended dry period. The findings of this study indicated that organic carbon content was not a controlling factor on the efflux of CO_2, and CO_2 emissions appeared to largely originate from surface peat. The lack of relationship between VMC and RWL during periods of the year, and the demonstrated importance of surface peat towards CO_2 emissions, may lead to explain why there have been such contrasting results in the literature with respect to the optimum water table depth to reduce CO_2 from drained peatlands.

Chapter 5

Spatiotemporal variability of surface elevation in a drained agricultural peatland

5.1 Introduction

The surfaces of drained peatlands do not remain static over time (Strack et al., 2005). Occurring over long time scales, subsidence results in an irreversible loss of soil carbon (through peat oxidation), and induces changes to soil physical and hydraulic characteristics (Kuntze, 1965; Price et al., 2003; Liu & Lennartz, 2019). Superimposed on the rate of irreversible subsidence, is the shrinking and swelling behaviour of drained peatlands that operate on hourly to seasonal time scales (Peatland surface oscillation, PSO; Egglesmann, 1984; Camporese et al., 2006). These reversible fluctuations in surface elevation reflect considerable changes to peat volume in response to variable hydrological conditions (Egglesmann, 1984) imposing different effective stresses on the soil matrix (Price, 2003).

In a drained peatland in the Waikato Region, spatially explicit and high-resolution temporal oscillations in peat surface elevation were measured at two sites for ten months. The objective was to quantify reversible spatiotemporal variations in peat surface elevation, as related to hydrological variability and soil physical properties, and compare these to long-term irreversible subsidence rates.

5.2 Methods

Spatial patterns of changes in surface elevation were assessed along the hydrological transects at the two sites (Figure **3.2**). The transects were equipped with four benchmarks, one at either end of the transect, and two within the transect as survey accuracy checkmarks. Each benchmark consisted of a steel rod inserted through the peat and approximately 1.5 m into the underlying Hinuera Formation, to prevent vertical movement. The upper 2 m of the benchmark rods were run through PVC tubes to prevent the steel rods contacting shallow peat. Benchmark elevations were determined on February 22, 2019, with real-time kinematic (RTK) surveying (Viva GS16 GNSS Smart Receiver and CS20 Controller, Leica

Geosystems, Heerbrugg, Switzerland), for which local geodetic marks (Land Information New Zealand) were used to obtain an accurate vertical datum. Every month, repeated peat surface elevation surveys were carried out, using a total station (VX DR Plus and TSC3 Controller, Trimble, Sunnyvale, CA, USA; 10 mm accuracy) with precision within 9 mm.

Half-hourly fluctuations in peat surface elevation were measured at two sites along each transect, at hump and mid-slope topographic positions, by implementing a paired pressure transducer methodology adapted from Fritz et al. (2008). At each site, two pressure transducer probes (INW LevelSCOUT, Seametrics, Kent, WA, USA) were deployed within a single dipwell (Figure **5.1**). One probe was suspended on a braided stainless steel wire from a steel benchmark rod adjacent to the dipwell, fixed in place (AWL). The other was suspended from a steel rod bridging two aluminium channels affixed to the peat just below the soil surface, free to move with the peat (RWL). The water table acted as a mobile benchmark, where changes in surface elevation were calculated by subtracting RWL from AWL (Fritz et al., 2008).

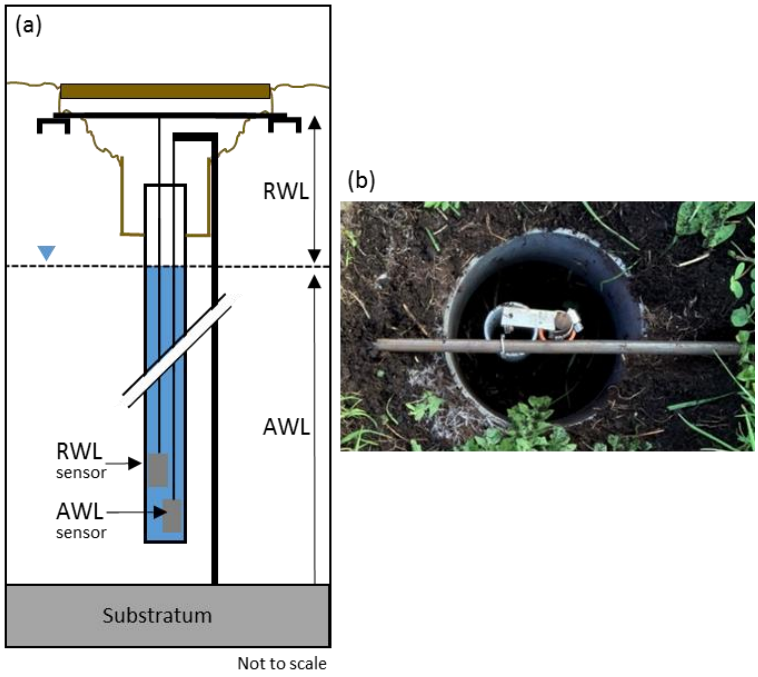

Figure 5.1 (a) Cross-sectional diagram of the paired pressure transducer method, showing the steel rod bridging the aluminium channels either side of the dipwell, from which the RWL probe is suspended, and the vertical benchmark rod from which the AWL probe hangs, (b) vertical photograph of a dipwell containing paired pressure transducers.

5.3 Results

5.3.1 Climate and hydrology

Rainfall between 1 March and 31 December 2019, totalled 779 mm for Site 1 and 801 mm for Site 2; 77% and 79% of the long-term average rainfall totals of 1013.5 mm in Cambridge (1981-2010; NIWA, 2017) for these months, respectively. Both sites were subject to non-normal conditions before shrinkage measurements began, where December 2018 was 256% wetter than normal, which was followed by low rainfall (32% of average) in January and February 2019 (Figure **4.2**). The study period can be separated into three distinct periods. The first period, March to June, was characterised by rainfall that totalled only 65% of the long-term average. In July, August and September, rainfall was 120% above average. In October to December rainfall amounted to 38% of the long-term average, which was particularly pronounced in November (14%).

Figure **5.2** shows hydrological patterns prior to and during the time period of interest. Low precipitation in January and February 2019 meant that a considerable drawdown in RWL and VMC had occurred by March. Between March and June, RWL at Site 2 continued to get deeper, however, Site 1 RWL appeared to level off and remain relatively constant during this time. VMC during this period was much lower at Site 1, despite having a water table closer to the surface. Sporadic rainfall events that occurred between April and June recharged VMC but were not of sufficient size to significantly affect RWL.

Rainfall at the beginning of June increased both RWL and VMC. RWL over the wet winter period (June to October 2019) was, in general closer to the peat surface at Site 2 (Figure **4.5**), although RWL fluctuations at both sites followed a similar pattern. VMC at Site 1 increased more gradually than at Site 2 over the wet period, likely due to hydrophobic behaviour from excessive drying over the extended summer drought. The same trend was not observed at Site 2, likely because the soil was able to sustain a higher moisture content between February and May. VMC at both sites were similar between late August and early September, after which a sudden increase was measured at Site 1. This increase was measured by all soil probes at Site 1 and corroborated with manual measurements. It was therefore

unlikely to be a sampling issue, instead suggesting hydrophobicity was overcome. Extremely low rainfall from late October caused RWL and VMC to drawdown.

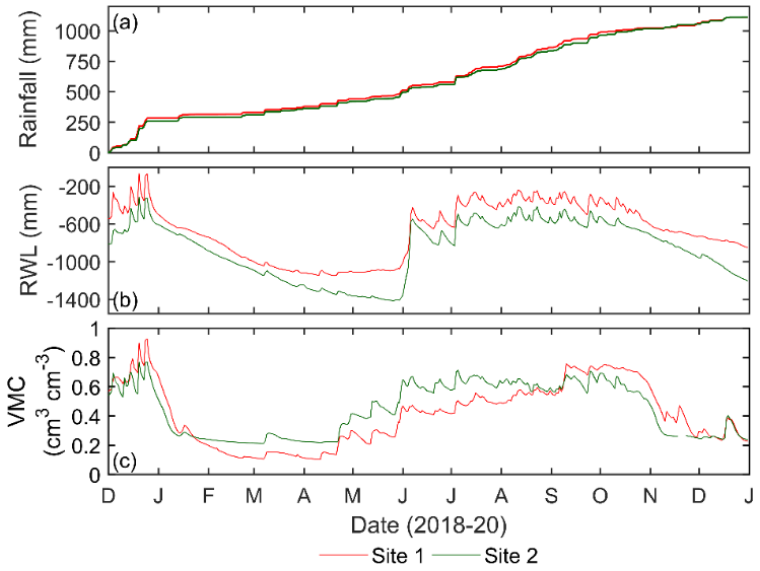

Figure 5.2 Time series of (a) cumulative rainfall, (b) daily mean relative water level (RWL), and (c) daily mean soil volumetric moisture content (VMC) at 10 cm depth, at Sites 1 and 2 between December 2018 and December 2019.

Hydrological variation existed between the transects at each site (

Table **5.1**), with manual RWL measurements along the transect at Site 1 averaging -562 mm and Site 2, -696 mm. Intra-site differences were more pronounced across the paddocks than the drains, with mean RWL beneath the paddocks at Site 1 being -784 mm and Site 2, -911 mm. This difference was also evident in the total range of RWL manual measurements, 1067 mm at Site 1 and 1227 mm at Site 2. However, the range of RWL in the drains contrasted this, where Site 1 had a range of 1217 mm and Site 2, 1040 mm.

Table 5.1 Summary of mean manual relative water levels (RWL) and ranges for the whole transects, drains and paddocks, at Site 1 and 2 between 1 March, 2019, and 16 January, 2020.

	Site 1 (mm)	**Site 2 (mm)**
Mean RWL	-562	-696
Mean RWL (drains)	-260	-265
Mean RWL (paddocks)	-784	-911
RWL range	1655	1770
RWL range (drains)	1217	1040
RWL range (paddocks)	1067	1227

5.3.2 Soil physical properties

Soil bulk density (25 – 75 mm depth) displayed seasonal variation over the measurement period, and varied along the transects and between the sites (Figure **5.3**; Table **5.2**). Consistently higher bulk density was measured at Site 2, with the mean over the paddocks being 0.36 g cm^{-3}, compared to Site 1, with a mean of 0.30 g cm^{-3} (Table **5.2**); a difference that was statistically significant ($p < 0.05$). When compared to the paddocks, bulk density was higher in the drains at both sites, but the difference was not statistically significant.

Table 5.2 Mean bulk density values (mean ± 1 standard deviation) within the paddocks and adjacent to the drains for Sites 1 and 2. Letters represent whether the difference between sites was statistically significant ([a]) or not statistically significant ([b]) derived from paired T-tests.

	Site 1 (g cm^{-3})	**Site 2 (g cm^{-3})**
Mean bulk density (paddocks)	0.30 ± 0.04[a]	0.36 ± 0.01[a]
Mean bulk density (drains)	0.31 ± 0.05[b]	0.37 ± 0.02[b]

Soil bulk density increased during the initial wetting of the peat in June, and then decreased slightly over winter, which was more pronounced at Site 1. Mean bulk density increased at both sites near the end of the measurement period. Bulk density was more spatially variable at Site 1 than Site 2. For each measurement date, there was considerable variation between soil cores, which were sampled at various locations along the transect. The magnitude of variation can be inferred by the width of the error bars (Figure **5.3**).

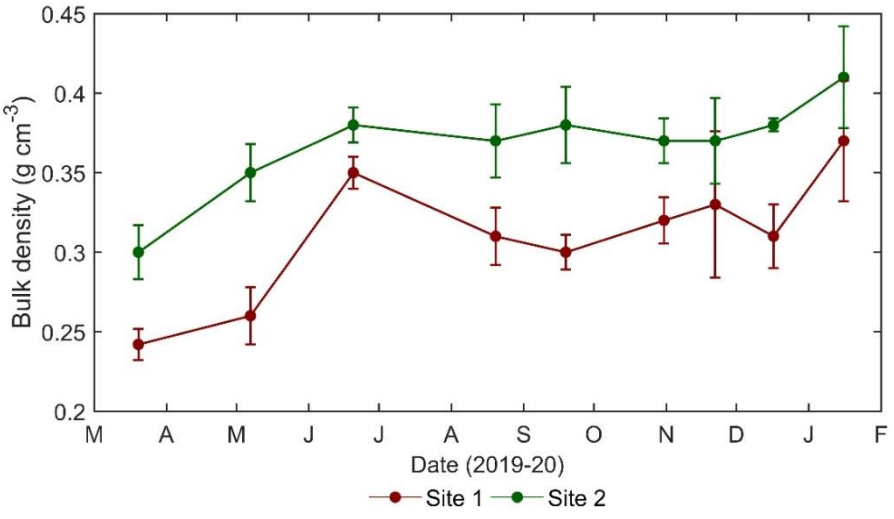

Figure 5.3 Time series of manual soil bulk density measurements at 25 – 75 mm depth (mean of four samples ± 1 standard deviation) between March and December 2019.

5.3.3 Spatial variability of peat surface elevation

Maximum peat surface elevations (SE) across Sites 1 and 2 were surveyed on 19 September, 2019, while minimum SE were surveyed on 16 January, 2020. During this period, peat shrinkage rates were spatially variable along the transects at both sites (Figure **5.4**). Peat close to the drains, where RWL was higher, shrank less than the peat in the middle of the paddocks, where RWL was lower (Table **5.3**). More shrinkage was apparent along the entirety of the transect at Site 1, a trend that was not reflected by differences in RWL during this period (
Table **5.1**), but was consistent with lower VMC (Figure **5.2**).

The mean range of SE change further portrays the spatial variability of PSO (Table **5.3**; Figure **5.4**). Parts of the paddocks at both sites shrank more than others, but this had no evident spatial trend. The range of SE over the paddocks was greater at Site 2, suggesting SE was more spatially variable than at Site 1.

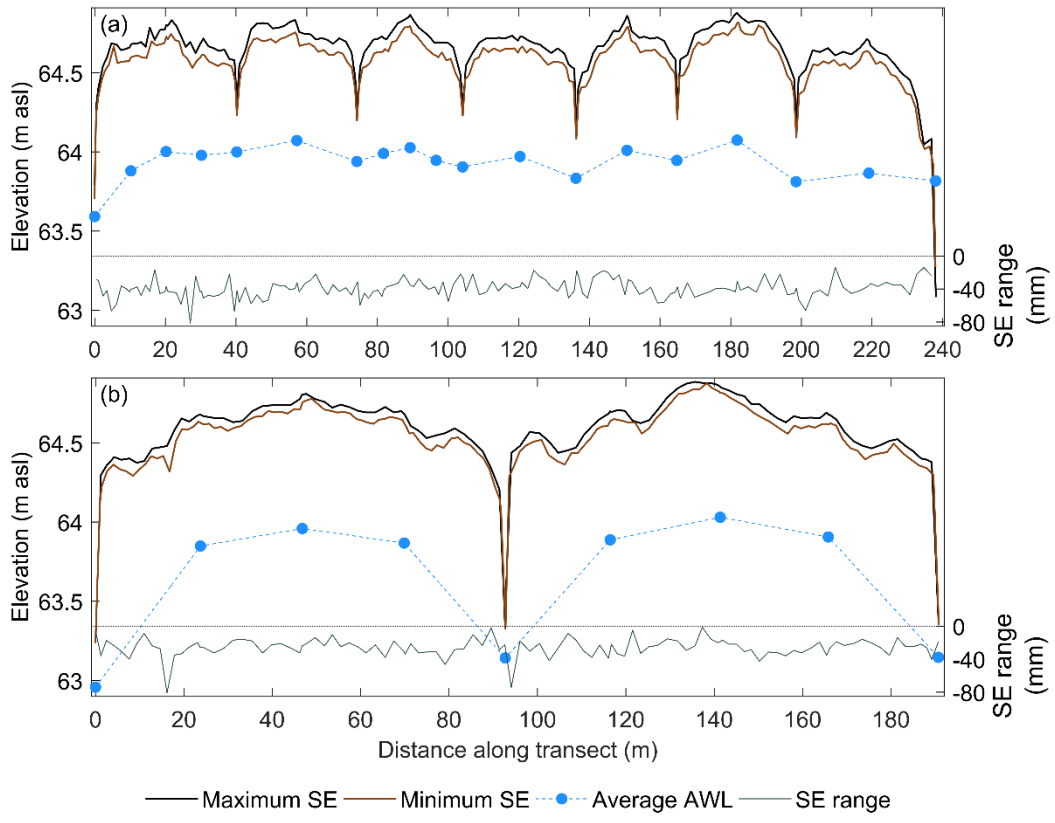

Figure 5.4 Spatial variability of peat surface elevation (SE) along the transects surveyed at (a) Site 1 and (b) Site 2, showing topographical differences and the range of SE change between maximum (19 September 2019) and minimum (16 January 2020) SE. Mean absolute water level (RWL) is also shown during that time, where each circle denotes the location of a dipwell.

Table 5.3 Summary of mean surface elevation (SE) changes and ranges (± 1 standard deviation) between maximum and minimum SE for the whole transect, drains and paddocks, at Site 1 and 2 between March 1, 2019, and January 16, 2020, from survey data.

	Site 1 (mm)	**Site 2 (mm)**
Mean SE change	39 ± 10	26 ± 11
Mean SE change (drains)	32 ± 8	15 ± 9
Mean SE change (paddocks)	39 ± 10	26 ± 11
SE range	67 ± 10	79 ± 11
SE range (drains)	24 ± 8	17 ± 9
SE range (paddocks)	67 ± 10	79 ± 11

5.3.4 Temporal variability of peat surface elevation

Based on the paired transducer probe time series, PSO exhibited a strong seasonal pattern between March and December 2019 (Figure **5.5**). The peat surface shrank during dry conditions and reached lowest elevation in May, followed by swelling processes during wet conditions, and highest elevation in September. PSO followed an opposite trend to bulk density between July and December, which was particularly pronounced at Site 1 (Figure **5.3**). Overall, PSO followed a similar pattern at each of the sites, indicating the underlying processes causing shrinkage and swelling were similar. Greater PSO occurred at Site 1.

Temporally, shrinking and swelling processes can be attributed to wetting and drying cycles. The first drying cycle, which persisted between March and June, was characterised by a continuous lowering of the peat surface at both sites. Site 1 had a higher rate of shrinkage, which caused the sites to deviate from one another (Figure **5.4**). Over these four months, shrinkage caused reductions in SE of 49 mm at Site 1 and 32 mm at Site 2 (Table **5.4**).

Coinciding with rainfall events in late May and early June, rapid peat expansion was indicated by increases in SE, marking the beginning of a wetting cycle. Like in the drying cycle, the rate at which the soil at Site 1 swelled also appeared to be greater than at Site 2. This behaviour caused the deviation between sites in SE change to narrow by late September, after which the sites behaved similarly in October. The wetting phase lasted until the end of October, during which time all reductions in SE that were observed over the previous drying cycle were more than

regained. Total surface swelling between June and October amounted to 66 mm at Site 1 and 46 mm at Site 2 (Table **5.4**).

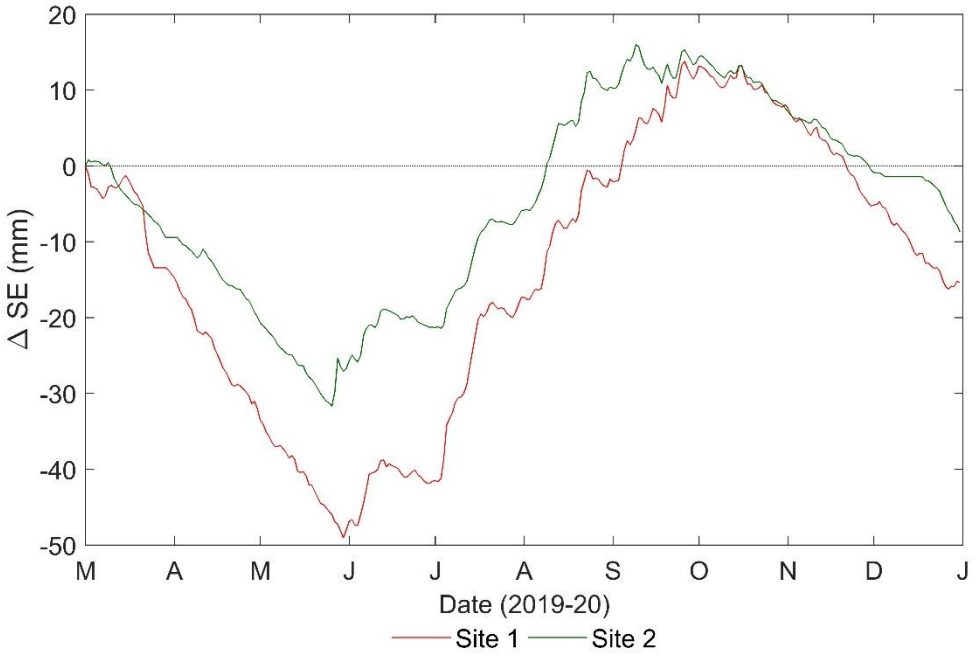

Figure 5.5 Time series plot of changes in peat surface elevation (SE) based on mean daily data from one of the paired transducer systems at Sites 1 and 2[8] between 1 March and 31 December 2019.

Table 5.4 Summary of total surface elevation (SE) changes for the drying (March – June 2019; October – December 2019) and wetting (June – October) cycles at Sites 1 and 2 over the measurement period, showing paired transducer and manual measurements (distance between the peat surface and the top of each dipwell over the paddocks).

	Site 1 (mm)	**Site 2 (mm)**
Paired transducer		
SE change (March – June)	-49	-32
SE change (June – October)	66	46
SE change (October – December)	-30	-24
Manual		
SE change (March - June)	-24	-24
SE change (June - October)	37	26
SE change (October - December)	-35	-30

[8] Only one probe was shown from Site 2, from a malfunction with one of the paired transducer systems resulting in SE changes that could not have been real (Figure **B.1**). For ease of comparison, only one probe is shown from Site 1.

Low precipitation from the end of October led to the beginning of another drying cycle. Initially, both sites had similar oscillations and shrank at the same rate. Extremely low rainfall in November caused the sites' shrinkage behaviour to depart from one another, and by the end of December, Site 1 shrank a total of 30 mm, and Site 2, 24 mm. The shrinkage rate at the beginning of this drying cycle (0.51 mm day^{-1} and 0.25 mm day^{-1} at Sites 1 and 2, respectively) occurred at a slightly slower rate than at the end of the previous drying cycle (0.39 mm day^{-1} and 0.27 mm day^{-1}) at Site 1, but not Site 2.

Manual shrinkage measurements of the surface peat (distance between the peat surface and the top of each dipwell) show the same seasonal variation in SE changes (Figure **5.6**), and indicate considerable shrinkage prior to commencement of paired transducer measurements in March 2019 (-34 mm and -15 mm for Sites 1 and 2, respectively). Manual measurements (Table **5.4**) indicate less shrinkage between March and June (24 mm for both sites), and less swelling between June and October (37 mm and 26 mm) than the paired transducers. During the second drying cycle, however, manual measurements indicated shrinkage of 35 mm and 30 mm, both of which were greater than measurements from the paired transducers. Similar to the survey results in Figure **5.4**, manual measurements portray the highly variable shrinkage processes along the transects, as inferred by the width of the error bars.

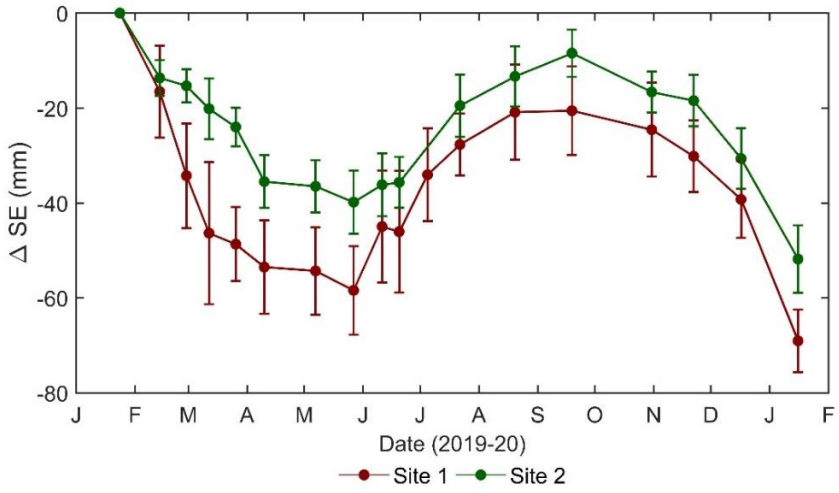

Figure 5.6 Time series of mean manual shrinkage measurements (mean ± 1 standard deviation) between January 2019 and January 2020, made by measuring the change in distance between the peat surface and the top of each dipwell.

The relationship between rainfall, VMC, RWL and PSO between 21 April and 28 June is shown in Figure **5.7**. This period represents the end of a drying cycle leading into a wetting cycle. Shrinkage behaviour at the beginning of this period was initially parallel between sites, with regards to both rate and magnitude of shrinkage. Rainfall on 27 May resulted in rapid swelling of peat at Site 2, causing a 6.7 mm increase in SE, a change which was not reflected by RWL or VMC; suggesting swelling occurred in the top 50 mm of peat above the soil moisture probes. Site 1 showed no response to this rainfall event and shrinkage at this site continued until 31 May, after which there was a response to rainfall.

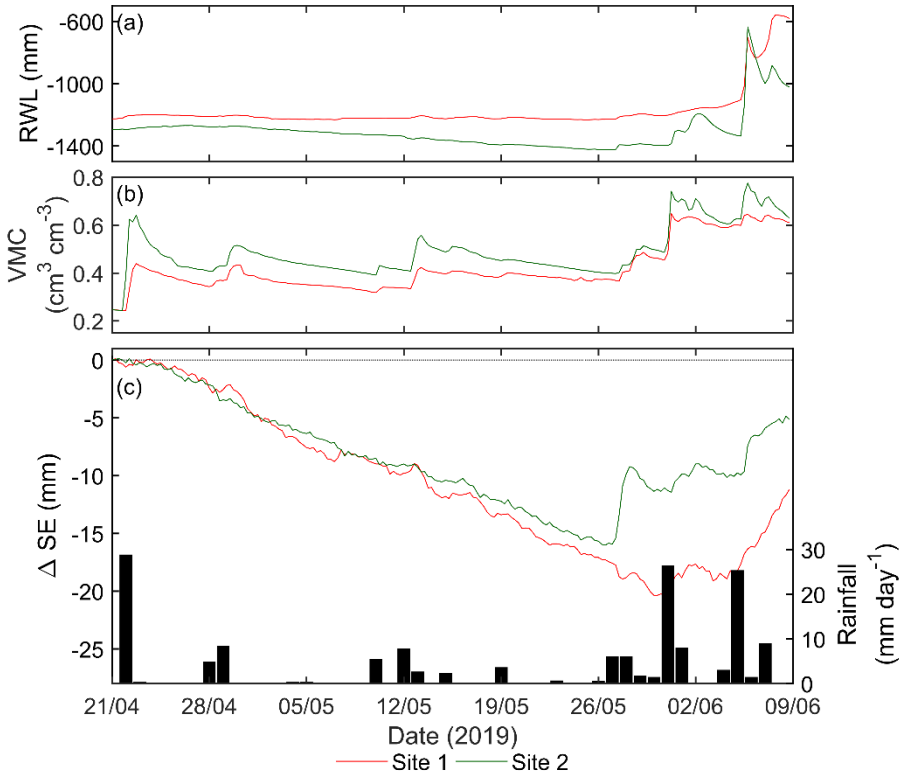

Figure 5.7 Time series plots of six-hourly mean (a) relative water level (RWL), (b) soil volumetric moisture content (VMC) at 5 cm depth, and (c) change in peat surface elevation (SE) and daily rainfall totals at Sites 1 and 2 for 48 days starting 21 April 2019, encompassing the end of the drying cycle and beginning of the wetting cycle.

Towards the end of the wetting cycle (Figure **5.8**), there was less short-term variation in SE than the end of the first drying cycle (Figure **5.7**). The peat was likely near saturation at both sites, which was particularly evident from VMC appearing to flatline at Site 1. PSO behaviour was almost identical at both sites, with peaks and troughs of SE observed at the same time. Site 1 was more responsive to hydrological changes, and showed an increased amount of SE fluctuation, despite lower RWL and VMC fluctuations than Site 2. Site 1 did, however, have a higher

VMC over this period. It is apparent that in the middle of wet periods SE was more correlated with fluctuations in RWL, due to a stronger relationship between VMC and RWL (Figure **4.9**).

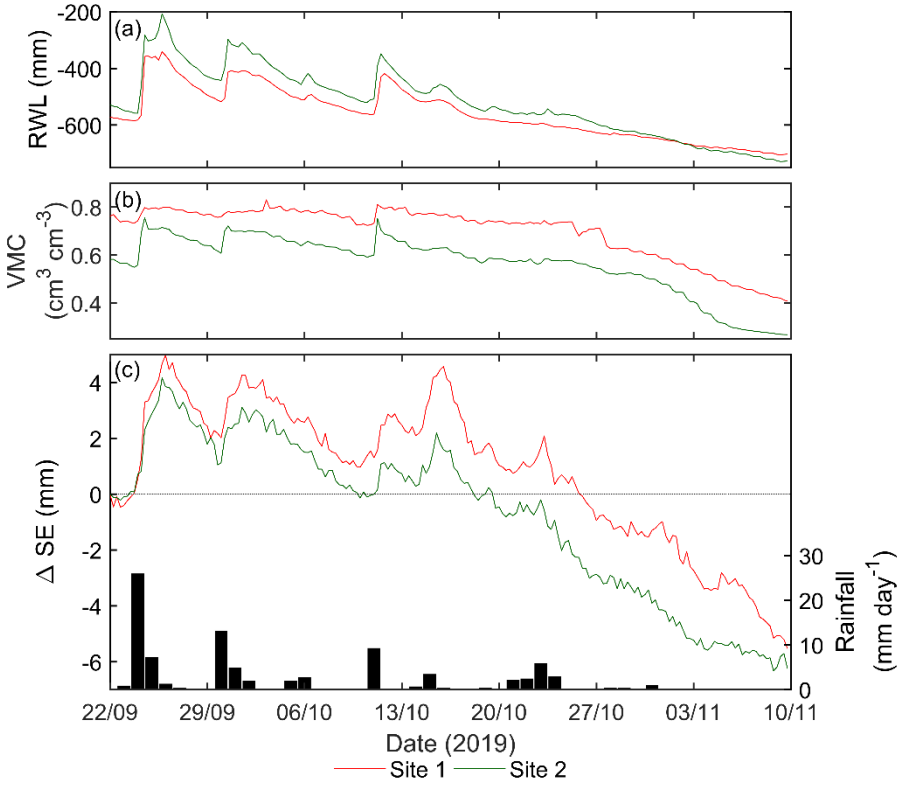

Figure 5.8 Time series plots of six-hourly mean (a) relative water level (RWL), (b) soil volumetric moisture content (VMC) at 5 cm depth, and (c) change in peat surface elevation (SE) and daily rainfall totals at Sites 1 and 2 for 48 days starting 22 September 2019, encompassing the end of the wetting cycle and beginning of the drying cycle.

5.3.5 Hysteretic surface elevation changes

The relationship between RWL and SE for both sites displayed substantial hysteretic behaviour (Figure **5.9**), which can be separated into five segments. In segment A (March to May), a rapid decrease in SE occurred (-49 mm and -32 mm for Sites 1 and 2, respectively), and to a lesser extent, RWL (-208 mm and -477 mm). The range of RWL change during this segment was greater at Site 2 than Site 1, as shown in Figure **5.2**. Segment B (May to June) encompassed the transition from drying cycle to wetting cycle. The peat was rewetted after an extended summer drought, which led to slightly increased SE (6 mm and 8 mm), and a larger, and delayed, response of RWL (605 mm and 757 mm; Figure **5.7**). Segment C represents the wetting cycle, when rainfall events increased RWL and SE. Considerable short-term hysteresis was evident during this segment due to

intermittent rainfall events, causing fluctuations in both SE and RWL. Visible as 'loops' in the data, these fluctuations were confounded by an evident delay between SE and RWL changes, where RWL was increasing while SE appeared to still be decreasing following the previous rainfall event.

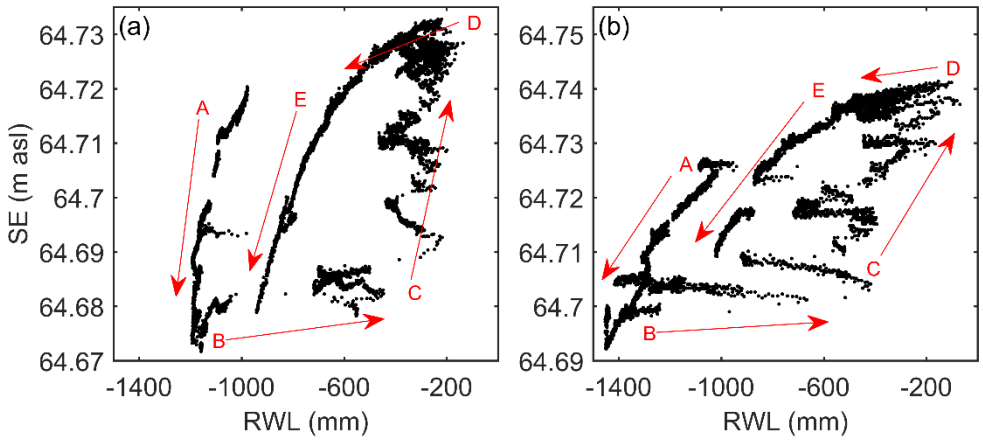

Figure 5.9 Half-hourly values of peat surface elevation (SE) plotted against relative water level (RWL) at (a) Site 1 and (b) Site 2, for the measurement period (1 March – December 2019) Note that the values on the Y axes differ between sites, but the ranges are the same. Arrows indicate the time sequence, and letters are referred to in the text.

In segment D (September to November), lower rainfall resulted in decreases in both SE and RWL. A greater change in RWL (-313 mm and -359 mm) relative to SE (-9 mm and -14 mm) occurred, because VMC was initially high (Figure **5.8**). Segment E, between November and January, was characterised by low rainfall forming the second distinct drying curve at both sites, offset compared to segment A. The behaviour between segments A and E, however, appeared to be very consistent. In comparison to Site 1, there was less drawdown in SE (-45 mm and -28 mm) relative to RWL (-429 mm and -466 mm) at Site 2.

5.4 Discussion

5.4.1 Temporal variability of peat surface elevation

The reversible peat surface elevation changes measured in this study were approximately 3.5 (Site 1) and 2.5 (Site 2) times greater than the regional irreversible subsidence rate of 19 mm yr^{-1} (Pronger et al., 2014). The ranges (66 mm and 46 mm from paired transducers at Sites 1 and 2, respectively) align well with other values in published literature, particularly at Site 2. Egglesmann (1984) reported oscillations of 40 mm in German drained peatlands, while Zanello et al.

(2011) and Teatini et al. (2004) measured reversible fluctuations as much as 40-50 mm in Italy, and in the Netherlands, Schothorst (1982) measured SE changes of 40-80 mm.

Seasonal variability of rainfall, VMC and RWL were closely followed by changes in SE at both sites, likely in response to different effective stresses imposed on the peat matrices (Price, 2003). As expected, the surfaces of both sites shrank to minimum elevation during a drying cycle and swelled to a maximum during a wetting cycle; a pattern that is typical of drained peatlands (Egglesmann, 1984; Zanello et al., 2011). At the beginning of the second drying cycle (November), shrinkage processes were initiated as soon as the peat began to dewater from near saturation, but at a slower rate at Site 1 when compared to the end of the previous drying cycle. As macropore collapse began, PSO was most correlated with VMC. The surface peat continued to dry (March), and the shrinkage rate appeared to have increased at Site 1, similar to the change in shrinkage rate that Oleszczuk et al. (2003) measured under laboratory conditions. PSO and VMC appeared to be no longer correlated at this point, and shrinkage could instead be explained by the drawdown of RWL; increasing effective stress on the peat matrix due to lower pore water pressure, and higher overburden stress from overlying peat layers (Oleszczuk et al., 2003). Further evidence for shrinkage at depth is provided by manual PSO measurements. These measurements indicated less shrinkage between March and June than the paired transducers, suggesting that the volume changes were not confined to surface peat. Similarly, Price and Schlotzhauer (1999) found shrinkage to take place deeper in the soil profile once the surface peat had dried and compressed.

Swelling dynamics in the wetting cycle (June) at Site 1 appeared initially to be affected by peat hydrophobicity, because only the soil at Site 2 swelled in response to a large rainfall event at the end of May. Hydrophobicity has been reported to affect peat soils that dry out below a VMC of 0.3 cm^3 cm^{-3} (Berglund & Persson, 1996), which occurred at both sites in this study but only appeared to affect Site 1 (Figure **4.8**). It appeared that VMC at Site 1 did not fully recover from surface peat hydrophobicity until September, however, rapid recharge of RWL in June caused swelling of the peat at both sites. This phenomenon has also been described by Schwärzel et al. (2002) and Schothorst (1982), which they attributed to preferential

flow pathways to the water table due to hydrophobic surface peat. The sudden increase in RWL would have reduced effective stress and caused swelling of the peat matrix, likely at depth. Later in the wetting cycle (September; Figure **5.8**), rainfall, VMC, and RWL were closely linked with PSO, whereby fluctuations in VMC, RWL and SE occurred rapidly in response to rainfall events.

The results of this study demonstrate that the temporal variability of PSO at both sites was influenced by the response of VMC and RWL to rainfall, each of which have varying degrees of importance depending on climatic conditions (Schothorst, 1982). Price (2003) also found a dependence of PSO on both VMC and RWL fluctuations. Other studies have found PSO to be most connected to rainfall and RWL (e.g. Teatini et al., 2004), VMC (e.g. Zanello et al., 2011), but in winter affected also by the diurnal variation in soil temperature which causes the peat to freeze and expand overnight (Teatini et al., 2004; Zanello et al., 2011). Freeze/thaw processes were not an influence on PSO in this study.

Bulk density should increase over the summer as the peat shrinks, and follow the reverse trend over winter; resulting in an inverse relationship with PSO (Price & Schlotzhauer, 1999). Surprisingly, this relationship was only apparent from July to December at both sites. Rather than being a real effect, this could be a measurement artefact, as monthly soil cores were sampled from different locations along the transects. Therefore, it is probable that differences in bulk density between sampling events were not solely a result of shrinkage, and the methodology did not adequately account for the large amount of spatial variation in soil physical properties.

5.4.2 Hysteretic behaviour of surface elevation changes

Peat soils are characterised by hysteretic effects (Ahti, 1987), and hysteresis has been measured in the relationship between WTD and VMC (Chapter 4), response of bulk density to VMC (Price & Schlotzhauer, 1999), and in the soil water retention curve (Schwärzel et al., 2006). On seasonal and intermittent time-scales, considerable hysteretic behaviour was found between SE and RWL at both sites, which formed distinct wetting (segment C) and drying (segments A and E) curves. A strong correlation between SE and RWL in segments A and E were congruent

with the findings of Fritz et al. (2008) from a pristine NZ peatland. Egglesmann (1981, as cited in Fritz et al., 2008), found a more substantial delay between decreasing SE and RWL in a drained peatland, where a rapid decrease in RWL initiated a decline in SE that lasted for several months, continuing even after RWL had recovered.

Short-term hysteresis occurred during the rewetting of peat in segment C, forming small loops characterised by decreasing RWL, and SE that was either static or increasing. Price (2003) measured a similar phenomenon in a drained cutover peatland, which he attributed to methane production at depth, and changes in VMC that were not reflected by PSO. Although this explanation may hold for this investigation, it is more likely that the small loops result from a lag between RWL fluctuations and SE; caused by changes in effective stress taking longer to equilibrate within the peat matrix than what it takes for RWL to increase, consistent with the findings of Fritz et al. (2008).

5.4.3 Spatial variability of peat surface elevation changes

The spatial pattern of PSO along the transects correlated well with the mean shape of the water table; there was less PSO near the drains where RWL was closer to the surface, which is in agreement with the findings of Wosten et al. (1997). The difference in shrinkage between these two landforms may also be attributed to differences in bulk density. Slightly higher, although not significantly different, bulk densities were measured near the drains than over the paddocks, at both sites. Previous research has highlighted that higher bulk density is indicative of a decreased total porosity (e.g. Waddington & Price, 2000), causing the soil to have lower compressibility and, consequently, less of a capacity to shrink.

Within each paddock along the transects, there were no evident spatial trends in PSO, likely a result of the high variability in peat physical and hydraulic properties over short distances that have been observed in drained peatlands (Norberg et al., 2018), and also measured in this investigation.

5.4.4 Intra-site differences

Although the spatiotemporal patterns in PSO were similar at both sites over the measurement period, there were considerable differences between sites, regarding the rates and, correspondingly, the amount of PSO that occurred. The rate of SE change was typically greater at Site 1, which led to variation between the sites temporally, spatially, and in hysteretic behaviour. It is proposed that differences between sites can be explained by differences in soil physical properties. Bulk density has an inverse relationship with pore size distribution (Waddington & Price, 2000), and the higher bulk density at Site 2 suggests a lower total porosity and greater abundance of micropores. Micropores are able to retain more moisture at higher suctions (Price et al., 2003), possibly explaining why VMC at Site 2 remained higher over the extended summer drought, and therefore why less shrinkage occurred relative to changes in water content (as reflected by VMC and RWL). Furthermore, peat soils with lower total porosity have been found to display less volumetric change in response to hydrology (Kennedy & Price, 2005). The thickness of the peat layer has previously been suggested to influence PSO, where a greater thickness of peat leads to a more variable SE (Almendinger et al., 1986). Peat thickness, along with soil physical properties, might serve to explain intra-site differences, since peat depth at Site 1 (7 m) was greater than at Site 2 (5 m).

PSO was spatially more variable within the paddocks at Site 2 and, although there was a smaller range in bulk density over the measurement period, RWL was consistently deeper. Similarly, in a pristine peatland in Sweden, Nijp et al. (2019) found that deeper RWL led to greater variation in peat SE along a transect.

5.4.5 Implications for measurement

The highly variable nature of PSO measured in this study, and others (e.g. Egglesmann, 1984; Teatini et al., 2004), highlights the importance of separately considering reversible surface deformations and long-term irreversible subsidence rates. Since the reversible PSO measured in this study were 250% – 350% greater than long-term annual shrinkage, yearly measurements to determine annual subsidence rates could yield very different results if measured on the same day each year. For example, comparing December 2018 with December 2019. These months had highly contrasting rainfall, and extremely high rainfall in December 2018

would have acted to ‘reset’ shrinkage processes that may have occurred in the preceding spring months. In contrast, the dry December 2019 followed a considerably drier November, and as such, considerable shrinkage had already occurred. Annual subsidence rates for the sites between December 2018 and December 2019 would therefore have been substantially overestimated. If, for some reason, irreversible subsidence measurements can only be measured annually, it is recommended that they are taken at the tail end of winter (e.g. September) to minimise over- or underestimation.

5.5 Conclusions

PSO has not been previously quantified for drained peatlands in Aotearoa New Zealand. In this investigation, PSO was found to be highly active (2.5 and 3.5 times higher than annual irreversible subsidence rates) at two sites on adjacent dairy farms within Moanatuatua drained peatland. The ranges of PSO at these sites align well with values in published literature, with both sites in the upper ranges of reported rates. The magnitude of PSO differed between sites, and Site 1 was much more reactive to hydrological changes. Consistently higher bulk density at Site 2 provides a potential explanation for this, indicating lower total porosity and therefore less susceptibility to SE change.

The seasonal variability of SE strongly followed patterns in rainfall, but correlations to varying magnitudes were observed between PSO, VMC and RWL. The relationships between SE and RWL displayed hysteretic behaviour that separated drying and wetting cycles, probably due to delayed equilibration of effective stresses on the peat matrix, causing SE to rise at a slower rate than RWL. PSO was not spatially uniform; less SE changes were measured near the drains due to higher RWL and lower bulk density. Across the paddocks, no spatial trends in PSO were evident, attributed to the highly variable nature of soil physical properties over short distances.

These findings have demonstrated that irreversible subsidence can only be determined with time periods surpassing twelve months, and highlight the importance of taking PSO into account when designing experimental procedure.

Chapter 6

Conclusions and recommendations

A hydrological investigation was conducted at Moanatuatua drained peatland, at two sites with similar agricultural management practices but different drainage designs and drainage histories, to quantify the nature of and controls on spatiotemporal variability of water table depth (relative water level, RWL) and soil moisture content (volumetric moisture content, VMC), as well as the relationship between these hydrological variables, for an improved understanding of Aotearoa New Zealand drained peat behaviour. Also, the impact of hydrological spatiotemporal variability on CO_2 emissions and reversible subsidence processes were investigated, and the two sites were compared and contrasted.

6.1 Major findings

6.1.1 Spatiotemporal variability of hydrology

RWL and VMC varied spatially at the two sites, where RWL was lower, and soils drier, in close proximity to the drains. At both sites, RWL drawdown appeared to be equal on either side of the drainage channels, creating a parabolic shape in the water table that was apparent with both drainage styles, year-round. VMC appeared to follow the same trend; however, the sampling design was not spatially detailed enough to adequately display this effect. Indicative that drainage design has limited control on the spatial pattern of hydrology, however, the deeper drains at Site 2 did appear to increase RWL depth, as well as the magnitude of RWL fluctuations throughout 2019. Site 1, which had much shallower drains, displayed less RWL fluctuation, and mounding of the water table was less pronounced across the paddocks. Previous research suggests that fluctuations in RWL would be greatest in close proximity to drains, however, the same pattern was not detected at either site, and drainage ditch RWL generally showed less variation than in-field RWL. The year of measurement, 2019, was a climatically warm and dry year, and consequently, drainage ditches were only active for a few months, which may have dampened in-field RWL fluctuations.

Temporally, both RWL and VMC were seasonally varying at both sites, and appeared to be largely driven by the water balance components, $P - E$. Differences between sites were evident and were a result of soil physical properties, and to a much lesser extent, drainage design. Such differences resulted in VMC being more variable at Site 1 and RWL more variable at Site 2. Higher soil bulk density at Site 2 indicated a greater abundance of micropores, leading to increased water holding capacity, reduced hydraulic conductivity, and stronger capillary rise processes at very high matric potentials during drying cycles. These characteristics appeared to prevent VMC at Site 2 from becoming as low as at Site 1 over a dry period and limited the effects of hydrophobicity, which Site 1 was evidently affected by. Active capillary rise processes also appeared to draw RWL further down at Site 2 between April and June, while RWL at Site 1 levelled off. Previous research has indicated that capillary rise processes are often no longer active when RWL is deeper than 1 m, and both sites appear to be exceptional in comparison, particularly Site 2. However, results from the 1.8 m deep peat cores extracted in March, when RWL was 1142 mm at Site 1 and 1146 mm at Site 2, showed deep capillary zones extending approximately 0.6 m above the water table at both sites. Rainfall events in June caused rapid reactions of RWL, likely due to preferential flow pathways (deep soil cracks) initiated during the extended summer drought. In some dipwells, an overreaction of the water table was measured during these rainfall events, which meant that water tables declined much quicker than in the other dipwells. At Site 1, VMC increase occurred at a much slower rate than at Site 2 between March and August, providing further evidence of hydrophobic behaviour. Furthermore, VMC at 10 cm depth surpassed VMC at 5 cm depth at Site 1, suggesting that hydrophobicity was primarily confined to peat near the surface.

6.1.2 Relationship between RWL and VMC

The relationship between RWL and VMC displayed substantial hysteresis, for which a dependent relationship was only apparent when the peat was near saturation. As a result, the two variables were correlated at the beginning of dry periods, and in the middle of the wet period. Hysteresis was most apparent in rewetting of the peat after the extended summer drought, where short-term hysteretic loops were also measured. These loops appeared to be caused by different and delayed responses of RWL and VMC to rainfall. Larger hysteretic loops were

observed at Site 2, due to an increased response of VMC to rainfall, further indicating that Site 1 was affected by hydrophobicity delaying full rewetting.

6.1.3 Hydrological influence on CO_2 emissions

At both sites, CO_2 emissions appeared to be predominantly influenced by VMC, and little affected by depth to water tables. Many studies have concluded RWL to be the dominant driver of CO_2 emissions, however, the apparent lack of a relationship between RWL and VMC year-round at Sites 1 and 2 indicate that the continued use of RWL as a proxy to estimate near-surface moisture conditions is flawed, especially for moisture-dependent processes such as CO_2 production. Aligning with previous research, CO_2 fluxes were also seasonally influenced by soil temperature, the effect of which was more pronounced when VMC was high during winter. The ability of Site 2 to retain a higher VMC over the extended summer drought meant that ecosystem respiration (ER) was less constrained by water availability than at Site 1. Evidence of the Birch effect at Site 1 during February further illustrated that low VMC reduced ER. As gross primary production (GPP) was very similar at the two sites, the ongoing differences between the sites' ER during dry conditions led to accumulated CO_2 emissions of approximately 5.6 t C ha^{-1} greater at Site 2 than at Site 1.

6.1.4 Spatiotemporal variability of PSO

Peatland surface oscillation (PSO), the reversible component of subsidence, was found to be a highly active process at both sites, where vertical movements over a period of 10 months were between 2.5 – 3.5 times greater than the average annual irreversible subsidence rate for the Waikato region (Pronger et al., 2014). This puts both sites in the upper range of published PSO values. PSO was seen to be correlated with rainfall, RWL and VMC, each of which had varying influence during the year. Considerable hysteresis was seen in the relationship between surface elevation and RWL, separating drying and wetting cycles. Short-term hysteresis within the wetting cycle was also measured, which was likely induced by a delay between RWL and surface elevation change, due to the time taken for effective stresses to equilibrate within the peat matrix before a change in surface elevation occurs. Across both transects, less PSO was measured adjacent to drainage channels which correlated with higher bulk density, but across the

paddocks, there were no evident spatial trends. Consistently lower bulk density at Site 1 led to increased PSO compared to Site 2.

6.2 Intra-site differences

Although the two sites had similar management practices and contrasting drainage designs, it appeared that the differences between sites described above were predominantly a result of the drainage history, and potentially affected by the recontouring event at Site 2 in 2016. Site 2 was drained approximately 15 years prior to Site 1, and as a result, decomposition and secondary pedogenic processes had been initiated much earlier. It is widely accepted that peat decomposition acts to decrease total porosity as well as increase bulk density and the abundance of micropores by breaking down organic matter to smaller fragments (Moore et al., 2005). Furthermore, the ability of micropores to hold moisture at lower pore water pressures (Price et al., 2003), increases the water holding capacity of the soil (Kuntze, 1965). Another characteristic of a peat soil with higher microporosity is reduced hydraulic conductivity (Price, 2003), and increased vertical capillary flows (Price et al., 2003).

Site 2 had consistently higher bulk density in the surface soil than Site 1, lower hydraulic conductivity at all suction potentials, as well as an evidently greater connection between surface soil and the underlying saturated capillary zone. This suggests that the degree of peat decomposition was more advanced at Site 2 when compared to Site 1. The differences in hydrology, CO_2 and shrinkage between sites appear to have all been influenced by these dissimilarities in soil physical properties, which raises many questions with regards to the adverse environmental effects of peatland drainage and their continued use as agricultural ecosystems. Because Site 2 had a smaller range of PSO than Site 1, this environmental effect appears to be dampened as time goes on. However, the likely increased water-holding ability during severe drying and connection of the capillary zone to surface moisture conditions at Site 2, meant that ER was less constrained by water limitations and able to continue at a higher rate during an extended summer drought period, having major implications for the carbon balances of drained peatlands. As international literature suggests, these properties continue to be enhanced over time, and worryingly, so too may CO_2 emissions during dry periods.

6.3 Management implications

If current land management practices on drained peatlands are continued, CO_2 emissions and irreversible land subsidence will persist for decades, and based on the findings of this study, may even increase, especially if the frequency and intensity of droughts are increased with ongoing climate change. Moving forward, when considering the need to feed a growing global population whilst adhering to international and national greenhouse gas emission reduction targets, it is clear that changes to the ways we use drained peatlands are imperative.

So how may we achieve this? Aotearoa New Zealand is in a unique position where we can draw on and modify mitigation measures that have been implemented in other countries which have longer, and more extensive, research backgrounds. In the Netherlands, a technique known as subsurface irrigation through the use of submerged drains, has been said to reduce subsidence and CO_2 emissions by at least 50% (Van den Akker & Hendriks, 2017). Submerged drains lie perpendicular to the traditional drainage ditches at approximately -0.8 m depth; in summer acting to irrigate subsurface soil, while in winter removing excess water. Van den Akker and Hendriks (2017) found this method to be highly beneficial from both an environmental and agricultural perspective, being economically feasible for farmers to implement, able to maintain sufficient land trafficability for dairy cattle, and decreasing irreversible subsidence and CO_2 emissions. However, based on the findings in Chapter 4, soils at both sites were near saturation below a depth of approximately -0.5 m, and CO_2 emissions were higher when ER was not water-limited, meaning further research would be required to determine the suitability of this mitigation measure, and how it may be adapted for Aotearoa New Zealand's advantage.

Peatland conservation, through rewetting drained peatlands back to their natural state or raising water tables for modified (e.g. paludiculture) or continued agricultural use, are the most frequently suggested mitigation measures to reduce CO_2 emissions and subsidence (e.g. Norberg et al., 2018; Murdiyarso et al., 2019). Renger et al. (2002) suggested that by raising the water table depth from 70 cm to 30 cm below the surface, 90% of optimum plant production was achieved, CO_2 emissions were reduced by 40 – 50% and subsidence was reduced. In Ireland, Renou-Wilson et al. (2014) suggested that a government-led approach would be

best, to implement a reduction in grazing regimes to actively promote carbon uptake, as well as maintaining higher water tables. However, with both of these mitigation options, agricultural productivity and trafficability would be considerably constrained, impacting wide adoption in Aotearoa New Zealand unless policy was implemented to enforce this. Furthermore, maintaining the water table at a specific level is difficult (Norberg et al., 2018), particularly in the context of a changing climate affecting precipitation patterns, drought intensity, and water availability.

In a review on sustainable drained peatland management in Switzerland, Ferré et al. (2019) concluded that the main challenges for adopting change were current land use profitability and the difficulty of integrating new management practices, particularly in smaller farming operations. Furthermore, they found there to be considerable difficulty in designing policies which promoted alternative and more sustainable land use. Some of their proposed ideas were: payments for environmental services that drained peatlands provide in terms of protecting the carbon stock; subsidies for farmers which maintain high water tables; carbon credits associated with rewetting drained peatlands; product labelling allowing farmers to charge more for their products; and increasing public awareness on the loss of drained peatlands and the associated ecosystem services (Ferré et al., 2019). Each of these ideas may be feasible within Aotearoa New Zealand, but it is clear that we first require a strong scientific background before top-down approaches such as these can be implemented.

Naturally induced changes to soil physical characteristics caused by peat decomposition processes are unavoidable in drained peatlands unless these ecosystems are returned to their natural state or their water tables raised. However, human-induced changes to physical characteristics (e.g. bulk density) that result from intensive agricultural use might be able to be limited wherever possible, as these appeared to have a substantial effect on PSO and CO_2 emissions at the two research sites. Potential approaches that are easily implemented at farm level include reducing stocking rates, reducing livestock weight, increasing length of grazing rotations, cut and carry techniques, and using stand-off pads in winter when VMC is high.

6.4 IPCC reporting

Emission reporting for organic soils under grassland in Aotearoa New Zealand currently adheres to an outdated Tier 1 International Panel for Climate Change (IPCC) framework, based on emission factors (EF) for two climate classes; cold temperate (0.25 ± 0.23 t C ha^{-1} yr^{-1}) and warm temperate (2.5 ± 2.3 t C ha^{-1} yr^{-1}) from the 2006 IPCC guidelines (Ministry for the Environment, 2019). The 2013 Wetlands Supplement (IPCC, 2014) reflects considerable scientific advances made on organic soils, with EF estimates improved and additional categories such as nutrient status and drainage depth included (IPCC, 2014), although as of 2019 Aotearoa New Zealand had not yet adopted this approach (Ministry for the Environment, 2019).

Based on the most recent EFs for organic soils from the Wetlands Supplement, measured CO_2 emissions in 2019 of 1.05 ± 0.66 t C ha^{-1} at Site 1 sits well below the EF for shallow-drained grassland (3.6 t C ha^{-1} yr^{-1}), as well as the 95% confidence interval (1.8 – 5.4 t C ha^{-1} yr^{-1}). CO_2 emissions of 6.66 ± 0.63 t C ha^{-1} at Site 2, however, sits above the EF for deep-drained grassland (6.1 t C ha^{-1} yr^{-1}), but within the 95% confidence interval (5.0 – 7.3 t C ha^{-1} yr^{-1}). Furthermore, emissions at Site 2 far exceed the EF currently used in Aotearoa New Zealand (2.5 ± 2.3 t C ha^{-1} yr^{-1}), and Site 1 sits within the 95% confidence interval. The substantial spatial variability in CO_2 emissions, between the two geographically similar sites, suggests that Tier 1 reporting does not adequately represent emissions from drained peatlands around Aotearoa New Zealand. Correspondingly, there is a need to derive country-specific EFs.

Aotearoa New Zealand should, at least, aspire to Tier 2 reporting and incorporate sub-categories, such as time since drainage and type of management system, allowing for more detailed and comprehensive emission estimates. This is especially imperative as the results of this study indicate that CO_2 emissions may get worse as time since drainage increases. Furthermore, the results of various international studies indicate that different management practices with regards to nutrient amendments will influence CO_2 emissions (e.g. Pinsonneault et al., 2016; Säurich et al., 2019a). Tier 3 reporting improves estimates further, through the construction of models which incorporate driving factors of CO_2 emissions, such as temperature or hydrological temporal variability (IPCC, 2014). While this

approach will lead to best estimates of emissions from drained peatlands in Aotearoa New Zealand, it is resource-intensive and a significant undertaking, especially given the relatively limited extent of research when compared to European countries, such as Germany or the Netherlands.

An example of country-specific greenhouse gas reporting was described by Tiemeyer et al. (2020). In their study, spatially detailed modelling was used for a large emissions dataset, segregated to nine land-use categories. Emissions responses to driving variables (land use category, mean annual water table depth from each category, and type of organic soil) were statistically analysed with two models (multivariate linear and non-linear), to which they were verified and compared to IPCC default EFs (Tiemeyer et al., 2020). As temporal water table variability data were not nationally available, they simplified Tier 3 reporting to a spatially representative Tier 2 approach. Overall, they concluded that their approach led to improved EF estimates specific to Germany, and could be implemented at project level and in other countries providing sufficient data were available (Tiemeyer et al., 2020).

6.5 Future work

To improve on the current study, it would be beneficial to alter aspects of the methodological design. Firstly, it became apparent that the monthly manual soil core sampling strategy did not adequately characterise the whole transect at each of the sites. It is suggested that the number of samples is doubled to eight, and at least three of these be retrieved from adjacent to the drainage ditches. Furthermore, when considering a time series of soil bulk density for the PSO study, there should be some samples which are repeatedly taken from the same locations along each transect. An additional four cores could be taken at each sampling time to achieve this. Secondly, like any temporal scientific study, it would be beneficial to extend measurements past a year-long dataset. This would help determine whether the results presented in Chapters 4 and 5 were primarily a result of an uncharacteristically dry year, or whether they are representative of a long term trend.

To gain an enhanced understanding of the differences between Sites 1 and 2, detailed measurements of peat physical properties need to be conducted, encompassing both space and depth. While both sites were tested for total porosity, VMC and water release characteristics in October, the results of these measurements were not yet available at the time of thesis completion. These measurements will provide more conclusive evidence regarding the soil characteristics of each site and whether, for our sites, total porosity decreases and water holding capacity increases over time. It is recommended that more sites within Moanatuatua drained peatland be tested for soil physical and hydraulic properties, to develop a chronosequence with regards to time since drainage and soil physical characteristics. This should be extended to other drained peatlands in the Waikato region, or elsewhere in Aotearoa New Zealand, to gain a comprehensive understanding of how different drained peatlands behave over time and space. Furthermore, to supplement these data with respect to their environmental impacts, eddy covariance sites to measure CO_2 fluxes should be established.

References

Ahti, E. (1987). *Water balance of drained peatlands on the basis of water table simulation during the snowless period*. Finnish Forest Research Institute.

Almendinger, J. C., Almendinger, J. E., & Glaser, P. H. (1986). Topographic fluctuations across a spring fen and a raised bog in the Lost River Peatland, Northern Minnesota. *Journal of Ecology, 74*, 393-401. https://doi.org/10.2307/2260263

Anshari, G. Z., Afifudin, M., Nuriman, M., Gusmayanti, E., Arianie, L., Susana, R., Nusantara, R. W., Sugardjito, J., & Rafiastanto, A. (2010). Drainage and land use impacts on changes in selected peat properties and peat degradation in West Kalimantan Province, Indonesia. *Biogeosciences, 7*, 3403-3419. https://doi.org/10.5194/bg-7-3403-2010

Armentano, T. V. (1980). Drainage of organic soils as a factor in the world carbon cycle. *Bioscience, 30*, 825-830. https://doi.org/10.2307/1308375

Armentano, T. V., & Menges, E. S. (1986). Patterns of change in the carbon balance of organic soil-wetlands of the temperate zone. *The Journal of Ecology, 74*, 755-774. https://doi.org/10.2307/2260396

Baden, W., & Egglesmann, R. F. (1963). Zur Durchlassigkeit der Moor-boden. On the permeability of marshland. *A. Kulturtech Flurberein, 4*, 226-254.

Balaine, N., Clough, T. J., Beare, M. H., Thomas, S. M., Meenken, E. D., & Ross, J. G. (2013). Changes in relative gas diffusivity explain soil nitrous oxide flux dynamics. *Soil Science Society of America Journal, 77*, 1496-1505. https://doi.org/10.2136/sssaj2013.04.0141

Baldocchi, D. (2008). 'Breathing' of the terrestrial biosphere: lessons learned from a global network of carbon dioxide flux measurement systems. *Australian Journal of Botany, 56*. https://doi.org/10.1071/bt07151

Baldocchi, D. D. (2003). Assessing the eddy covariance technique for evaluating carbon dioxide exchange rates of ecosystems: past, present and future. *Global Change Biology, 9*, 479-492. https://doi.org/10.1046/j.1365-2486.2003.00629.x

Baldocchi, D. D., & Meyers, T. (1988). A spectral and lag-correlation analysis of turbulence in a deciduous forest canopy. *Boundary-Layer Meteorology, 45*, 31-58. https://doi.org/10.1007/BF00120814

Berglund, K., & Persson, L. (1996). Water repellence of cultivated organic soils. *Acta Agriculture Scandinavia, Section B, Soil and Plant Science, 46*, 145-152. https://doi.org/10.1080/09064719609413127

Berglund, Ö., & Berglund, K. (2011). Influence of water table level and soil properties on emissions of greenhouse gases from cultivated peat soil. *Soil Biology and Biochemistry, 43*, 923-931. https://doi.org/10.1016/j.soilbio.2011.01.002

Berglund, Ö., Berglund, K., Jordan, S., & Norberg, L. (2019). Carbon capture efficiency, yield, nutrient uptake and trafficability of different grass species on a cultivated peat soil. *Catena, 173*, 175-182. https://doi.org/10.1016/j.catena.2018.10.007

Blodau, C. (2002). Carbon cycling in peatlands — A review of processes and controls. *Environmental Reviews, 10*, 111-134. https://doi.org/10.1139/a02-004

Boelter, D. H. (1965). Hydraulic conductivity of peats. *Soil Science, 100*, 227-231. https://doi.org/10.1097/00010694-196510000-00001

Boelter, D. H. (1969). Physical properties of peats as related to degree of decomposition. *Soil Science Society of America Journal, 33*, 606-609. https://doi.org/10.2136/sssaj1969.03615995003300040033x

Boelter, D. H. (1972). Preliminary results of water level control on small plots in a peat bog. In *The Use of Peatland for Agriculture, Horticulture, and Forestry. Fourth International Peat Congress Proceedings* (pp. 347-354).

Brouns, K., Eikelboom, T., Jansen, P. C., Janssen, R., Kwakernaak, C., van den Akker, J. J., & Verhoeven, J. T. (2015). Spatial analysis of soil subsidence in peat meadow areas in Friesland in relation to land and water management, climate change, and adaptation. *Environ Manage, 55*, 360-72. https://doi.org/10.1007/s00267-014-0392-x

Burba, G. (2013). *Eddy covariance method for scientific, industrial, agricultural and regulatory applications: A field book on measuring ecosystem gas exchange and areal emission rates*. LI-Core Biosciences.

Burke, W. (1967). Principles of drainage with special reference to peat. *Irish Forestry, 24*, 1-7.

Campbell, D., & Jackson, R. (2004). Hydrology of wetlands. *Freshwaters of New Zealand*, 20.1-20.14.

Campbell, D. I., Wall, A. M., Nieveen, J. P., & Schipper, L. A. (2015). Variations in CO_2 exchange for dairy farms with year-round rotational grazing on drained peatlands. *Agriculture, Ecosystems & Environment, 202*, 68-78. https://doi.org/10.1016/j.agee.2014.12.019

Camporese, M., Ferraris, S., Putti, M., Salandin, P., & Teatini, P. (2006). Hydrological modeling in swelling/shrinking peat soils. *Water Resources Research, 42*. https://doi.org/10.1029/2005wr004495

Camporese, M., Putti, M., Salandin, P., & Teatini, P. (2008). Spatial variability of CO_2 efflux in a drained cropped peatland south of Venice, Italy. *Journal of Geophysical Research: Biogeosciences, 113*. https://doi.org/10.1029/2008jg000786

Candra, R. A., Gusmayanti, E., & Anshari, G. (2016). The relation between water contents and CO_2 fluxes from drained tropical peats. In *15^{TH} International Peat Congress*. Kuching, Sarawak, Malaysia.

Carlson, K. M., Goodman, L. K., & May-Tobin, C. C. (2015). Modeling relationships between water table depth and peat soil carbon loss in Southeast Asian plantations. *Environmental Research Letters, 10*. https://doi.org/10.1088/1748-9326/10/7/074006

Chapin, F. S., Woodwell, G. M., Randerson, J. T., Rastetter, E. B., Lovett, G. M., Baldocchi, D. D., Clark, D. A., Harmon, M. E., Schimel, D. S., Valentini, R., Wirth, C., Aber, J. D., Cole, J. J., Goulden, M. L., Harden, J. W., Heimann, M., Howarth, R. W., Matson, P. A., McGuire, A. D., Melillo, J. M., Mooney, H. A., Neff, J. C., Houghton, R. A., Pace, M. L., Ryan, M. G., Running, S. W., Sala, O. E., Schlesinger, W. H., & Schulze, E. D. (2006). Reconciling carbon-cycle concepts, terminology, and methods. *Ecosystems, 9*, 1041-1050. https://doi.org/10.1007/s10021-005-0105-7

Charman, D. (2002). *Peatlands and environmental change*. John Wiley & Sons Ltd.

Clarkson, B., Thompson, K., Schipper, L., & McLeod, M. (1999). Moanatuatua Bog—proposed restoration of a New Zealand restiad peat bog ecosystem. In *An international perspective on wetland rehabilitation* (pp. 127-137). Springer.

Clarkson, B. R., Ausseil, A.-G. E., & Gerbeaux, P. (2013). Wetland ecosystem services. In J. R. Dymond (Ed.), *Ecosystem services in New Zealand: conditions and trends*. Manaaki Whenua Press, Lincoln, New Zealand.

Clarkson, B. R., Schipper, L. A., & Lehmann, A. (2004). Vegetation and peat characteristics in the development of lowland restiad peat bogs, North Island, New Zealand. *Wetlands, 24*, 133-151. https://doi.org/10.1672/0277-5212(2004)024[0133:VAPCIT]2.0.CO;2

Clymo, R. S. (1963). Peat. In A. J. P. Gore (Ed.), *Ecosystems of the World. Mires: Swamp, Bog, Fen and Moor* (pp. 159-224). New York, NY: Elsevier.

Couwenberg, J. (2011). Greenhouse gas emissions from managed peat soils: is the IPCC reporting guidance realistic? *Mires and Peat, 8*.

Couwenberg, J., Dommain, R., & Joosten, H. (2010). Greenhouse gas fluxes from tropical peatlands in South-East Asia. *Global Change Biology, 16*, 1715-1732. https://doi.org/10.1111/j.1365-2486.2009.02016.x

Cranwell, L. M. (1939). Native vegetation. Soils and agriculture of part of Waipa County. 23-29. https://doi.org/10.7931/DL1-SBP-0005.

DairyNZ. (2019). New Zealand dairy statistics 2018-19.

Davidson, E. A., & Janssens, I. A. (2006). Temperature sensitivity of soil carbon decomposition and feedbacks to climate change. *Nature, 440*, 165-73. https://doi.org/10.1038/nature04514

Davoren, A. (1978). *A survey of New Zealand peat resources*. (Vol. 14). New Zealand: University of Waikato for the National Water and Soil Conservation Organisation.

Dawson, Q., Kechavarzi, C., Leeds-Harrison, P. B., & Burton, R. G. O. (2010). Subsidence and degradation of agricultural peatlands in the Fenlands of Norfolk, UK. *Geoderma, 154*, 181-187. https://doi.org/10.1016/j.geoderma.2009.09.017

De Vleeschouwer, F., Chambers, F. M., & Swindles, G. T. (2010). Coring and sub-sampling of peatlands for palaeoenvironmental research. *Mires and peat, 7*.

Delta-T Devices Ltd. (2017). *User manual for the ML3 ThetaProbe*. https://www.delta-t.co.uk/wp-content/uploads/2017/02/ML3-user-manual-version-2.1.pdf.

Dettmann, U., Bechtold, M., Frahm, E., & Tiemeyer, B. (2014). On the applicability of unimodal and bimodal van Genuchten–Mualem based models to peat and other organic soils under evaporation conditions. *Journal of Hydrology, 515*, 103-115. https://doi.org/10.1016/j.jhydrol.2014.04.047

Dettmann, U., Bechtold, M., Viohl, T., Piayda, A., Sokolowsky, L., & Tiemeyer, B. (2019). Evaporation experiments for the determination of hydraulic properties of peat and other organic soils: An evaluation of methods based on a large dataset. *Journal of Hydrology, 575*, 933-944. https://doi.org/10.1016/j.jhydrol.2019.05.088

Deverel, S. J., Ingrum, T., & Leighton, D. (2016). Present-day oxidative subsidence of organic soils and mitigation in the Sacramento-San Joaquin Delta, California, USA. *Hydrogeol J, 24*, 569-586. https://doi.org/10.1007/s10040-016-1391-1

Deverel, S. J., & Leighton, D. (2010). Historic, recent, and furture subsidence, Sacramento-San Joaquin Delta, California, USA. *San Francisco Estuary and Watershed Science, 8*. https://doi.org/10.15447/sfews.2010v8iss2art1

Dietrich, O., Fahle, M., & Steidl, J. (2019). The role of the unsaturated xone for rainwater retention and runoff at a drained wetland site. *Water, 11*, 1104. https://doi.org/10.3390/w11071404

Dragoni, D., Schmid, H., Grimmond, C., & Loescher, H. (2007). Uncertainty of annual net ecosystem productivity estimated using eddy covariance flux measurements. *Journal of Geophysical Research: Atmospheres, 112*. https://doi.org/10.1029/2006JD008149

Drzymulska, D. (2016). Peat decomposition- shaping factors, significance in environmental studies and methods of determination; a literature review. *Geologos, 22*, 61-69. https://doi.org/10.1515/logos-2016-0005

Dunn, S., & Mackay, R. (1996). Modelling the hydrological impacts of open ditch drainage. *Journal of Hydrology, 179*, 37-66. https://doi.org/10.1016/0022-1694(95)02871-4

Egglesmann, R. F. (1976). Peat consumption under the influence of climate, soil condition, and utilisation. In *5th International Peat Congress* (pp. 233-247). Poznan.

Egglesmann, R. F. (1981). *Okohydrologische Aspekte von anthropogen beeinflußten und unbeeinflußten Mooren Norddeutschlands.* thesis, University of Oldenburg, Oldenburg.

Egglesmann, R. F. (1984). Subsidence of peatland caused by drainage, evaporation, and oxidation. In *Proceedings of the Third International Symposium on Land Subsidence* (pp. 497-505): IAHS Publication Venice, Italy.

Egglesmann, R. F., Heathwaite, A. L., Gross-Brauckmann, G., Kuster, E., Naucke, W., Schich, M., & Schweikle, V. (1993). Physical processes and properties of mires. In A. L. Heathwaite & K. H. Gottlich (Eds.), *Mires, Process, Exploration and Conservation* (pp. 172-262). Chichester: John Wiley and Sons.

Erkens, G., van der Meulen, M. J., & Middelkoop, H. (2016). Double trouble: subsidence and CO_2 respiration due to 1,000 years of Dutch coastal peatlands cultivation. *Hydrogeology Journal, 24*, 551-568. https://doi.org/10.1007/s10040-016-1380-4

Evans, C. D., Williamson, J. M., Kacaribu, F., Irawan, D., Suardiwerianto, Y., Hidayat, M. F., Laurén, A., & Page, S. E. (2019). Rates and spatial variability of peat subsidence in Acacia plantation and forest landscapes in Sumatra, Indonesia. *Geoderma, 338*, 410-421. https://doi.org/10.1016/j.geoderma.2018.12.028

Falge, E., Baldocchi, D. D., Olson, R., Anthoni, P., Aubinet, M., Bernhofer, C., Burba, G., Ceulemans, R., Clement, R., Dolman, H., Granier, A., Gross, P., Grunwald, T., Hollinger, D., Jensen, N.-O., Katul, G., Keronen, P., Kowalski, A., Ta Lai, C., Law, B. E., Meyers, T., Moncrieff, J. B., Moors, E., Munger, J. W., Pilegaard, K., Rannik, U., Rebmann, C., Suyker, A., Tenhunen, J., Tu, K., Verma, S., Vesala, T., Wilson, K., & Wofsy, S. C. (2001). Gap filling strategies for defensible annual sums of net ecosystem exchange. *Agricultural and Forest Meteorology, 107*, 43-69. https://doi.org/10.1016/S0168-1923(00)00225-2

Fang, C., & Moncrieff, J. B. (2001). The dependence of soil CO_2 efflux on temperature. *Soil Biology and Biochemistry, 33*, 155-165. https://doi.org/10.1016/S0038-0717(00)00125-5

Faul, F., Gabriel, M., Roßkopf, N., Zeitz, J., van Huyssteen, C. W., Pretorius, M. L., & Grundling, P.-L. (2016). Physical and hydrological properties of peatland substrates from different hydrogenetic wetland types on the Maputaland Coastal Plain, South Africa. *South African Journal of Plant and Soil, 33*, 265-278. https://doi.org/10.1080/02571862.2016.1141334

Ferré, M., Muller, A., Leifeld, J., Bader, C., Müller, M., Engel, S., & Wichmann, S. (2019). Sustainable management of cultivated peatlands in Switzerland: Insights, challenges, and opportunities. *Land Use Policy, 87*. https://doi.org/10.1016/j.landusepol.2019.05.038

Fritz, C., Campbell, D. I., & Schipper, L. A. (2008). Oscillating peat surface levels in a restiad peatland, New Zealand-magnitude and spatiotemporal

variability. *Hydrological Processes, 22*, 3264-3274. https://doi.org/10.1002/hyp.6912

Fuentes, J. P., Bezdicek, D. F., Flury, M., Albrecht, S., & Smith, J. L. (2006). Microbial activity affected by lime in a long-term no-till soil. *Soil and Tillage Research, 88*, 123-131. https://doi.org/10.1016/j.still.2005.05.001

Gaumont-Guay, D., Black, T. A., Griffis, T. J., Barr, A. G., Jassal, R. S., & Nesic, Z. (2006). Interpreting the dependence of soil respiration on soil temperature and water content in a boreal aspen stand. *Agricultural and Forest Meteorology, 140*, 220-235. https://doi.org/10.1016/j.agrformet.2006.08.003

Google Earth. (2019). Retrieved 10 November, 2019, from https://earth.google.com/web/@-37.94742753,175.3771848,63.45831618a,6881.02280753d,35y,-60.28961762h,45.03858955t,0r.

Grachev, A. A., Fairall, C. W., Blomquist, B. W., Fernando, H. J. S., Leo, L. S., Otárola-Bustos, S. F., Wilczak, J. M., & McCaffrey, K. L. (2020). On the surface energy balance closure at different temporal scales. *Agricultural and Forest Meteorology, 281*. https://doi.org/10.1016/j.agrformet.2019.107823

Haapalehto, T., Kotiaho, J. S., Matilainen, R., & Tahvanainen, T. (2014). The effects of long-term drainage and subsequent restoration on water table level and pore water chemistry in boreal peatlands. *Journal of Hydrology, 519*, 1493-1505. https://doi.org/10.1016/j.jhydrol.2014.09.013

Heathwaite, A., Eggelsmann, R., Gottlich, K., & Kaule, G. (1993). Ecohydrology, mire drainage and mire conservation. In A. L. Heathwaite (Ed.), *Mires: Processes, Exploitation and Conservation* (pp. 417-484). Chichester: Wiley.

Hobbs, N. B. (1986). Mire morphology and the properties and behaviour of some British and foreign peats. *Quarterly Journal of Engineering Geology and Hydrogeology, 19*, 7-80. https://doi.org/10.1144/GSL.QJEG.1986.019.01.02

Holden, J. (2005). Peatland hydrology and carbon release: why small-scale process matters. *Philosophical Transactions of the Royal Society A: Mathematical, Physical and Engineering Sciences, 363*, 2891-2913. https://doi.org/10.1098/rsta.2005.1671

Holden, J., Chapman, P., & Labadz, J. (2004). Artificial drainage of peatlands: hydrological and hydrochemical process and wetland restoration. *Progress in Physical Geography, 28*, 95-123. https://doi.org/10.1191/0309133304pp403ra

Holden, J., Evans, M. G., Burt, T. P., & Horton, M. (2006). Impact of land drainage on peatland hydrology. *J Environ Qual, 35*, 1764-78. https://doi.org/10.2134/jeq2005.0477

Holden, J., Wallage, Z. E., Lane, S. N., & McDonald, A. T. (2011). Water table dynamics in undisturbed, drained and restored blanket peat. *Journal of Hydrology, 402*, 103-114. https://doi.org/10.1016/j.jhydrol.2011.03.010

Hooijer, A., Page, S., Jauhiainen, J., Lee, W. A., Lu, X. X., Idris, A., & Anshari, G. (2012). Subsidence and carbon loss in drained tropical peatlands. *Biogeosciences, 9*, 1053-1071. https://doi.org/10.5194/bg-9-1053-2012

Howie, S. A., & Hebda, R. J. (2018). Bog surface oscillation (mire breathing): A useful measure in raised bog restoration. *Hydrological Processes, 32*, 1518-1530. https://doi.org/10.1002/hyp.11622

Huat, B., B. K., Kazemian, S., Prasad, A., & Barghchi, M. (2011). State of an art review of peat: General perspective. *International Journal of the Physical Sciences, 6*, 1988-1996. https://doi.org/10.5897/IJPS11.192

Hudson, J. A., & Roberts, G. (1982). The effect of a tile drain on the soil moisture content of peat. *Journal of Agricultural Engineering Research, 27*, 495-500. https://doi.org/10.1016/0021-8634(82)90088-9

Ingram, H. A. P. (1983). Hydrology. In A. J. P. Gore (Ed.), *Mires: Swamp, Bog, Fen and Moor. Ecosystems of the World 4A* (pp. 67-158). Elsevier, Amsterdam.

IPCC. (2006). *IPCC guidelines for national greenhouse gas inventories.* Japan.

IPCC. (2014). 2013 Supplement to the 2006 Inter-Governmental Panel on Climate Change guidelines for national greenhouse gas inventories: Wetlands. In T. Hiraishi, *et al.* (Eds.), (pp. 354). IPCC, Switzerland.

IPCC. (2019). Climate Change and Land: an IPCC special report on climate change, desertification, land degradation, sustainable land management, food security, and greenhouse gas fluxes in terrestrial ecosystems.

Jacobs, A. F. G., Heusinkveld, B. G., & Holtslag, A. A. M. (2008). Towards closing the surface energy budget of a mid-latitude grassland. *Boundary-Layer Meteorology, 126*, 125-136. https://doi.org/10.1007/s10546-007-9209-2

Jarvis, N. J. (2007). A review of non-equilibrium water flow and solute transport in soil macropores: principles, controlling factors and consequences for water quality. *European Journal of Soil Science, 58*, 523-546. https://doi.org/10.1111/j.1365-2389.2007.00915.x

Joosten, H., Sirin, A., Couwenberg, J., Laine, J., & Smith, P. (2016). The role of peatlands in climate regulation. In A. Bonn, *et al.* (Eds.), *Peatland Restoration and Ecosystem Services: Science, Policy and Practice* (pp. 63-76). Cambridge University Press.

Kaat, A., & Joosten, H. (2009). Factbook for UNFCCC policies on peat carbon emissions. *Wetlands International*.

Karki, S., Elsgaard, L., Kandel, T. P., & Laerke, P. E. (2016). Carbon balance of rewetted and drained peat soils used for biomass production: a mesocosm study. *GCB Bioenergy, 8*, 969-980. https://doi.org/10.1111/gcbb.12334

Kasimir-Klemedtsson, A., Klemedtsson, L., Berglund, K., Martikainen, P., Silvola, J., & Oenema, O. (1997). Greenhouse gas emissions from farmed organic

soils: a review. *Soil Use and Management, 13*, 245-250. https://doi.org/10.1111/j.1475-2743.1997.tb00595.x

Kelliher, F. M., van Koten, C., Lindsey, S. B., Wise, B., & Rys, G. (2016). Nitrous oxide emissions from drained peat soil beneath pasture. *New Zealand Journal of Agricultural Research, 59*, 363-376. https://doi.org/10.1080/00288233.2016.1212382

Kellner, E., & Halldin, S. (2002). Water budge and surface-layer water storage in a *Sphagnum* bog in central Sweden. *Hydrological Processes, 16*, 87-103.

Kennedy, G. W., & Price, J. S. (2005). A conceptual model of volume-change controls on the hydrology of cutover peats. *Journal of Hydrology, 302*, 13-27. https://doi.org/10.1016/j.jhydrol.2004.06.024

Kuntze, H. (1965). Physikalische Untersuchungsmethoden fur Moorund Anmoorboden (English Summary). *Landwirtschaftlishe Forschung, 18*, 178-191.

Kutikoff, S., Lin, X., Evett, S., Gowda, P., Moorhead, J., Marek, G., Colaizzi, P., Aiken, R., & Brauer, D. (2019). Heat storage and its effect on the surface energy balance closure under advective conditions. *Agricultural and Forest Meteorology, 265*, 56-69. https://doi.org/10.1016/j.agrformet.2018.10.018

Laiho, R. (2006). Decomposition in peatlands: Reconciling seemingly contrasting results on the impacts of lowered water levels. *Soil Biology and Biochemistry, 38*, 2011-2024. https://doi.org/10.1016/j.soilbio.2006.02.017

Lamaud, E., Ogee, J., Brunet, Y., & Berbigier, P. (2001). Validation of eddy flux measurements above the understorey of a pine forest. *Agricultural and Forest Meteorology, 106*, 187-203. https://doi.org/10.1016/S0168-1923(00)00215-X

Larmola, T., Bubier, J. L., Kobyljanec, C., Basiliko, N., Juutinen, S., Humphreys, E., Preston, M., & Moore, T. R. (2013). Vegetation feedbacks of nutrient addition lead to a weaker carbon sink in an ombrotrophic bog. *Glob Chang Biol, 19*, 3729-39. https://doi.org/10.1111/gcb.12328

Leifeld, J., & Menichetti, L. (2018). The underappreciated potential of peatlands in global climate change mitigation strategies. *Nat Commun, 9*, 1071. https://doi.org/10.1038/s41467-018-03406-6

Leifeld, J., Müller, M., & Fuhrer, J. (2011). Peatland subsidence and carbon loss from drained temperate fens. *Soil Use and Management, 27*, 170-176. https://doi.org/10.1111/j.1475-2743.2011.00327.x

Leuning, R., van Gorsel, E., Massman, W. J., & Isaac, P. R. (2012). Reflections on the surface energy imbalance problem. *Agricultural and Forest Meteorology, 156*, 65-74. https://doi.org/10.1016/j.agrformet.2011.12.002

Liu, H., & Lennartz, B. (2019). Hydraulic properties of peat soils along a bulk density gradient-A meta study. *Hydrological Processes, 33*, 101-114. https://doi.org/10.1002/hyp.13314

Lloyd, C. R. (2006). Annual carbon balance of a managed wetland meadow in the Somerset Levels, UK. *Agricultural and Forest Meteorology, 138*, 168-179. https://doi.org/10.1016/j.agrformet.2006.04.005

Lloyd, J., & Taylor, J. A. (1994). On the temperature dependence of soil respiration. *Functional ecology, 8*, 315-323. https://doi.org/10.2307/2389824

Loescher, H. W., Law, B. E., Mahrt, L., Hollinger, D., Campbell, J., & Wofsy, S. C. (2006). Uncertainties in, and interpretation of, carbon flux estimates using the eddy covariance technique. *Journal of Geophysical Research, 111*. https://doi.org/10.1029/2005JD006932

Logsdon, S., Schilling, K., Hernandez‐Ramirez, G., Prueger, J., Hatfield, J., & Sauer, T. (2010). Field estimation of specific yield in a central Iowa crop field. *Hydrological Processes: An International Journal, 24*, 1369-1377. https://doi.org/10.1002/hyp.7600

Luscombe, D. J., Anderson, K., Grand-Clement, E., Gatis, N., Ashe, J., Benaud, P., Smith, D., & Brazier, R. E. (2016). How does drainage alter the hydrology of shallow degraded peatlands across multiple spatial scales? *Journal of Hydrology, 541*, 1329-1339. https://doi.org/10.1016/j.jhydrol.2016.08.037

Luyssaert, S., Inglima, I., Jung, M., Richardson, A. D., Reichstein, M., Papale, D., Piao, S., Schulze, E. D., Wingate, L., & Matteucci, G. (2007). CO_2 balance of boreal, temperate, and tropical forests derived from a global database. *Global change biology, 13*, 2509-2537. https://doi.org/10.1111/j.1365-2486.2007.01439.x

Mäkiranta, P., Laiho, R., Fritze, H., Hytönen, J., Laine, J., & Minkkinen, K. (2009). Indirect regulation of heterotrophic peat soil respiration by water level via microbial community structure and temperature sensitivity. *Soil Biology and Biochemistry, 41*, 695-703. https://doi.org/10.1016/j.soilbio.2009.01.004

Maljanen, M., Liikanen, A., Silvola, J., & Martikainen, P. (2003). Nitrous oxide emissions from boreal organic soil under different land-use. *Soil Biology and Biochemistry, 35*, 689-700. https://doi.org/10.1016/S0038-0717(03)00085-3

Maljanen, M., Martikainen, P. J., Walden, J., & Silvola, J. (2001). CO_2 exchange in an organic field growing barley or grass in eastern Finland. *Global Change Biology, 7*, 679-692. https://doi.org/10.1046/j.1365-2486.2001.00437.x

Maljanen, M., Sigurdsson, B., GuDmundsson, J., Oskarsson, H., Hutten, J., & Martikainen, P. (2010). Greenhouse gas balances of managed peatlands in the Nordic countries - present knowledge and gaps. *Biogeosciences, 7*, 2711-2738. https://doi.org/10.5194/bg-7-2711-2010

Manaaki Whenua Landcare Research. (2019). *MWLR infiltrometer manual.*

Manaaki Whenua Landcare Research. (2020). *Laboratory tests*. Retrieved 6 February, 2020, from

https://www.landcareresearch.co.nz/resources/laboratories/soil-physics-laboratory/services-offered/tests.

Marwanto, S., Sabiham, S., & Funakawa, S. (2019). Importance of CO_2 production in subsoil layers of drained tropical peatland under mature oil palm plantation. *Soil and Tillage Research, 186*, 206-213. https://doi.org/10.1016/j.still.2018.10.021

McGlone, M. S. (2009). Postglacial history of New Zealand wetlands and implications for their conservation. *New Zealand Journal of Ecology*, 1-23.

McLay, C., Allbrook, R., & Thompson, K. (1992). Effect of development and cultivation on physical properties of peat soils in New Zealand. *Geoderma, 54*, 23-37. https://doi.org/10.1016/0016-7061(92)90096-P

Minasny, B., Berglund, Ö., Connolly, J., Hedley, C., de Vries, F., Gimona, A., Kempen, B., Kidd, D., Lilja, H., Malone, B., McBratney, A., Roudier, P., O'Rourke, S., Rudiyanto, Padarian, J., Poggio, L., ten Caten, A., Thompson, D., Tuve, C., & Widyatmanti, W. (2019). Digital mapping of peatlands – A critical review. *Earth-Science Reviews, 196*. https://doi.org/10.1016/j.earscirev.2019.05.014

Ministry for the Environment. (2019). New Zealand's greenhouse gas inventory. *1*.

Minkkinen, K., Laine, J., Shurpali, N. J., Mäkiranta, P., Alm, J., & Penttilä, T. (2007). Heterotrophic soil respiration in forestry-drained peatlands. *Boreal Environment Research, 12*, 115-126.

Mitsch, W. J., & Gosselink, J. G. (2000). The value of wetlands: importance of scale and landscape setting. *Ecological economics, 35*, 25-33.

Moore, T. R., Trofymow, J. A., Siltanen, M., Prescott, C., & CIDET Working Group. (2005). Patterns of decomposition and carbon, nitrogen, and phosphorus dynamics of litter in upland forest and peatland sites in central Canada. *Canadian Journal of Forest Research, 35*, 133-142. https://doi.org/10.1139/X04-149

Morton, P. A., & Heinemeyer, A. (2019). Bog breathing: the extent of peat shrinkage and expansion on blanket bogs in relation to water table, heather management and dominant vegetation and its implications for carbon stock assessments. *Wetlands Ecology and Management, 27*, 467-482. https://doi.org/10.1007/s11273-019-09672-5

Motorin, A. S., Iglovikov, A. V., & Bukin, A. V. (2018). Changing in Water-physical Properties of Drained Peat Soils during Extraction and Exploration of Minerals in the Conditions of the Northern Urals. *IOP Conference Series: Earth and Environmental Science, 194*. https://doi.org/10.1088/1755-1315/194/8/082026

Murdiyarso, D., Lilleskov, E., & Kolka, R. (2019). Tropical peatlands under siege: the need for evidence-based policies and strategies. *Mitigation and Adaptation Strategies for Global Change, 24*, 493-505. https://doi.org/10.1007/s11027-019-9844-1

Mustamo, P., Hyvärinen, M., Ronkanen, A. K., Kløve, B., & Moffat, A. J. (2016). Physical properties of peat soils under different land use options. *Soil Use and Management, 32*, 400-410. https://doi.org/10.1111/sum.12272

Nieveen, J. P., Campbell, D. I., Schipper, L. A., & Blair, I. J. (2005). Carbon exchange of grazed pasture on a drained peat soil. *Global Change Biology, 11*, 607-618. https://doi.org/10.1111/j.1365-2486.2005.00929.x

Nijp, J. J., Metselaar, K., Limpens, J., Bartholomeus, H. M., Nilsson, M. B., Berendse, F., & Zee, S. E. A. T. M. (2019). High ‐ resolution peat volume change in a northern peatland: Spatial variability, main drivers, and impact on ecohydrology. *Ecohydrology, 12*. https://doi.org/10.1002/eco.2114

NIWA. (2010). *National Climate Database*. from https://www.niwa.co.nz/education-andtraining/schools/resources/climate.

NIWA. (2017). *Annual climate summary.* Retrieved 25 December 2019, from https://cliflo.niwa.co.nz/.

Norberg, L., Berglund, Ö., & Berglund, K. (2018). Impacts of drainage and soil properties on carbon dioxide emissions from intact cores of cultivated peat soils. *Mires and Peat, 21*, 1-14. https://doi.org/10.19189/MaP.2017.OMB.284

Oechel, W. C., Vourlitis, G. L., Hastings, S. J., Ault Jr, R. P., & Bryant, P. (1998). The effects of water table manipulation and elevated temperature on the net CO_2 flux of wet sedge tundra ecosystems. *Global Change Biology, 4*, 77-90. https://doi.org/10.1046/j.1365-2486.1998.00110.x

Oikawa, P. Y., Sturtevant, C., Knox, S. H., Verfaillie, J., Huang, Y. W., & Baldocchi, D. D. (2017). Revisiting the partitioning of net ecosystem exchange of CO_2 into photosynthesis and respiration with simultaneous flux measurements of $^{13}CO_2$ and CO_2, soil respiration and a biophysical model, CANVEG. *Agricultural and Forest Meteorology, 234*, 149-163. https://doi.org/10.1016/j.agrformet.2016.12.016

Oleszczuk, R., Bohne, K., Stzatylowicz, J., Brandyk, T., & Gnatowski, T. (2003). Influence of load on shrinkage behavior of peat soils. *Journal of Plant Nutrition and Soil Science, 166*, 220-224. https://doi.org/10.1002/jpln.200390032

Papale, D., & Valentini, R. (2003). A new assessment of European forests carbon exchanges by eddy fluxes and artificial neural network spatialization. *Global Change Biology, 9*, 525-535. https://doi.org/10.1046/j.1365-2486.2003.00609.x

Parmentier, F. J. W., van der Molen, M. K., de Jeu, R. A. M., Hendriks, D. M. D., & Dolman, A. J. (2009). CO_2 fluxes and evaporation on a peatland in the Netherlands appear not affected by water table fluctuations. *Agricultural and Forest Meteorology, 149*, 1201-1208. https://doi.org/10.1016/j.agrformet.2008.11.007

Petersen, L., & Madsen, H. B. (1978). Possible effects of ground water lowering on some peat soils in Sjælland. *Geografisk Tidsskrift-Danish Journal of Geography, 77*, 25-35. https://doi.org/10.1080/00167223.1978.10649089

Pinsonneault, A. J., Moore, T. R., & Roulet, N. T. (2016). Effects of long-term fertilization on peat stoichiometry and associated microbial enzyme activity in an ombrotrophic bog. *Biogeochemistry, 129*, 149-164. https://doi.org/10.1007/s10533-016-0224-6

Price, J. S. (1997). Soil moisture, water tension, and water table relationships in a managed cutover bog. *Journal of Hydrology, 202*, 21-32. https://doi.org/10.1016/S0022-1694(97)00037-1

Price, J. S. (2003). Role and character of seasonal peat soil deformation on the hydrology of undisturbed and cutover peatlands. *Water Resources Research, 39*. https://doi.org/10.1029/2002wr001302

Price, J. S., Heathwaite, A. L., & Baird, A. J. (2003). Hydrological processes in abandoned and restored peatlands: An overview of management approaches. *Wetlands Ecology and Management, 11*, 65-83. https://doi.org/10.1023/A:1022046409485

Price, J. S., & Schlotzhauer, S. M. (1999). Importance of shrinkage and compression in determining water storage changes in peat: the case of a mined peatland. *Hydrological Processes, 13*, 2591-2601. https://doi.org/10.1002/(SICI)1099-1085(199911)13:16<2591::AID-HYP933>3.0.CO;2-E

Pronger, J., Schipper, L. A., Hill, R. B., Campbell, D. I., & McLeod, M. (2014). Subsidence rates of drained agricultural peatlands in New Zealand and the relationship with time since drainage. *J Environ Qual, 43*, 1442-9. https://doi.org/10.2134/jeq2013.12.0505

Querner, E. P., Jansen, P. C., van den Akker, J. J. H., & Kwakernaak, C. (2012). Analysing water level strategies to reduce soil subsidence in Dutch peat meadows. *Journal of Hydrology, 446-447*, 59-69. https://doi.org/10.1016/j.jhydrol.2012.04.029

Ratcliffe, J. L., Campbell, D. I., Clarkson, B. R., Wall, A. M., & Schipper, L. A. (2019). Water table fluctuations control CO_2 exchange in wet and dry bogs through different mechanisms. *Sci Total Environ, 655*, 1037-1046. https://doi.org/10.1016/j.scitotenv.2018.11.151

Regan, S., Flynn, R., Gill, L., Naughton, O., & Johnston, P. (2019). Impacts of groundwater drainage on peatland subsidence and Its ecological implications on an Atlantic raised bog. *Water Resources Research, 55*, 6153-6168. https://doi.org/10.1029/2019WR024937

Regina, K., Sheehy, J., & Myllys, M. (2014). Mitigating greenhouse gas fluxes from cultivated organic soils with raised water table. *Mitigation and Adaptation Strategies for Global Change, 20*, 1529-1544. https://doi.org/10.1007/s11027-014-9559-2

Regina, K., Syvasalo, E., Hannukkala, A., & Esala, M. (2004). Fluxes of N_2O from farmed peat soils in Finland. *European Journal of Soil Science, 55*, 591-599. https://doi.org/10.1111/j.1365-2389.2004.00622.x

Reichstein, M., Falge, E., Baldocchi, D., Papale, D., Aubinet, M., Berbigier, P., Bernhofer, C., Buchmann, N., Gilmanov, T., & Granier, A. (2005). On the separation of net ecosystem exchange into assimilation and ecosystem respiration: review and improved algorithm. *Global change biology, 11*, 1424-1439. https://doi.org/10.1111/j.1365-2486.2005.001002.x

Renger, M., Wessolek, G., Schwärzel, K., Sauerbrey, R., & Siewert, C. (2002). Aspects of peat conservation and water management. *Journal of Plant Nutrition and Soil Science, 165*, 487-493. https://doi.org/10.1002/1522-2624(200208)165:4<487::AID-JPLN487>3.0.CO;2-C

Renou-Wilson, F., Barry, C., Müller, C., & Wilson, D. (2014). The impacts of drainage, nutrient status and management practice on the full carbon balance of grasslands on organic soils in a maritime temperate zone. *Biogeosciences, 11*, 4361-4379. https://doi.org/10.5194/bg-11-4361-2014

Rezanezhad, F., Price, J. S., Quinton, W. L., Lennartz, B., Milojevic, T., & Van Cappellen, P. (2016). Structure of peat soils and implications for water storage, flow and solute transport: A review update for geochemists. *Chemical Geology, 429*, 75-84. https://doi.org/10.1016/j.chemgeo.2016.03.010

Ritchie, J. T. (1998). Soil water balance and plant water stress. In *Understanding options for agricultural production* (pp. 41-54). Springer, Dordrecht.

Rothwell, R. L., Silins, U., & Hillman, G. R. (1996). The effects of drainage on substrate water content at several forested Alberta peatlands. *Canadian Journal of Forest Research, 26*, 53-62. https://doi.org/10.1139/x26-006

Roulet, N., Lafleur, P. M., Richard, P. J., Moore, T. R., Humphreys, E., & Bubier, J. L. (2007). Contemporary carbon balance and late Holocene carbon accumulation in a northern peatland. *Global Change Biology, 13*, 397-411. https://doi.org/10.1111/j.1365-2486.2006.01292.x

Rowson, J. G., Gibson, H. S., Worrall, F., Ostle, N., Burt, T. P., & Adamson, J. K. (2010). The complete carbon budget of a drained peat catchment. *Soil Use and Management, 26*, 261-273. https://doi.org/10.1111/j.1475-2743.2010.00274.x

Säurich, A., Tiemeyer, B., Dettmann, U., & Don, A. (2019a). How do sand addition, soil moisture and nutrient status influence greenhouse gas fluxes from drained organic soils? *Soil Biology and Biochemistry, 135*, 71-84. https://doi.org/10.1016/j.soilbio.2019.04.013

Säurich, A., Tiemeyer, B., Don, A., Fiedler, S., Bechtold, M., Amelung, W., & Freibauer, A. (2019b). Drained organic soils under agriculture — The more degraded the soil the higher the specific basal respiration. *Geoderma, 355*. https://doi.org/10.1016/j.geoderma.2019.113911

Schipper, L. A., & McLeod, M. (2002). Subsidence rates and carbon loss in peat soils following conversion to pasture in the Waikato Region, New Zealand. *Soil Use and Management, 18*, 91-93. https://doi.org/10.1079/SUM2001106

Schlotzhauer, S. M., & Price, J. S. (1999). Soil water flow dynamics in a managed cutover peat field, Quebec: Field and laboratory investigations. *Water Resources Research, 35*, 3675-3683. https://doi.org/10.1029/1999wr900126

Schothorst, C. J. (1977). Subsidence of a low moor peat in the western Netherlands. *Geoderma, 17*, 265-291. https://doi.org/10.1016/0016-7061(77)90089-1

Schothorst, C. J. (1982). Drainage and behaviour of peat soils. In H. de Bakker & M. W. van den Berg (Eds.), *Proceedings of the Symposium on Peatlands Below Sea Level* (pp. 130-163). Institute of Land Reclamation and Improvement, Wageningen.

Schwärzel, K., Renger, M., Sauerbrey, R., & Wessolek, G. (2002). Soil physical characteristics of peat soils. *Journal of Plant Nutrition and Soil Science, 165*, 479-486. https://doi.org/10.1002/1522-2624(200208)165:4<479::AID-JPLN479>3.0.CO;2-8

Schwärzel, K., Šimůnek, J., van Genuchten, M. T., & Wessolek, G. (2006). Measurement and modeling of soil-water dynamics evapotranspiration of drained peatland soils. *Journal of Plant Nutrition and Soil Science, 169*, 762-774. https://doi.org/10.1002/jpln.200621992

Shih, S. F., Glaz, B., & Barnes, R. E. (1998). Subsidence of organic soils in the everglades agricultural area during the past 19 years. In *Soil and Crop Science Society of Florida* (Vol. 57, pp. 20-29).

Silins, U., & Rothwell, R. L. (1999). Spatial patterns of aerobic limit depth and oxygen diffusion rate at two peatlands drained for forestry in Alberta. *Canadian Journal of Forest Research, 29*, 53-61. https://doi.org/10.1139/x98-179

Sinclair, A. L., Graham, L. L. B., Putra, E. I., Saharjo, B. H., Applegate, G., Grover, S. P., & Cochrane, M. A. (2020). Effects of distance from canal and degradation history on peat bulk density in a degraded tropical peatland. *Sci Total Environ, 699*, 134199. https://doi.org/10.1016/j.scitotenv.2019.134199

Stenberg, L., Haahti, K., Hökkä, H., Launiainen, S., Nieminen, M., Laurén, A., & Koivusalo, H. (2018). Hydrology of drained peatland forest: Numerical experiment on the role of tree stand heterogeneity and management. *Forests, 9*. https://doi.org/10.3390/f9100645

Stewart, A. J., & Lance, A. N. (1983). Moor-draining: A review of impacts on land use. *Journal of Environmental Management, 17*, 81-99.

Strack, M., Kellner, E., & Waddington, J. M. (2005). Dynamics of biogenic gas bubbles in peat and their effect on peatland biogeochemistry. *Global Biogeochemical Cycles, 19*. https://doi.org/10.1029/2004GB002330

Swift, M. J., Heal, O. W., Anderson, J. M., & Anderson, J. (1979). *Decomposition in terrestrial ecosystems*. (Vol. 5). Univ of California Press.

Szajdak, L., & Szatylowicz, J. (2010). Impact of drainage on hydrophobicity of fen peat-moorsh soils. *Mires Peat*, 158-174.

Teatini, P., Putti, M., Gambolati, G., Ferraris, S., & Camporese, M. (2004). *Reversible/Irreversible peat surface displacements and hydrological regime in the Zennare Basin, Venice.* Scientific Research and Safeguarding of Venice (CORILA Research Program 2001-2003, 2002 Results). 93-106p.

Tiemeyer, B., Albiac Borraz, E., Augustin, J., Bechtold, M., Beetz, S., Beyer, C., Drosler, M., Ebli, M., Eickenscheidt, T., Fiedler, S., Forster, C., Freibauer, A., Giebels, M., Glatzel, S., Heinichen, J., Hoffmann, M., Hoper, H., Jurasinski, G., Leiber-Sauheitl, K., Peichl-Brak, M., Rosskopf, N., Sommer, M., & Zeitz, J. (2016). High emissions of greenhouse gases from grasslands on peat and other organic soils. *Glob Chang Biol, 22*, 4134-4149. https://doi.org/10.1111/gcb.13303

Tiemeyer, B., Freibauer, A., Borraz, E. A., Augustin, J., Bechtold, M., Beetz, S., Beyer, C., Ebli, M., Eickenscheidt, T., Fiedler, S., Förster, C., Gensior, A., Giebels, M., Glatzel, S., Heinichen, J., Hoffmann, M., Höper, H., Jurasinski, G., Laggner, A., Leiber-Sauheitl, K., Peichl-Brak, M., & Drösler, M. (2020). A new methodology for organic soils in national greenhouse gas inventories: Data synthesis, derivation and application. *Ecological Indicators, 109*. https://doi.org/10.1016/j.ecolind.2019.105838

Tubiello, F., Biancalani, R., Salvatore, M., Rossi, S., & Conchedda, G. (2016). A worldwide assessment of greenhouse gas emissions from drained organic soils. *Sustainability, 8*. https://doi.org/10.3390/su8040371

Unger, S., Máguas, C., Pereira, J. S., David, T. S., & Werner, C. (2010). The influence of precipitation pulses on soil respiration–Assessing the "Birch effect" by stable carbon isotopes. *Soil Biology and Biochemistry, 42*, 1800-1810. https://doi.org/10.1016/j.soilbio.2010.06.019

Van den Akker, J. J. H., & Hendriks, R. F. A. (2017). Diminishing peat oxidation of agricultural peat soils by infiltration via submerged drains. In *Global Symposium on Soil Organic Carbon*. Rome, Italy.

van der Schaaf, S. (2012). Subsidence in bogs: Moving catchment boundaries, changing flow paths and slopes, self-sealing and effects on drying and natural rewetting. In T. Lindholm & R. Heikkila (Eds.), *Mires from pole to pole* (pp. 295-312).

Verhoeven, J. T., & Setter, T. L. (2010). Agricultural use of wetlands: opportunities and limitations. *Ann Bot, 105*, 155-63. https://doi.org/10.1093/aob/mcp172

Waddington, J., Rotenberg, P., & Warren, F. (2001). Peat CO_2 production in a natural and cutover peatland: implications for restoration. *Biogeochemistry, 54*, 115-130. https://doi.org/10.1023/A:1010617207537

Waddington, J. M., Griffis, T. J., & Rouse, W. R. (1998). Northern Canadian wetlands: Net ecosystem CO_2 exchange and climatic change. *Climate Change, 40*, 267-275. https://doi.org/10.1023/A:1005468920206

Waddington, J. M., & Price, J. S. (2000). Effect of peatland drainage, harvesting, and restoration on atmospheric water and carbon exchange. *Physical Geography, 21*, 433-451. https://doi.org/10.1080/02723646.2000.10642719

Wall, A. M., Campbell, D. I., Mudge, P. L., Rutledge, S., & Schipper, L. A. (2019). Carbon budget of an intensively grazed temperate grassland with large quantities of imported supplemental feed. *Agriculture, Ecosystems & Environment, 281*, 1-15. https://doi.org/10.1016/j.agee.2019.04.019

Warner, K. D. (1999). *Net ecosystem CO_2 exhcange in natural, harvested and restored peatlands. Effect on peatland drainage and harvesting on CO_2 efflux.* thesis, McMaster University, Hamilton, Ontario, Canada.

Wehr, R., Munger, J. W., McManus, J. B., Nelson, D. D., S., Z. M., Davidson, E. A., Wofsy, S. C., & Saleska, S. R. (2016). Seasonality of temperate forest photosynthesis and daytime respiration. *Nature, 534*, 680-683. https://doi.org/10.1038/nature17966

Wessolek, G., Schwärzel, K., Renger, M., Sauerbrey, R., & Siewert, C. (2002). Soil hydrology and CO_2 release of peat soils. *Journal of Plant Nutrition and Soil Science, 165*, 494-500. https://doi.org/10.1002/1522-2624(200208)165:4<494::AID-JPLN494>3.0.CO;2-K

Whittington, P., Strack, M., van Haarlem, R., Kaufman, S., Stoesser, P., Maltez, J., Price, J. S., & Stone, M. (2007). The influence of peat volume change and vegetation on the hydrology of a kettle-hole wetland in Southern Ontario, Canada. *Mires and Peat, 2*, 1-14.

Wilson, K., Goldstein, A., Falge, E., Aubinet, M., Baldocchi, D. D., Berbigier, P., Bernhofer, C., Ceulemans, R., Dolman, A. J., Field, C., Grelle, A., Ibrom, A., Law, B. E., Kowalski, A., Meyers, T., Moncrieff, J. B., Monson, R., Oechel, W., Tenhunen, J., Valentini, R., & Verma, S. (2002). Energy balance closure at FLUXNET sites. *Agricultural and Forest Meteorology, 113*, 223-243. https://doi.org/10.1016/S0168-1923(02)00109-0

Wosten, J. H. M., Ismail, A. B., & Van Wijk, A. L. M. (1997). Peat subsidence and its practical implications: a case study in Malaysia. *Geoderma, 78*, 25-36. https://doi.org/10.1016/S0016-7061(97)00013-X

Xu, J., Morris, P. J., Liu, J., & Holden, J. (2018). PEATMAP: Refining estimates of global peatland distribution based on a meta-analysis. *Catena, 160*, 134-140. https://doi.org/10.1016/j.catena.2017.09.010

Zanello, F., Teatini, P., Putti, M., & Gambolati, G. (2011). Long term peatland subsidence: Experimental study and modeling scenarios in the Venice coastland. *Journal of Geophysical Research, 116*. https://doi.org/10.1029/2011jf002010

Appendices

Appendix A

Table 6.1 Artificial neural network (ANN) input variable selections for daytime and night-time models for net ecosystem CO_2 exchange (NEE) and latent heat fluxes (LE). Rn = net radiation, PPFD = photosynthetic photon flux density, u = horizontal wind speed, VPD = saturation vapour pressure deficit, Ta = air temperature, Ts, 4 cm = soil temperature at 4 cm depth, VMC5 & 10 cm = soil volumetric moisture content at both 5 cm and 10 cm depths, ΔNEE described in Wall et al. (2019).

Driver variable	NEE day	NEE night	LE day	LE night
R_n			✓	✓
PPFD	✓			
u		✓	✓	✓
VPD	✓		✓	✓
T_a	✓	✓	✓	✓
$T_{s,4\ cm}$	✓	✓		
$VMC_{5\ \&\ 10\ cm}$	✓	✓	✓	✓
ΔNEE	✓	✓	✓	

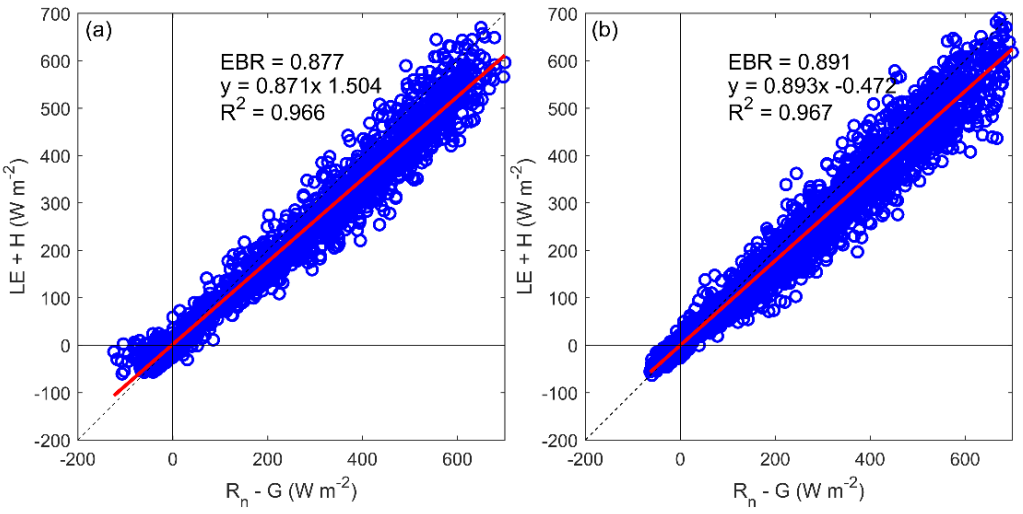

Figure A.1 Energy balance closure ratios at (a) Site 1 and (b) Site 2 between 1 January and 31 December 2019.

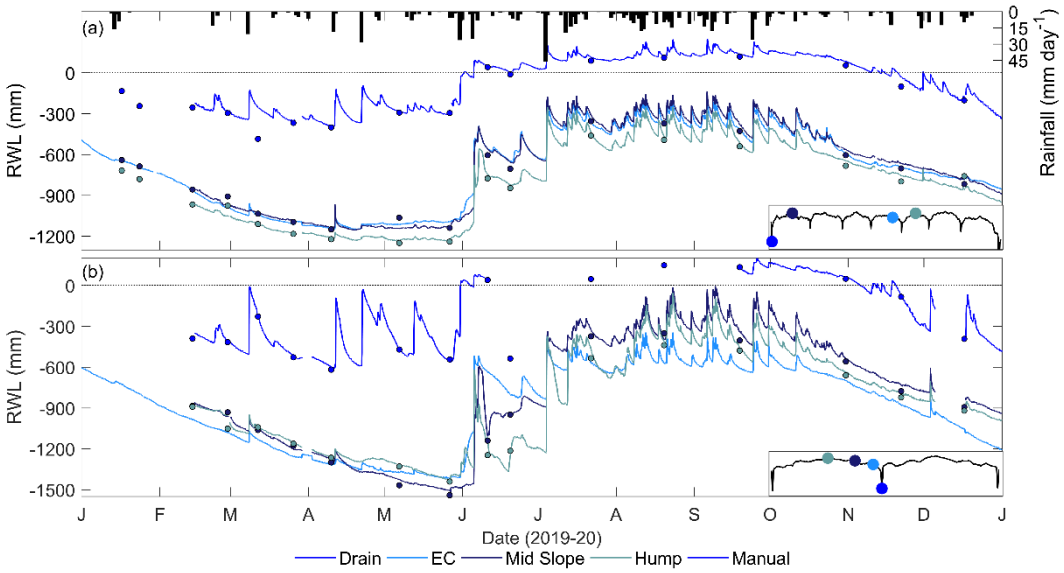

Figure A.2 Time series of daily rainfall totals and half-hourly mean relative water level (RWL) from automatic probes, and manual RWL:measurements (circle colour corresponds to dipwell position) between 1 January and 31 December 2019 at (a) Site 1 and (b) Site 2, with the inset graphical legend showing relative locations of the automatic probes along each of the transects. The horizontal black dotted line at RWL = 0 represents the peat surface. Note that the values on the Y axes differ between sites, but the ranges are the same, and missing data corresponds to probe errors.

Table A.2 Summary of spatial soil volumetric moisture content from the monthly manual surface soil cores. Not all sampling dates are shown as these represent when no core was sampled adjacent to a drain.

	Site 1(cm^3 cm^{-3})				Site 2 (cm^3 cm^{-3})			
Date	**Paddock 1**	**Paddock 2**	**Paddock 3**	**Drain**	**Paddock 1**	**Paddock 2**	**Paddock 3**	**Drain**
14/02/2019	0.21	0.16	0.21	0.24	0.17	0.16	0.17	0.12
20/03/2019	0.23	0.22	0.26	0.22	0.24	0.21	0.31	0.26
7/05/2019	0.26	0.37	0.34	0.39	0.38	0.45	0.42	0.33
20/06/2019	0.37	0.58	0.44	0.59	0.53	0.55	0.53	0.49
20/08/2019	0.62	0.55	0.59	0.45	0.63	0.62	0.63	0.51
31/10/2019	0.63	0.54	0.69	0.39	0.62	0.52	0.62	0.39

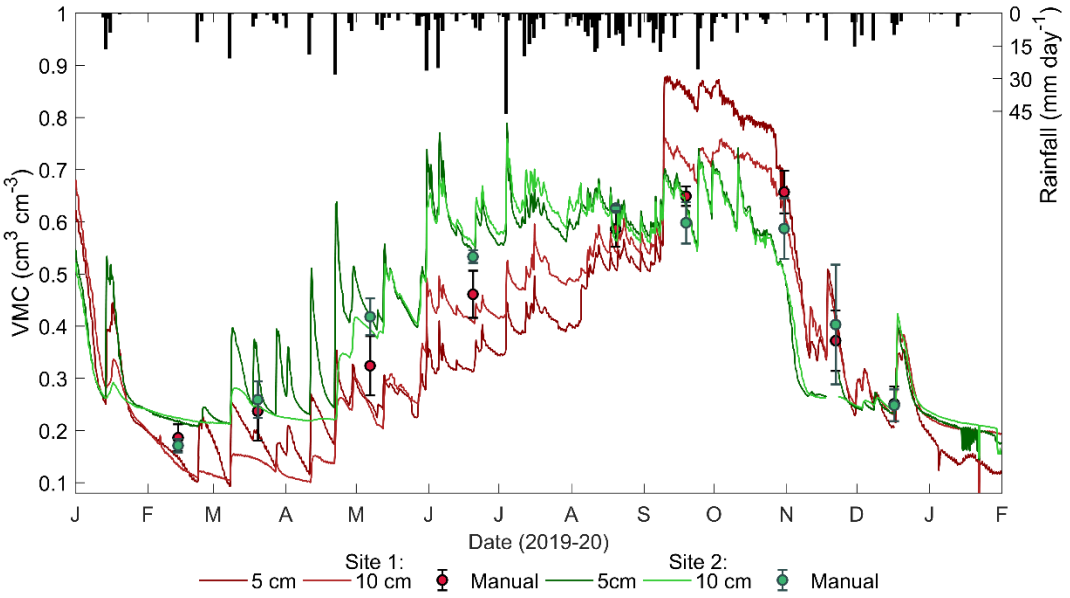

Figure A.3 Time series of daily rainfall totals, six-hourly mean soil volumetric moisture content (VMC) from the automatic probes at 5 cm and 10 cm depths, and manual measurements (mean ± 1 standard deviation) at 2.5 – 7.5 cm depth along the transects at Sites 1 (red) and 2 (green) between 1 January 2019 and 1 February 2020. Note that the data has not been filtered for probe dropouts between 1 January and 1 February 2020.

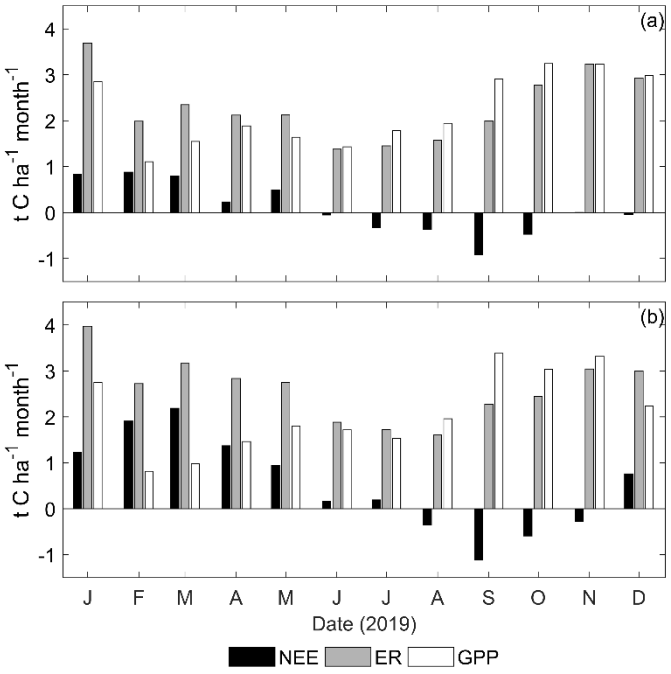

Figure A.4 Monthly totals of net ecosystem exchange (NEE), ecosystem respiration (ER) and gross primary production (GPP) at (a) Site 1 and (b) Site 2 between January and December 2019.

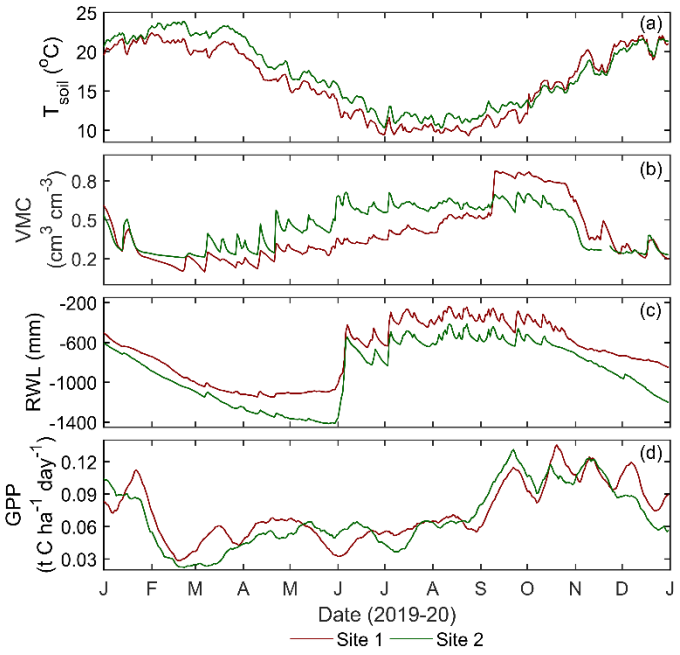

Figure A.5 Time series plots of (a) soil temperature (T_{soil}), (b) soil volumetric moisture content (VMC) and (c) relative water level (RWL) based on daily means, and (d) 15 day moving mean of gross primary production (GPP) at Sites 1 and 2 between 1 January and 31 December 2019.

Appendix B

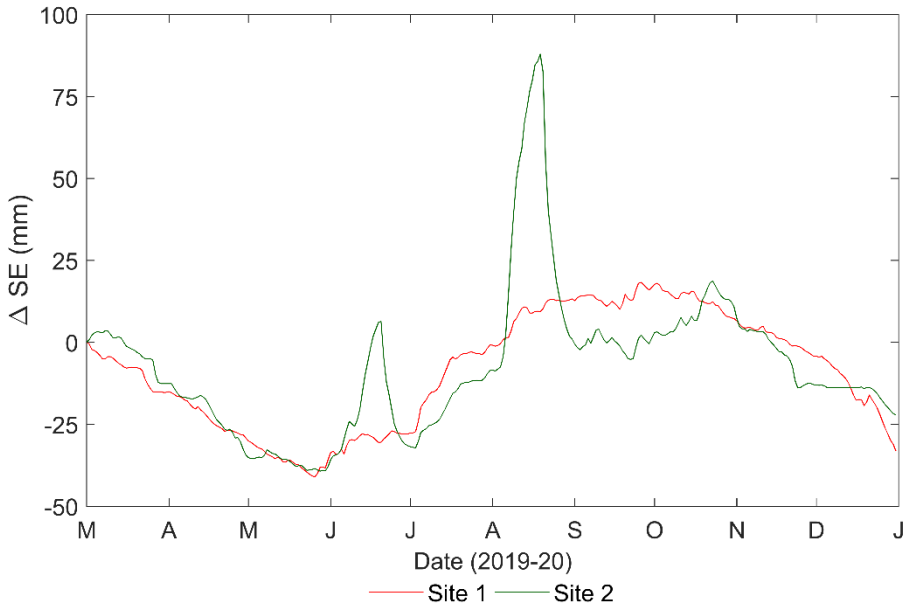

Figure B.1 Time series plot of changes in peat surface elevation (SE) based on mean daily data from the paired transducer systems at Sites 1 and 2 not shown in Chapter 5.